Regulation of Type-2 Airway Inflammation in Cystic Fibrosis and Asthma

by

Mason L. Donnell

Bachelor of Science, Missouri University of Science & Technology, 2017

Submitted to the Graduate Faculty of the

School of Medicine in partial fulfillment

of the requirements for the degree of

Doctor of Philosophy

University of Pittsburgh

2020

UNIVERSITY OF PITTSBURGH

SCHOOL OF MEDICINE

This dissertation was presented

by

Mason L. Donnell

It was defended on

July 27, 2020

and approved by

Charleen T. Chu, MD, PhD, Professor, Department of Pathology

Luis A. Ortiz, MD, Professor, Department of Medicine

Corrine R. Kliment, MD, PhD, Assistant Professor, Department of Pathology

Jonathan K. Alder, Assistant Professor, Department of Pathology

Dissertation Director: Tim D. Oury, MD, PhD, Professor, Department of Pathology

Regulation of Type-2 Airway Inflammation in Cystic Fibrosis and Asthma

Mason L. Donnell, PhD

University of Pittsburgh, 2020

Asthma, chronic obstructive pulmonary disease (COPD) and cystic fibrosis (CF) patients can all experience type-2 airway inflammation. The aim of this research was to understand how type-2 airway inflammation is regulated in models of CF and asthma by the receptor for advanced glycation endproducts (RAGE). Previous studies indicate RAGE is crucial for induction of type-2 airway inflammation. Intriguingly, RAGE and type-2 proinflammatory cytokines are elevated in CF patient sputum and during infection with *Pseudomonas aeruginosa*. This led to the hypothesis that RAGE regulates IL-13 induced mucus production seen in CF patients.

Using a RAGE antagonist, this study shows RAGE regulates mucin gene *MUC5AC* expression, the expression of transcription factors regulating mucous metaplasia (*CLCA1*, *SPDEF* and *FOXA3*) and exotoxin-2 production in Non-CF and CF human bronchial epithelial cells (HBECs). By transfecting Non-CF and CF HBECs with dicer substrate siRNA (dsiRNA) to deplete *RAGE* expression, this study shows RAGE regulates these phenomena through activation of STAT6 upstream of mucous gene expression. CF HBECs were hyperresponsive to IL-13 treatment with elevated *MUC5AC*, *CLCA1* and *FOXA3* expression, which may be driven by sustained activation of STAT6. To test the role of RAGE *in vivo*, exotoxin derived from *P. aeruginosa* was used to model type-2 airway inflammation in WT and RAGE knock-out mice (RAGE-/-). WT animals treated with exotoxin were found to develop mucus production, though this was absent in RAGE-/- animals.

In a second study, RAGE regulation of IL-33 initiation of type-2 allergic airway inflammation (AAI) was investigated. Prior work shows WT mice exposed to allergens upregulate

IL-33 in the lung, while RAGE-/- mice do not significantly upregulate the cytokine alarmin. To further understand how RAGE regulates IL-33 production, this study hypothesized RAGE expressing type-1 alveolar epithelial cells (ATIs) release IL-33 in response to allergens. After stimulation with *Alternaria alternata* (*AA*), RAGE expressing murine ATIs did not release IL-33. Human alveolar organoids were also tested but were unable to release IL-33 after stimulation with *AA*. Collectively, these studies show RAGE plays a role in IL-13 induced mucus production in CF HBECs and that ATIs are not solely responsible for IL-33 release.

Table of Contents

Preface xiv

Acknowledgement xv

Key Nomenclature xvii

1.0 Pathology of Cystic Fibrosis & Asthma 1

1.1 Cystic Fibrosis 3

1.1.1 CFTR function, structure and mutations 3

1.1.2 Pathophysiology of CF 5

1.1.3 Current and future treatment of CF 7

1.1.4 Experimental models of CF 12

1.2 Asthma 14

1.2.1 Genetic and environmental factors of asthma 14

1.2.1.1 Genetic factors 14

1.2.1.2 Environmental factors 16

1.2.2 Pathophysiology of asthma 19

1.2.3 Current and future treatment of asthma 23

1.2.4 Experimental models of asthma 25

2.0 The Receptor for Advanced Glycation Endproducts (RAGE) regulates mucus production & airway inflammation in models of Cystic Fibrosis 28

2.1 RAGE 28

2.1.1 RAGE structure and isoforms 28

2.1.2 RAGE ligands 29

2.1.3 RAGE signaling pathways 31

2.1.4 RAGE in CF type-2 airway inflammation 34

2.2 Materials and Methods 36

2.2.1 Animals and reagents 36

2.2.2 Modeling type-2 airway inflammation *in vivo* 36

2.2.3 Culture of primary human bronchial epithelial cells (HBECs) 37

2.2.4 Modeling airway mucus production *in vitro* 38

2.2.5 Pharmacological Inhibition of RAGE 38

2.2.6 Knockdown of RAGE expression using dicer substrate siRNA (dsiRNA) .. 39

2.2.7 Quantitative RT-PCR 39

2.2.8 Western blot analysis 40

2.2.9 Periodic-acid Schiff (PAS) Stain 41

2.2.10 Immunofluorescence (IF) imaging 42

2.2.11 ELISA for Eotaxin-2 42

2.2.12 Statistical Analysis 43

2.3 Results 44

2.3.1 RAGE expression in CF vs. Non-CF HBECs 44

2.3.2 Pharmacological inhibition of RAGE blocks mucus production and CF HBEC hyperplasia 45

2.3.3 RAGE regulates expression of mucous metaplasia transcription factors 51

2.3.4 Inhibition of RAGE reduces production of an eosinophil chemoattractant 54

2.3.5 Inhibition of RAGE reduces STAT6 phosphorylation 56

2.3.6 Knock-down of RAGE expression reduces STAT6 phosphorylation 59

2.3.7 RAGE-/- mice have reduced mucus production in response to exotoxin derived from *P. aeruginosa* 62

2.4 Discussion 66

3.0 IL-33 is not released from murine Type-1 Alveolar Epithelial Cells or Human Alveolar Organoids *in vitro* 73

3.1 Interlukin-33 (IL-33) 73

3.1.1 IL-33 structure and function 73

3.1.2 RAGE regulation of IL-33 in type-2 allergic airway inflammation 75

3.1.3 Cellular localization of IL-33 release in the lung 76

3.2 Materials and Methods 77

3.2.1 Isolation of primary murine type-1 alveolar epithelial cells (ATIs) 77

3.2.1.1 Lung perfusion and digestion 77

3.2.1.2 Fluorescence-activated cell sorting (FACS) 78

3.2.1.3 Culture of primary murine ATIs 79

3.2.2 Culture of human induced pluripotent stem cells (hiPSCs) and alveolar organoids 79

3.2.3 Modeling allergen exposure *in vitro* 81

3.2.4 Western blot analysis 81

3.2.5 Immunofluorescence (IF) and fluorescence microscopy 82

3.2.5.1 IF: hiPSC characterization 82

3.2.5.2 Fluorescence microscopy: Alveolar organoid characterization 83

3.2.6 ELISA for murine and human IL-33 83

3.2.6.1 Murine IL-33 ELISA: Murine ATI media and lysates 83

3.2.6.2 Human IL-33 ELISA: Alveolar organoid media, matrigel supernatant and lysates 84

3.2.7 Statistics 84

3.3 Results 85

3.3.1 Isolated primary WT and RAGE KO murine ATIs do not release IL-33 in response to *Alternaria alternata* 85

3.3.2 hiPSCs express human pluripotency markers 97

3.3.3 Organoids express marker of type-2 alveolar epithelial cells (ATIIs) 98

3.3.4 Organoids do not release IL-33 in response to *Alternaria alternata* 99

3.4 Discussion 100

3.5 Final Conclusions: Chapter 2 & 3 103

4.0 Future Directions 107

4.1 Rage regulation of mucus production in Cystic Fibrosis 107

4.1.1 Role of RAGE in CF 107

4.1.2 *Pseudomonas aeruginosa* driven type-2 airway inflammation in CF 108

4.1.3 Future investigations: Regulation of type-2 airway inflammation in CF .. 110

4.1.3.1 Extended dsiRNA *in vitro* experiments 110

4.1.3.2 Exotoxin *in vitro* experiments 112

4.1.3.3 sRAGE in vitro experiments 112

4.1.3.4 G82S RAGE expression *in vitro* 114

4.1.3.5 Extended exotoxin *in vivo* experiments 115

4.1.3.6 sRAGE *in vivo* experiments 116

4.2 IL-33 release during allergic airway inflammation 117

4.2.1 Role of IL-33 in type-2 AAI 117

4.2.2 Lung epithelial cell type expression of IL-33 118

4.2.3 Future investigations: cell specific IL-33 release during type-2 AAI 120

4.2.3.1 Murine *in vivo* and *in vitro* experiments 120

4.2.3.2 Human *in vitro* experiments 121

Appendix A 124

Bibliography 132

List of Tables

Table 1: Non-CF and CF HBEC samples 124

List of Figures

Figure 1: Major hypotheses and type-2 airway inflammation 2

Figure 2: *RAGE* expression in differentiated HBECs 45

Figure 3: Mucin gene expression in differentiated HBECs 47

Figure 4: PAS stains of differentiated HBECs 49

Figure 5: IF images of differentiated HBECs 51

Figure 6: Expression of TFs regulating mucous metaplasia in differentiated HBECs 53

Figure 7: Eotaxin-2 production in differentiated HBECs 55

Figure 8: IL-13 signaling pathway 57

Figure 9: STAT6 phosphorylation in differentiated HBECs 58

Figure 10: dsiRNA knock-down of RAGE expression in undifferentiated HBECs 62

Figure 11: Exotoxin treated WT and RAGE-/- mice 65

Figure 12: Initial FACS isolation protocol for primary murine ATIs 86

Figure 13: Western blot of murine ATI markers 87

Figure 14: IL-33 release from primary murine lung cells 88

Figure 15: FACS isolation of WT primary murine ATIs 89

Figure 16: Culture of WT primary murine ATIs 90

Figure 17: Western blot of murine ATI markers 91

Figure 18: FACS isolation of WT primary murine ATIs 93

Figure 19: Culture of WT and RAGE-/- primary murine ATIs 94

Figure 20: Immunoblot of WT and RAGE-/- murine ATI markers 95

Figure 21: IL-33 release from WT and RAGE-/- primary murine lung cells 96

Figure 22: hiPSCs express pluripotency markers..... 97

Figure 23: Alveolar organoid culture and characterization 98

Figure 24: Human IL-33 release from alveolar organoids..... 99

Figure 25: CF HBECs have sustained activation of STAT6 111

Figure 26: Immunofluorescent images of Non-CF HBECs..... 125

Figure 27: Immunofluorescent images of CF HBECs 126

Figure 28: Total STAT6 is not significantly depleted at 24 hours..... 127

Figure 29: Power analyses on *RAGE* expression and RAGE inhibition experiments 128

Figure 30: Brown-Forsythe test for *MUC5AC* expression at 48 and 96 hours..... 129

Figure 31: Brown-Forsythe test for *CLCA1*, *SPDEF* and *FOXA3* expression at 48 hours 130

Figure 32: Brown-Forsythe test for *CLCA1*, *SPDEF* and *FOXA3* expression at 96 hours 131

Preface

Chapters of this dissertation may contain results, figures and discussion from a manuscript I will be submitting as first author.

Acknowledgement

Thank you first to my family and loved ones. Without their support, I would not have the financial or emotional ability to pursue my undergraduate and graduate education. To my niece Vivian Donnell, you are the reason I came to the University of Pittsburgh to study cystic fibrosis and have fueled my passion for research, science and medicine. I hope this work allows you to see your mind can dream and make it reality.

To my mentor Dr. Tim Oury, thank you for your broad medical knowledge, open mind, understanding personality and laughter. Throughout my rotations, your lab and its members felt the most like home. You have given me a plethora of opportunities and allowed me to pursue my dream of studying cystic fibrosis, and for that I am forever grateful. To Dr. Tim Perkins, thank you for being a role model and sharing your experimental advice. You have motivated me throughout this experience through your work ethic, sharp mind and love for what you do in the lab. To Gina Dutz, thank you for introducing me to the lab and being a great listener and friend. To our collaborator, Dr. Mike Myerburg, your expertise and contribution to this work was greatly appreciated. Thank you for consulting with me on many of my experiments involving the maintenance and genetic transduction of primary human cells. These samples provided by the staff at the Lung Tissue Core were indispensable for this work. For consultation with the statistical analysis of these samples, I would like to thank PhD candidate Channing Parker. You have been an asset and it was a joy working with you.

I would also like to thank the members of my committee, including Dr. Chu, Dr. Kliment, Dr. Alder and Dr. Ortiz. Your guidance has been enlightening and has developed my skills as a scientist. Specifically, I would like to thank Dr. Chu and Dr. Kliment. Dr. Chu, I want to thank

you and your lab for giving me indispensable training on working with human induced pluripotent stem cells, which was a highlight of my work. Dr. Kliment, thank you for giving me knowledgeable career advice and for guiding me experimentally with immunofluorescence and genetic transduction. Lastly, thank you to the Cystic Fibrosis Foundation (CFF) for funding our lab and the ARCS Scholar program. These funds have greatly supported this work and have been vital to my success and ability to keep moving forward even when things got stressful.

Key Nomenclature

A. muciniphila	*Akkermansia muciniphila*
AA	*Alternaria alternata*
AAI	Allergic Airway Inflammation
ACK	Ammonium-Chloride-Potassium
AERD	Aspirin-Exacerbated Respiratory Disease
AGE	Advanced Glycation Endproduct
AGER	RAGE Gene Locus
AKT	Protein Kinase B
ALI	Air Liquid Interface
ANOVA	Analysis of Variance
AQP5	Aquaporin-5
ASL	Airway Surface Liquid
ATI	Type-1 Alveolar Epithelial Cell
ATII	Type-2 Alveolar Epithelial Cell
ATP	Adenosine Triphosphate
BALF	Bronchoalveolar Lavage Fluid
Bcl-2	B-cell lymphoma 2 Protein
BEGM	Bronchial Epithelial Growth Medium
BSA	Bovine Serum Albumin
CaCC	Calcium Activated Chloride Conductance Channels
cAMP	Cyclic Adenosine Monophosphate
Cas9	CRISPR Associated Peptide-9
CBD	Cannabidiol
CD31	Platelet Endothelial Cell Adhesion Molecule
CD45	Protein Tyrosine Phosphatase Receptor Type C
Cdk4	Cyclin-Dependent Kinase 4
cDNA	Complementary DNA
CF	Cystic Fibrosis
CFRD	Cystic Fibrosis Related Diabetes
CFTR	Cystic Fibrosis Transmembrane Conductance Regulator
CHAPS	3-((3-Cholamidopropyl) Dimethylammonio)-1-Propanesulfonate
ClcA1	Chloride Channel Accessory 1 mRNA
IgER	IgE Receptor or FCεRII
IκB	Inhibitor of κB
IL-#	Interleukin
IL-13Rα1	IL-13 Receptor Alpha 1
IL-4Rα	IL-4 Receptor Alpha
IL-5Rα	IL-5 Receptor Alpha
ILC#	Group-# Innate Lymphoid Cell
ILD	Interstitial Lung Disease
IMDM	Iscove's Modified Dulbecco's Media
IPF	Idiopathic Pulmonary Fibrosis
Jak Kinase	Janus Kinase
Mac	Macrophage
MAP Kinase	Mitogen-Activated Protein Kinase
MBP	Granular Major Basic Protein
MEK Kinase	Mitogen-Activated Protein Kinase Kinase
MHC II	Major Histocompatibility Complex 2
mRNA	Messenger RNA
MSD	Membrane Spanning Domain
MTG	1-Thioglycerol
Muc5ac	Mucin 5ac mRNA
NBD	Necleotide Binding Domain
NF-κB	Nuclear Factor Kappa-light-chain-enhancer of activated B Cells
NKX2.1	NK2 Homeobox 1
OVA	Ovalbumin
P. aeruginosa	*Pseudomonas aeruginosa*
PAS	Periodic acid–Schiff
PBMCs	Peripheral Blood Mononuclear Cells
PBS	Phosphate-Buffered Saline
PEP	Positive Expiratory Pressure
PFA	Paraformaldehyde
PI3K	Phosphatidylinositol-3 Kinase
PM	Particulate Matter

COPD	Chronic Obstructive Pulmonary Disorder	proSPC	Pro-Surfactant Protein-C
Cre	Causes Recombination	PRR	Pattern Recognition Receptor
CRISPR	Clustered Regulatory Interspaced Short-Palindromic Repeats	pSTAT6	Phospho-STAT6 Protein
DAMP	Damage Associated Molecular Pattern	RA	Reumathoid Arthritis
DC	Dendritic Cell	RAGE	Receptor for Advanced Gycation Endproducts
DEP	Diesel Exhaust Particle	*RAGE*	RAGE mRNA
Dia-1	Diaphanous-1	RAGE-/-	RAGE global knock-out mice
DIGE	Difference Gel Electrophoresis	RCF	Relative Centrifugal Force
DMEM	Dulbecco's Modified Eagle Medium	RD	Regulatory Domain
DNA	Deoxyribonucleic Acid	rKGF	Reccombinant Human Keratinocyte Growth Factor
dsiRNA	Dicer Substrate Interfering RNA	RNA	Ribonucleic Acid
DTT	Dithiothreitol	RNAi	RNA Interference
ECL	Enhanced Chemilumineescence	ROS	Reactive Oxygen Species
ECM	Extracellular Matrix	RT	Room Temperature
ELISA	Enzyme-linked Immunosorbent Assay	RT-qPCR	Quantitative Reverse Transcription Polymerase Chain Reaction
Eos	Eosinohil	S100A12	S100 calcium-binding protein A12 (enRAGE)
ERT2	Ethylene-Regulated Transcript 2	SDS	Sodium Dodecyl Sulfate
ES	Embryonic Stem	SDS-PAGE	Sodium Dodecyl Sulfate Polyacrylamide
FBS	Fetal Bovine Serum	siRNA	Small Interfering RNA
FDA	Food and Drug Administration	SLC26	Solute Carrier 26
FEV1	Forced Expiratory Volume in One Second	SNP	Single Nucleotide Polymorphism
FoxA3	Forkhead Box Protein-A3 mRNA	*Spdef*	SAM Pointed Domain Containing ETS Transcription Factor mRNA
FPS-ZM1	N-Benzyl-4-chloro-N-cyclohexylbenzamide	sRAGE	Soluble RAGE
FVC	Forced Vital Capacity	SSEA-#	Cell Surface Stage Specfic Antigen-#
GAPDH	Glyceraldehyde 3-Phosphate Dehydrogenase	ST2	IL-33 Receptor
GFP	Green Fluorescent Protein	STAT6	Signal Transducer and Activator of Transcription-6 Protein
GTSCD	Glutathione S-Transferase C-terminal Domain-Containing	T1-α	Podoplanin
GWAS	Genome Wide Association Study	TCR	T-cell Receptor
HBEC	Human Bronchil Epithelial Cell	TGF-β	Transforming Growth Factor-β
HDM	House Dust Mite	Th-#	T-helper
HFCWO	High-Frequency Chest Wall Oscillation	*THSD4*	Thrombospondin Type 1 Domain Containing 4 Gene Locus
HHIP	Hedgehog-Interacting Protein Gene Locus	TLR-#	Toll-like Receptor-#
hiPSC	Human Induced Pluripotent Stem Cell	TNF-α	Tumor Necrosis Factor-Alpha
HMGB1	High Mobility Group Box 1 Protein	*TNS1*	Tensin-1 Gene Locus
HTR4	5-Hydroxytryptamine (serotonin) Receptor 4	TRA-1-81	Anti-Keratin Sulfate Associated Antigen
IBD	Inflammatory Bowel Disease	TRITC	Tetramethylrhodamine
IBMX	3-Isobutyl-1-Methylxanthine	TRM	Resident Memory T-cell

IF	Immunofluorescence
Ig_	Immunoglobulin-E, G, M
TSLP	Thymic Stromal Lymphopoietin
VCAM-1	Vascular Cell Adhesion Molecule-1
WT	Wild-Type

1.0 Pathology of Cystic Fibrosis & Asthma

This study will address two major hypotheses of how RAGE regulates type-2 airway inflammation in cystic fibrosis and asthma. Prior studies have indicated RAGE regulates IL-13 induced mucus production in mice and human airway epithelial cells. CF patients have increased levels of type-2 inflammation, which led to the hypothesis that RAGE regulates IL-13 induced mucus production in CF human airway epithelial cells (Fig. 1, H1). The second hypothesis addresses a previous finding that RAGE-/- mice treated with allergens have depleted levels of IL-33, which activates type-2 innate lymphoid cells to produce IL-13 in the lung. Yet, it is still not understood which lung epithelial cells release IL-33 in response to allergens (Fig. 1, H2). This led to the hypothesis that RAGE expressing type-1 alveolar epithelial cells regulate IL-33 release during allergen stimulation. In order to address these hypotheses, is important to understand the pathology of CF and asthma and how type-2 inflammation plays a role in both diseases.

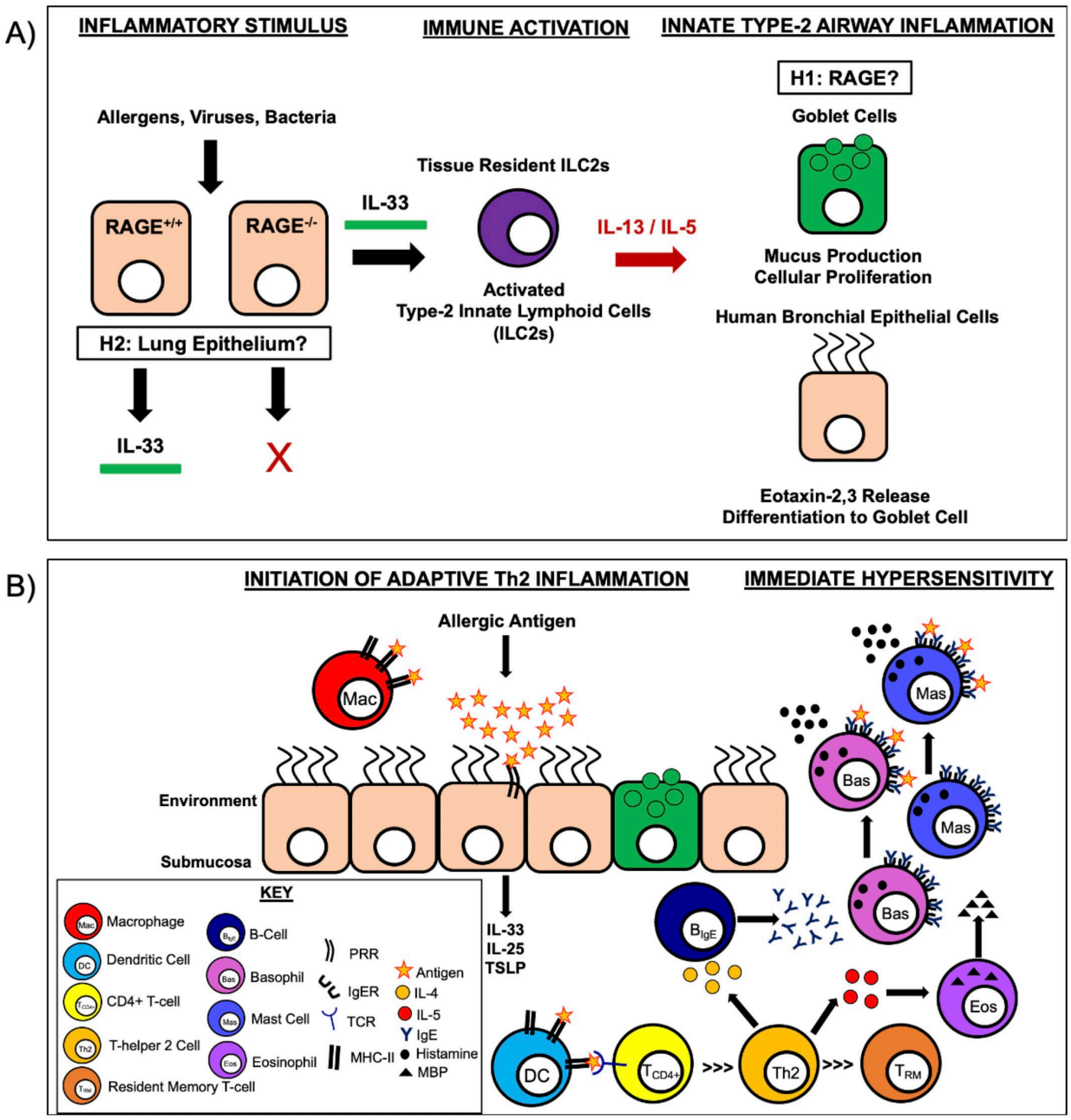

Figure 1: Major hypotheses and type-2 airway inflammation

Inflammatory Stimulus: Exposure to allergens, viruses, or bacteria induce release of IL-33 from airway cells. RAGE-/- animals exposed to allergens do not upregulate IL-33 like their WT counterparts. Immune Activation: IL-33 then bind to type-2 innate lymphoid cells (ILC2s, purple) activating their expansion and production of type-2 proinflammatory cytokines IL-13 and IL-5 (red). Type-2 Airway Inflammation: IL-13 and IL-5 then induce mucus production, mucous hyperplasia (goblet cell proliferation), mucous metaplasia (differentiation to goblet cell) and

eotaxin-2 release to recruit eosinophils to the lung. H1=Hypothesis 1 addressing RAGE regulation of IL-13 effects on Non-CF and CF bronchial epithelium. H2=Hypothesis 2 addressing which lung epithelial cell is responsible for IL-33 release in response to allergens (A). Lung epithelial cells recognize the presence of an allergen through pattern recognition receptor (PRR) signaling induced by allergen antigens. This then induces the epithelium to release cytokines alarmins, IL-33, IL-25 thymic stromal lymphopoietin (TSLP). These alarmins can then activate dendritic cells (DC) for antigen presentation. Antigen presenting cells, such as dendritic cells and alveolar macrophages (Mac) play a key role in type-2 airway inflammation. These immune cells express major histocompatibility complex II (MHC-II) that binds to the foreign antigen and presents it to the T-cell receptor (TCR) expressed on CD4+ T-cells activating their expansion to T-helper 2 (Th2) cells, which can further differentiate to Resident Memory T-cells (T_{RM}). Activated Th2 cells produce type-2 cytokines, where IL-4 activates B-cells to produce polyclonal IgE and IL-5 activates eosinophils (Eos) to release major basic protein (MBP). Polyclonal IgE then binds with high affinity to IgE receptors (IgER or FCεRII) expressed on mast cells (Mas) and basophils (Bas), sensitizing them to the allergen. Upon re-exposure of the allergic antigen, IgE crosslinks with the antigen and activates mast cells and basophils to degranulate and release histamines, which induces an immediate type-2 hypersensitivity reaction within minutes (B).

1.1 Cystic Fibrosis

1.1.1 CFTR function, structure and mutations

CF is an autosomal recessive genetic disorder caused by mutations in the cystic fibrosis transmembrane conductance regulator (*CFTR*). *CFTR* is located on chromosome 7 in humans and is expressed in multiple epithelial tissues, including the lung, pancreas, skin (sweat glands), brain and gastrointestinal tract [1,2]. It is a part of the ATP-binding cassette family of transporters facilitating the transport of chloride and bicarbonate ions into or out of the cell by utilizing ATP hydrolysis [3]. The transporter is comprised of seven domains: the N- and C-terminus, two

membrane spanning domains with six transmembrane helices each (MSD1 & 2), two nucleotide binding domains (NBD1 & 2) and a regulatory domain (RD) [4]. Activation of CFTR conductance is induced by cyclic-AMP (cAMP) activation of protein-kinase A (PKA) [5]. PKA then phosphorylates multiple residues on CFTR's R-domain, leading to a conformational change that engages the NBD domains for ATP hydrolysis [4,6]. Mutations in CFTR are classified into six or seven subsets based on the effect of CFTR conductance, stability or expression.

Traditionally, class I mutations of CFTR have been defined by no CFTR protein due to nonsense, frameshift or canonical splice site mutations (e.g. Gly542X, Arg553X). Class I has now been split into two classes (Class IA and Class IB) based on the specific mutation effect, though both still result in no CFTR protein [7]. Class IA is defined by mutations resulting in no mRNA (e.g. 1717-1G-A), whereas Class 1B (e.g. Gly542X) is defined by no protein. Class II mutations result in misfolded CFTR that is degraded by proteases during trafficking from the endoplasmic reticulum to the golgi apparatus. This class is based on missense or amino acid deletion mutations (e.g. Phe508del, Asn1303Lys) [8]. Class III mutations result in CFTR production and successful trafficking to the membrane, though the transport's gating function is impaired due to missense or aminoacid substitution mutations (e.g. Gly551Asp, Ser549Asn) [4]. Class IV missense and amino acid substitution mutations result in reduced chloride conductance through CFTR (e.g. Arg117His, Ala455Glu). Class V mutations occur due to splicing defects or missense mutations that result in decreased full length *CFTR* mRNA formation and therefore lack of functional CFTR (e.g. 3849+10kbC-T, 2789+5G-A). Lastly, class VI mutations result in production of mRNA and protein, but decrease CFTR's membrane stability (e.g. Gln412X) [2,8]. Rescued CFTR in patients who are on novel CFTR correctors may still retain plasma membrane instability even though the trafficking defect has been corrected ((r-rescued) Phe508del) [9].

1.1.2 Pathophysiology of CF

Over 85,000 individuals suffer from CF across the world with an expected life expectancy of around 50 years old [10]. CF pathophysiology is centered around aberrant or missing anion secretion or absorption through CFTR. Since CFTR is expressed in multiple tissues, its mutations affects multiple organs, including the skin, pancreas, intestines, brain and the lungs [8,11]. Humans have been documented to display signs of pancreatic inefficiency and salty skin since the 1600's, which are both characteristic of CF pathophysiology [12]. Increased levels of sodium chloride build up on the skin of CF patients due to a net reduction in Cl^- ion absorption through CFTR, which also reduces Na^+ ion absorption. Pancreatic insufficiency is caused by lack of CFTR secretion of HCO_3^- from pancreatic ductal cells. This causes pancreatic juices to increase in acidity and dehydrate, which leads to decreased enzyme secretion via exocytosis and primes the gland for pancreatitis and fibrosis [13]. Fibrosis can then lead to destruction of beta cells in the pancreatic islets, which in turn decreases insulin resistance and insulin secretions [14]. This disruption in glucose regulation leads to 30-50% of CF patients developing CF related diabetes (CFRD), where patients with class I, II or II mutations are at higher risk [15–17]. CFTR mutations also affect the gastrointestinal track, where lack of CFTR Cl^- secretions leads to increased acidity, dehydration, meconium ileus at birth, an altered microbiome and acid reflux disease [1,18].

CFTR is also expressed in the central and peripheral nervous systems. In pigs CFTR is expressed in neurons and glial cells, however in humans CFTR has only been identified in neuronal cells [19,20]. Since chloride ions play an excitatory role (depolarization) in peripheral neurons and an inhibitory role (hyperpolarization) in central neurons, it is plausible lack of CFTR may impede peripheral neuron signaling and enhance central neuron signaling [21]. Indeed, a study looking at peripheral nerve signaling in CF patients found 56% of patients had at least one abnormal signal,

which was typically a reduced sensory nerve action potential [22]. CFTR has also been shown to affect intervention of peripheral nerves and the development of the central nervous system [19,21]. In CF human fetal tissue, CFTR dramatically increases in expression during fetal development in the cerebral cortex, ventricular zone and cortical plate [20]. Though overall, cerebral development is not affected by mutations in CFTR, with only a slight delay in maturation of the neuroepithelium and choroid plexus [20].

Intriguingly, both CFRD and microbiome diversity are associated with airway function, which is the primary cause of morbidity in CF patients [18,23,24]. Airway ciliated epithelial and submucosal cells harbor CFTR in their apical membranes where it acts as the primary route for chloride and bicarbonate conductance [13,25,26]. Chloride conductance across the cell membrane acts to enhance water secretion, which poises CFTR as a key regulator of the airway surface liquid (ASL) pH, composition and volume [13,27]. Its bicarbonate secretion in particular is tied to airway mucus viscosity and clearance as the absence of HCO_3^- ions dampens mucociliary transport [28]. HCO_3^- ions also drive mucus solubilization by complexing with Ca^{2+} or H^+ cations on mucins, exposing the proteins' negatives charge and providing a repulsive force to drive mucus granule expansion and solubilization [29,30].

Other anion channels and exchangers in the plasma membrane of airway epithelial cells contribute to the regulation of the ASL and mucus viscosity. Calcium activated chloride conductance channels (CaCC) and the solute carrier 26 (SLC26) family of transporters contribute to chloride and bicarbonate transport, while also interacting with CFTR. CFTR has been shown to inhibit Ca^{2+} stimulated Cl^- currents in CaCC channels, while solute carrier variants such as SLC26A3 and SLC26A9 share direct contact with CFTR via their C-terminal domain with CFTR's phosphorylated R domain [13,31]. Recent studies have also found class II CFTR mutations affect

SLC26A9 anion secretion, which highlights the importance of CFTR to regulate anion secretion, ASL volume and mucus viscosity [32].

Regulation of the ASL and mucus viscosity by anion secretion through CFTR is crucial to the health of CF patients as they ultimately affect the proficiency of mucociliary clearance, the primary innate immune response in the airways [33]. This ultimately leads to persistent infections over the life span and decreases in lung function measured by the forced expiratory volume in one second (FEV_1) [34]. While *Pseudomonas aeruginosa* is the most common infection associated with CF patients, *Staphylococcus aureus* infections are more prevalent during adolescence [35]. Critically, these infections induce Th17 and Th2 immune responses within the lung creating mucus biofilms that promote antibiotic resistance over time [36–38]. This remains a critical field of investigation for CF treatment since bacterial infections are enhanced by viral co-infection and current small molecular modulators of CFTR function do not ameliorate all types of infections in CF patients [39–41]. In total, lack of CFTR ion absorption and secretion affects organ physiology, immunology and microbiology, ultimately leading to mortality due to decreased lung function.

1.1.3 Current and future treatment of CF

Treatment of CF has expanded greatly over the past several decades, with patients living until their mid-40s and even late 60s if they possess less severe mutations (Classes IV, V and VI) [7,8,42]. Upon the discovery of CF, most patients were treated for pancreatic insufficiency using exogenous pancreatic enzymes to increase absorption of fats and proteins [2]. Concomitantly, CF patients are advised to eat a high caloric diet rich in fat, salt and protein to offset malnutrition [43]. In severe cases of malnutrition, patents may require a gastrostomy enteral tube for direct delivery

of nutrients to the stomach [44,45]. Other groups are also working on methods to measure risk of malnutrition, which is associated with pulmonary function [46].

Before FDA approval of CFTR small molecule modulators, CF patients were still able to live past their teenage years due to multiple treatment strategies targeted at pulmonary function [2]. This includes physical hand-percussion starting at birth and elevates to wearing a high-frequency chest wall oscillation (HFCWO) vest and applying a positive expiratory pressure (PEP) mask, which are designed to loosen mucus [47]. Adherence to these treatments varies, though randomized clinical trials are testing novel devices using sound waves, which do not require chest wall compression and may increase adherence [48]. To further disrupt mucus during these treatments, CF patients inhale hypertonic saline and DNAse enzymes (Pulmozyme, Genentech) that increase the fluidity of the airway-surface liquid (ASL) and breakdown viscous DNA released by neutrophils in the airway [49,50]. Aerosolized β-adrenergic bronchodilators (e.g. albuterol) are also administered during treatment to relax the airway smooth muscle cells and increase lung compliance. While albuterol has been shown to increase Cl^- concentrations in sputum, other studies have found albuterol may decrease production of cAMP and reduce CFTR activation during treatment with CFTR modulators [51,52].

The advancement of CFTR modulators has made the future bright for CF patients. These revolutionary small molecules were initially screened in primary human bronchial epithelial cell cultures from CF patients, where anion conductance and ciliary function served as end-point measures [8]. CFTR modulators are now used in combination and serve different purposes based on how they affect CFTR plasma membrane trafficking and anion conductance. The first FDA approved modulator (VX-770, Ivacaftor or Kalydeco) acts as a potentiator, meaning it increases the amount of time CFTR is open for conductance [53,54]. Its effects were most pronounced in

patients who possessed class II, IV and V mutations since CFTR is still trafficked to the plasma membrane, though lacks in number or gating function. In order to further apply modulators to the most common CFTR mutation (i.e. Phe508del), which prevents membrane trafficking and affects gating, new small molecules were found to increase CFTR protein in the plasma membrane (tezacaftor-VX-661 and lumacaftor-VX-809) [55,56].

Combination of lumacaftor and ivacaftor (Orkambi) then became the first FDA approved modulator therapy for patients homozygous for Phe508del [54]. Though, patients heterozygous for Phe508del who possess mutations unresponsive to ivacaftor potentiation or result in lack of CFTR in the plasma membrane were not responsive (as measured by FEV_1) to Orkambi treatment [57]. This led to further development of new correctors, of which elexacaftor in combination with tezacaftor and ivacaftor was successful in improving FEV_1 and decreasing pulmonary exacerbations by 63% in patients heterozygous for Phe508del [58]. This led to the newest FDA approval of the combinatorial CFTR modulator coined TRIKAFTA (elexacaftor-tezacaftor-ivacaftor), which may also eliminate lumacaftor's pulmonary adverse side effects [54,59].

While CFTR modulators have been shown to significantly enhance lung function and may also ameliorate pancreatic insufficiency, they do not cure CF patients and have limited effects on lung inflammation due to chronic and resistant infections [60,61]. In one study looking at the UK CF registry, ivacaftor treatment was associated with reduced infection from *P. aeruginosa* after 3-years of treatment. While *S. aureus* infection was also reduced, this was seen only in the last two years of treatment, and infections with *Burkholderia cepacian* complex were not reduced [62].

Importantly, infection with resistant strains of *P. aeruginosa* or *B. cepacian* are a hallmark of end-stage lung disease in CF patients where lung transplantation is considered. Criteria for transplantation include an $FEV_1 < 30\%$, frequent exacerbations due to chronic infection and

increased oxygen requirements [63]. Studies have found patients with resistant *P. aeruginosa* infections have decreased survival following lung transplant, though two year post-transplant survival curves are comparable between patients with non-resistant or resistant *P. aeruginosa* infection and transplantation is still advised [64,65]. Conversely, CF patients with *B. cepacian* complex infection have greatly reduced survival within the first year, with one study finding only 29% of patients with *B. cepacian* complex survived the first year after lung transplant [66]. Other comorbidities also affect whether a patient receives a lung transplantation, including malnutrition and CFRD. Though since these morbidities can be managed, they are often considered modifiable risk factors before transplantation [65]. In total, the average increase in lifespan for CF patients receiving a lung transplant in 2014 was 8.3 years, and as modulator therapies develop, the need for lung transplantation may be delayed in CF patients [67,68]. However, development of new drugs to target antibiotic resistant bacterial infections remains a major concern for CF patients.

In order to address chronic and resistant infections, researchers are investigating novel combinations of already approved antibiotics that have synergistic effects against lung damaging *B. cepacian* infection [69]. However new combinatory antibiotics may not suffice to kill drug resistant microbes due to their protection in mucus biofilms. This has led to new formulations for the most commonly used antibiotic in CF patients: tobramycin. By encapsulating tobramycin with hypromellose, aerosolized particles do not bind together and drug delivery to lower airways is enhanced [70]. Other studies have combined tobramycin and other antibiotics by encapsulating these drugs in *N*-acetylcysteine, a mucolytic drug, which together inhibits growth of *P. aeruginosa* biofilms [71]. This has led to research in encapsulating antibiotics in other compounds such as neutral-charged polymeric nanoparticles that do not interact with negatively charged mucins [72]. Other therapies, such as cationic antimicrobial peptides, degrade the extracellular matrix (ECM)

of bacterial biofilms and prevents microbial communication that confers drugs resistance [39]. Since antibiotics must always keep up with bacterial evolution, the most fundamental way to treat CF patients is to target the mutation in CFTR.

CF has been the desirable model to test the therapeutic efficacy of genetic therapy since it is a monogenetic disease where correction of one allele can reverse disease progression. In order to change CFTR gene expression, DNA or RNA must be introduced to the cell. This can be accomplished by a multitude of transport systems, including adenoviruses, adeno-associated viruses and non-viral vectors made up of polymers or liposomes [72,73]. The first clinical trial to open the door to genetic manipulation of CFTR utilized adenoviral delivery of cDNA encoding WT CFTR to the nasal epithelium in three CF patients [74]. While chloride conductance was enhanced in these patients, larger trials using adenoviruses delivered CFTR cDNA via aerosol delivery to the lungs or lobular instillation failed to show enhanced lung function, with some patients experiencing fever and increased sputum production [75]. These results, along with lack of expression of the coxsackie-adenovirus receptor in human airway epithelial cells, led to the investigation of adeno-associated viruses (AAVs). Engineered AAVs and other parvovirus capsids, such as human Bocavirus-type-1 (HBoV1), have higher tissue tropism and have been shown to correct CFTR in mouse nasal epithelial cells, CF patient derived intestinal organoids and ferret airway epithelial cells [73]. While AAVs may have a higher transduction rate, clinical trials failed to show increases in lung function 30 days from AAV delivery of full-length CFTR cDNA [76,77].

While viruses have co-evolved with mammalian cells for opportune transduction, non-viral delivery methods have several benefits including higher carrying capacity, scalability and are non-immunogenic [72]. Though, delivery of CFTR cDNA to the nucleus of the cell using non-viral

cationic liposomes still proves challenging. Phase 2 clinical trials using this approach with delivery every 28 days for 1-year have shown only modest improvement in lung function and did not show increases in CFTR expression [78]. This has led to investigation of mRNA targeted approaches, which eliminate the need to enter the nucleus. The oligonucleotide eluforsen shares 100% homology to WT *CFTR* mRNA and increased expression and chloride conductance in human bronchial epithelial cell cultures and in a murine model of Phe508del CFTR.

As of this year, phase 1 clinical trials showing its safety after inhalation of eluforsen in CF patients look promising [79,80]. The main caveat of both viral and non-viral delivery methods is the repetitive treatment to maintain full-length CFTR expression. This is countered by the advancement clustered regulatory interspaced short-palindromic repeats (CRISPR) and the CRISPR associated peptide-9 (Cas9) endonuclease, which enable correction of CFTR mutations before lung development in human induced pluripotent stem cell (hiPSC) organoids [81]. CRISPR/Cas9 corrected organoids serve as a translatable human model to test both genetic and small molecular modulator therapies. Patient derived organoids may also serve as a cell engraftment strategy for CF patients, which would reduce the dosage rate of genetic therapies [82–84].

1.1.4 Experimental models of CF

Since the gene responsible for CF was identified in 1989, researchers have created an array animal models to study the molecular and cellular pathology of CF. Each of these *in vivo* systems has their benefits and draw backs, which has led to the standardization of *ex vivo* primary human cell and organoid cultures for testing pharmacologic and genetic therapies [8,85]. To recapitulate the disease pathology, CFTR knock-out (KO) mice, pigs, ferrets, rats and rabbits have been

developed. CFTR KO mice exhibit intestinal blockage similar to meconium ileus at birth seen in humans, but do not develop spontaneous lung infections, mucosal inflammation in the airway, pancreatic inflammation or liver pathology [86]. This is mainly due to alternative chloride ion channel expression in mice and their lack of respiratory bronchioles [85,86]. Though, transgenic mice possessing WT CFTR that over express the sodium channel ß-ENaC do develop spontaneous infections and mucosal inflammation, which is due to sodium and airway liquid hyperabsorption preventing mucociliary clearance [87]. However, it should be noted that the ubiquitously used C57BL/6J mice strain is responsive to *Pseudomonas aeruginosa* infection, which 80% of CF patients experience [88–90].

Other than rodents, both pig and ferret CFTR KO models possess most of the human pathologies associated with CF. This includes pancreatic inefficiency and spontaneous lung infection at birth, which is due to their possession of respiratory bronchioles and submucosal glands within the airway [85]. While animal models provide important organ system insights, the gold standard in modeling CF is cultured primary human bronchial epithelial cells (HBECs) since they possess patient specific CFTR mutations and other potential genetic or environmental factors relevant to CF pathology [91]. Obtaining HBECs is challenging to due extensive processing and delays in CF patient lung transplants due to CFTR modulator therapies [67]. Although when HBECs are isolated from lung tissue and cultured in factor supplemented media, these cells can be differentiated into pseudostratified monolayers with beating cilia [92]. Differentiation is supported by addition of extracellular matrix components and by culturing primary HBECs on air-liquid interface (ALI) filters [91,93]. As well, coculture with other cell types, such as fibroblast, enhance cell passaging and doubling rates [92]. Since primary HBECs are hard to come by, researchers also use CF patient derived iPSCs. These stem cells can be easily stored and passaged

with the ability to differentiate into multiple tissue types [82,94]. This had led to their utilization in studying CFTR function in response to both genetic and pharmacologic treatments [81,83,95].

1.2 Asthma

1.2.1 Genetic and environmental factors of asthma

1.2.1.1 Genetic factors

Asthma is a chronic inflammatory airway disease characterized by airway hyperresponsiveness and obstruction, where both genetic and environmental risk factors contribute to disease severity. Hundreds of genes have been identified to be associated with asthma, which is anywhere from 35 to 95% heritable [96]. In order to better understand which genes may play a more significant role in asthma, metanalyses of genome-wide association studies (GWAS) have tried to identify loci associated with airway obstruction. In the clinic, airway obstruction is measured by the forced expiratory volume in one-second (FEV_1) and the ratio of FEV_1 to the forced vital capacity (FEV_1/FVC). These measures are associated with all-cause mortality, cardiovascular disease and asthma [97–99]. In one GWAS study, a cohort of 20,288 patients from 14 different databases was screened for top loci associated with FEV_1 or FEV_1/FVC. This was followed-up by analyzing these hits against an additional 54,276 member cohort, which led to six loci associated with measures of airway obstruction [97]. These included *HHIP*, *TNS1, GTSCD, HTR4, AGER* (RAGE gene locus) and *THSD4*. In a separate meta-analysis of GWAS studies including 20,890 individuals, eight loci were significantly associated with FEV_1/FVC and one was associated with FEV_1 alone [98].

To determine these loci, both studies corrected for smoking exposure, which would greatly affect pulmonary function measures. Of note, loci identified in both studies included *HHIP*, *HTR4*, *GSTCD* and *AGER* [97,98]. The hedgehog-interacting protein (*HHIP*) gene was first implicated in airway obstruction in a GWAS study of over 7,000 individuals from Massachusetts [100]. Prior, HHIP was found to regulate branching lung morphogenesis. Absence of *HHIP* in mice leads to formation of only one right and left lung lobe and predisposes mice to developing airway obstruction when compared to WT mice [101,102]. The *HTR4* gene codes for the 5-hydroxytryptamine (serotonin) receptor 4, which is a G-protein coupled receptor. When serotonin is released from blood platelets, it acts on HTR4, increasing heart rate and vasoconstriction [103]. Since serotonin was known to be elevated in asthmatic patients, *in vitro* studies using human airways showed serotonin binding to HTR4 induces airway constriction [104]. Serotonin is also found in cells of the innate immune system, including basophils and mast cells. Conversely, HTR4 is found most highly expressed within the alveoli of the lung, which further implicates the serotonin system in immunity and lung function [105,106].

GSTCD or glutathione s-transferase C-terminal domain-containing protein has been implicated in asthma based on its function in regulating oxidative stress. Based on structural homology to other GST enzymes, GSTCD has been proposed to function in oxidative stress by reducing reactive oxygen species, which protects DNA and proteins in the cell from oxidative damage [97]. Absence of *GSTCD* in mice predisposes these mice to developing lung cancer and non-cancerous lesions within the mucosal glands of the lung [107]. It is possible that SNPs within GSTCD may alter its enzymatic activity, thus promoting oxidative stress in the lung and worsening asthma symptoms [108]. Indeed, the SNP identified within GSTCD was highly correlated to FEV_1 compared to other genes identified in the meta-analysis [98].

The loci identified in the receptor for advanced glycation endproducts (RAGE, *AGER-gene*) associated with FEV_1/FVC leads to a glycine-to-serine (G82S) substitution in the receptors ligand binding V-domain [98,109,110]. Conversion from the non-polar to polar residue results in increased binding affinity of the RAGE ligand, enRAGE (S100A12), to G82S RAGE. When G82S RAGE is expressed in human polymorphonuclear cells, treatment with enRAGE led to increased phosphorylation of MEK and MAP kinase enhancing proinflammatory cytokine production [109]. Since enRAGE is known to be elevated in asthmatic patients, this may explain how mutations in RAGE contribute to airway obstruction through enhanced signaling of RAGE ligands, which promote airway inflammation [111]. Indeed, studies from our lab have shown RAGE regulates type-2 allergic airway inflammation (AAI). Using RAGE-/- mice and primary human bronchial epithelial cells, previous studies have found RAGE regulates allergen induced IL-33 expression, innate immune cell recruitment, and production of IL-13, IL-5 and mucins, which are hallmarks of type-2 AAI [112–114]. Concomitantly, SNPs in *IL-33* were found to be associated with asthma diagnosis in a meta-analysis across three ethnic groups, including European Americans, African Americans/African Caribbeans and Latinos [115]. While there are many loci attributed to pathological consequences of asthma, environmental factors including local environment, climate change and diet also have been found to have significant effects on asthma severity.

1.2.1.2 Environmental factors

Several environmental pollutants have been attributed to asthma pathogenesis through inflammation and cell death. These includes automobile fuel exhaust, ozone and particulate matter in the air [116]. Diesel exhaust particles (DEPs) are known to enhance Th17 immune cell activation and IL-17A production in primary human bronchial epithelial cells [117,118]. This finding is corroborated by increased expression of IL-17A in asthmatic patients who live near high traffic

areas compared to low traffic areas [118]. DEPs are also known to enhance type-2 AAI through release of IL-33 from the airway epithelium. Mice exposed to house dust mite (HDM) and DEPs accumulate IL-33 and produce type-2 proinflammatory cytokines. In contrast, mice lacking expression of the IL-33 receptor (ST2) stimulated with HDM and DEPs showed decreased levels of type-2 proinflammatory cytokines IL-13 and IL-5, as well as other markers of type-2 AAI [119].

Ozone plays a role in airway inflammation, cell death and lung compliance. Ozone is formed from oxygen in the atmosphere reacting with volatile organic compounds and nitrogen oxide gases produced from fossil fuel exhaust. Ozone has been known to stimulate alveolar macrophages to produce proinflammatory cytokines, such as IL-6 and TNF-α [120]. IL-6 in particular is seen elevated in the bronchoalveolar lavage fluid (BALF) from asthma patients, and blockade of the IL-6 receptor in mouse models of asthma lower levels of type-2 cytokines [121,122]. Due to its powerful oxidation capacity, ozone induces the production of reactive oxygen species (ROS) in bronchial epithelial cells, which leads to cell death through activation of caspase-9 [123]. ROS production due to ozone exposure has also been shown to decrease cilia formation, cilia beating and lung compliance measured by the end tidal volume and elastance [116,123]. In total, the impact of ozone on asthmatic patients is projected to lead to over 3,000 unnecessary emergency department visits between the years 2045 and 2055 due to climate change and weather patterns supporting ozone formation [124].

Ultrafine carbon particles (<100 nm) and particulate matter (PM) are also increasing in the atmosphere due to the continual use of fossil fuels and coal. One study looking at non-smoking asthma patients exposed to air downstream of the airport LAX for only 2-hours found that ultrafine particles and airway traffic were associated with increased levels of circulating IL-6 or decreased FEV_1 [125]. Interestingly, ultrafine carbon particles have also been shown to elevate IL-6 in

primary human bronchial epithelial cells [126]. While the bronchial epithelial cells responded to carbon particles by enhancing cytokine production, nasal epithelial cells exposed to carbon particles significantly lost their viability [126]. Mouse alveolar macrophages exposed to low concentrations of ultrafine particles have been shown to enhance proliferation, higher dosages induce caspase-8 mediated cell death [127]. These studies show particulate matter may differentially affect cells within the airway, and suggest exposure time and PM concentration alter the pathological consequences of PM exposure in asthmatic patients.

Weather and seasonal patterns also affect asthma patients. Temperature changes are known to contribute to allergic symptoms, and cold dry air challenge can even be used to measure airway hyperreactivity and bronchoconstriction [116,128,129]. While other measures of weather including humidity, wind speed and precipitation have no founded direct effects on the airway, these factors play a role in the seasonal adaptation of plants. Plants require specific signals from weather patterns to initiate their lifecycle, and thus produce pollen. Increases in global temperature and CO_2 lead to plants producing pollen earlier, shifting their life cycle and even lengthening pollen production [130,131]. While allergic reactions to pollen is dependent on the plant species and length of exposure, pollen can react with air pollutants, such as ozone, creating more allergenic particles [132,133].

Although many environmental factors contributing to asthma are found in the air, what's for dinner can also affect the immune system and severity of asthma. The microbiome is composed of trillions of microorganisms, including bacteria, fungi and viruses, whose diversity and function are largely shaped by our diets as well as our parents' diets [134]. During birth in both humans and mice, the microbiome is passed to offspring from the mother and can significantly affect the development of the immune system, particularly the spleen in mice [135,136]. Interestingly, obese

asthma patients compared to non-obese asthma patients have higher levels of eosinophils in the bronchoalveolar lavage fluid (BALF) and increased activation of IL-13 driven JAK-STAT6 signaling that leads to mucin gene expression [137,138]. In the same study, it was found severe asthmatic patients had reduced levels of the bacteria *A. muciniphila* in their gut. After chronic challenge with HDM in mice, administration of *A. muciniphila* reduced eosinophils, neutrophils, T-cells and B-cells in the airway [137]. More global perturbations of the gut microbiome also play a role in asthma. Specifically, asthma diagnosis at the age of five is associated with increased usage of antibiotics along with a decrease in the diversity of the microbiome [139]. These studies suggest specific gut bacterial species, as well as overall microbial diversity, can have significant immunologic consequences in the lung.

1.2.2 Pathophysiology of asthma

Asthma is a heterogeneous chronic inflammatory disease of the airways involving the airway epithelium, connective tissue, endothelium, smooth muscle and the immune system. Over 26 million Americans suffer from asthma and are estimated to lose 15.46 million quality adjusted life years between 2018-2038 [140]. Symptoms of asthma include, but are not limited to, wheezing, coughing, increased sputum production, airway obstruction and ultimately pulmonary exacerbations or “asthma attacks” [96]. The most common type of airway inflammation seen in asthma patients is type-2 allergic airway inflammation (AAI). This innate inflammatory response is centrally mediated by group-2 innate lymphoid cells (ILC2s) that receive molecular cues from the lung epithelium that drive their activation, expansion and abundant production of type-2 proinflammatory cytokines [141].

Other types of innate lymphoid cells have also been discovered, including group 1 and 3 innate lymphoid cells (ILC1 and ILC3s). All ILCs are derived from the same common bone marrow progenitor and become tissue resident immune cells that reside at mucosal barriers and surfaces in organs. Each express specific transcription factors (TFs) that define their functions in different forms of innate inflammation [142]. Specifically, ILC1s function in type-1 inflammation in response to bacteria and viruses, such as *clostridium difficile* (*C. diff*) and hepatis B [143,144]. They are activated by IL-12, IL-15 and IL-18 produced by macrophages and dendritic cells, and subsequently produce interferon gamma (INF-γ) [144,145]. ILC3s play a vital role in the gut by protecting the intestinal epithelium from microbial species by enhancing production of IgA, facilitating the formation of gut associated lymphatic structures and inducing intestinal stem cell repair [146,147]. ILC3s are activated by IL-1 produced by neutrophils and epithelial cells, and subsequently produce IL-17 and IL-22 [145]. ILC3s may also play a role in airway inflammation in asthma patients who do not have elevated levels of type-2 cytokines by inducing IL-8 production from lung epithelial cells though IL-17 signaling [148].

Type-2 inflammation in the airways is activated by allergens, smoke, viruses or parasitic infections that stimulate airway epithelial cells to release cytokine alarmins such as thymic stromal lymphopoietin (TSLP), IL-25 and IL-33 [141,149]. Specifically, type-2 inflammation can be induced by viruses such as influenza A and Sendai virus leading to IL-33 production in the lung [150,151]. Parasitic infections such as infections with parasitic worms or helminths can also induce type-2 airway inflammation [152,153]. It has been assumed that type-2 immunity evolved due to prior evolutionary pressures from these organisms, which can be unintendedly activated by allergens such as house dust mite, *Alternaria alternata* (*AA*) or pollen [154]. However, there is no structural similarity in antigens present on helminths or allergens, nor are the reactions to helminths

and allergens similar in severity or time [155]. Thus, it has been proposed type-2 immunity evolved to protect from many types of environmental stimuli present in our evolutionary history.

Antigen presenting cells, such as dendritic cells and alveolar macrophages play a key role in type-2 airway inflammation. These immune cells express major histocompatibility complex II (MHC-II) that binds to the foreign antigen and presents it to the T-cell receptor (TCR) expressed on CD4+ T-cells activating the adaptive immune system [156] (Fig. 1 B). Presentation of an allergic antigen by dendritic cells within the submucosa then induces the clonal expansion of T-helper 2 (Th2) cells, which later differentiate into T-resident memory (T_{RM}) cells that survive long-term and readily produce type-2 cytokines upon the next exposure to an allergen [157]. CD4+ T-cells can also clonally expand into Th1 cells, which react to antigens from intracellular parasites or bacteria [158]. Th1 cells produce type-1 cytokines such as INF-γ which activates phagocytosis by macrophages and helps regulate the balance of Th1 and Th2 responses, where lack of the INF-γ receptor in mice results in enhanced Th2 responses [159]. Conversely, activated Th2 cells produce the type-2 cytokine IL-4, which activates B-cells to go through Ig class switching to produce polyclonal IgE antibodies that bind with high affinity to the IgE receptor (IgER or FCεRII) expressed on mast cells and basophils [141,149,160]. Mast cells and basophils are now sensitized to the allergen, and upon a later exposure to the allergic antigen, IgE antibodies crosslink with the antigen and induce mast cells and basophils to degranulate, releasing histamines and proteases that induce an immediate type-2 hypersensitivity reaction characterized by vasoconstriction, vascular permeability and further immune cell infiltration [154,161–163] (Fig. 1 B). Mast cells and basophils have also been shown to produce type-2 cytokines, such as IL-4 and may play a role in the activation of Th2 cells [164].

ILC2s are activated by cytokine alarmins IL-33, IL-25 and TSLP and are responsible for the production of type-2 proinflammatory cytokines IL-5 and IL-13 from ILC2s [165]. The release of cytokine alarmins is thought to occur by recognition of allergens by pattern recognition receptors, such as RAGE and Toll-like receptors [114,166]. These cytokine alarmins then activate ILC2s and facilitate type-2 airway inflammation by activating antigen presenting dendritic cells as well as CD4+ T-cells [154,167]. Type-2 proinflammatory cytokines IL-5 derived from either ILC2s or Th2 cells then lead to activation of eosinophils that release granule major basic protein, which can have damaging affects to the bronchial epithelial cells and contributes to the type-2 hypersensitivity reaction [168,169]. Eosinophils may also communicate to the adaptive immune system through antigen presentation to naïve T-cells, furthering clonal expansion of Th2 cells [154].

While type-2 airway inflammation is common in asthma, many patients do not possess elevated levels of type-2 cytokines. This has led the classification of asthma into endotypes based on the specific molecular pathology of a patient. Currently, Th2 “high” and Th2 “low” are used to broadly categorize patients [149]. Th2 “high” patients are characterized by elevated IgE in serum, increased IL-13 and IL-5 expression, elevated eosinophils within the blood and BALF, increased mucin gene expression and increased basement membrane thickens [170]. Th2 “low” asthmatics lack these profiles, are less responsive to bronchodilators and glucocorticoids, but display airway hyperreactivity and neutrophilic influx [148,170]. While the pathology of Th2 “low” airway inflammation is not fully understood, the Th17 immune response has been implicated in neutrophilic influx. Specifically, IL-17 produced by Th17 cells induces airway epithelial cells to release IL-8, which subsequently activates neutrophilic inflammation [148]. Though due to the

heterogeneity of asthma, more specific pathological categories exist, including early-onset mild allergic asthma, obesity related asthma and severe atopic asthma [171].

Consequences of inflammation manifest in the airway and extrapulmonary organs. Within the airway mucosa, Th2 and Th17 cytokines induce mucous hyperplasia in humans and mucous metaplasia in rodent models of allergic airway inflammation [172–174]. Inflammation affects the airway submucosa by inducing smooth muscle cell hyperplasia, blood vessel development and deposition of extra cellular matrix (ECM) proteins [149]. This reduces the mechanical properties of the airways leading to fibrosis, constriction and obstruction [170,175,176]. Consequences of inflammation affecting the mucosa and submucosa ultimately lead to increased risk of a pulmonary exacerbations or "asthma attacks", which is associated with mortality in asthma patients [99,177]. Outside of the airway, inflammation contributes to multiple comorbidities. These include inflammatory bowel disease (IBD), atopic dermatitis, obesity, and cardiovascular disease, which is associated with increased mortality in asthma patients [178–181]. In total, the severity of asthma is dependent on the degree of inflammation in the airway and other organs.

1.2.3 Current and future treatment of asthma

Treatments for asthma vary depending on a patient's specific pathology and symptoms. Administration of β_2-agonist (albuterol, levalbuterol etc.) and inhaled corticosteroids (fluticasone, budesonide etc.) are common and effective treatments for allergic or Th2 "high" asthma, though inhaled corticosteroids are not as effective for Th2 "low" asthma patients [170,181]. β_2-agonists act on the airway smooth muscle cells by binding to β_2-adrenergic receptors, which reduces Ca^{2+} influx and muscle contraction, opening the airways [182]. Inhaled corticosteroids act on the airway vasculature as non-specific anti-inflammatories by reducing inflammation and angiogenesis [183].

While Th2 “low” asthmatics respond to β_2-agonists, treatment with fluticasone does not enhance FEV_1 when compared to placebo controls [170]. While the mechanisms driving Th2 “low” asthma have not been fully elucidated, smoking may be a confounding factor that reduces the effectiveness of corticosteroids and enhances neutrophilic inflammation in Th2 “low” patients [148].

In more severe cases, patients presenting with pulmonary exacerbations due to an infection may require further treatment with systemic corticosteroids (prednisone, dexamethasone etc.) or ipratropium bromide [181,184]. Treatment schedules using systemic corticosteroids vary and are controversial in the field due to their known side effects, including high blood pressure, ulceration of the gastrointestinal tract and mental illness [185]. Still, systemic corticosteroids have been found to reduce emergency room admission rates and are alone effective in reducing the relapse rate of pulmonary exacerbations [184]. Ipratropium bromide acts as a competitive inhibitor of cholinergic receptors, reducing constriction of airway smooth muscle cells. In combination with traditional β_2-agonists, it provides an synergistic effect on bronchodilation for patients dealing with severe pulmonary exacerbations and reduces side effects compared to albuterol alone [181,186].

In order to more specifically treat asthma patients, clinical trials have focused on developing biologics targeting mediators of airway inflammation. These include monoclonal antibodies (mAbs) targeting a gamut of type-2 cytokines and their receptors, including IL-4, IL-4Rα, IL-13, IL-13Rα, IL-5, IL-5Rα and TSLP [187]. mAbs raised to IgE (omalizumab), IL-5 (mepolizumab and reslizumab) and the IL-4Rα/IL-13Rα complex (depilumab) have been FDA approved based on their ability to reduce pulmonary exacerbations, eosinophilia and the need to use corticosteroids [187–189]. While effective treatments for Th2 “high” patients, these treatments do not enhance lung function in patients with Th2 “low” asthma [187]. Since Th17 driven neutrophilia has been implicated in Th2 “low” asthma, clinical trials using mAbs targeting IL-17A

(secukinumab) and IL-17RA (brodalumab) have been conducted with limited effectiveness and consistency in improving lung function [148,187,190]. Thus, further investigation into the mechanism driving neutrophilia in Th2 “low” asthma patients is crucial.

Other non-pharmacologic treatments have also been investigated for the treatment of asthma. Physical therapy, including breathing exercises and inspiratory muscle training, have been shown to decrease airway inflammation in asthma patients [191]. Metanalyses studying this effect have shown physical therapy reduces the incidence of asthma and can significantly improve the forced vital capacity (FVC) of asthma patients [192,193]. Dietary changes may also aid obesity related asthma patients by regulating the microbiome [137,179,194]. In one study using mice treated with house dust mite (HDM), a high fiber diet enhanced microbiome diversity and reduced Periodic acid Schiff (PAS) staining and the expression of IgE, IL-4 and IL-17 in the lung [194]. Natural substances, such as cannabidiol (CBD), can also reduce airway inflammation. In a mouse model using ovalbumin, intraperitoneal CBD was shown to reduce several markers of type-2 AAI, including IL-4, IL-5, IL-13 and eosinophil chemoattractant eotaxin-2 [195]. In summary, non-pharmacologic treatments are advantageous to patients due to their inherent reduced cost and lack of serious side effects. Though, in order to most effectively treat asthma, clinicians should use a multifactorial approach including pharmacologic, biologic and integrative medicine treatments.

1.2.4 Experimental models of asthma

There are many experimental models for asthma which mimic the endotypes seen in patients. This primarily includes mouse models displaying elevated Th2 inflammation, Th17 inflammation or a skewed response with both types of inflammation present [172]. While guinea pigs, rats, horses and non-human primate models have been also been used, these animals either

do not produce IgE as the primary anaphylactic antibody or do not lend themselves to genetic manipulation or immunological analysis [196]. Still mice do not naturally develop asthma, so various sensitization and treatment protocols have been developed. This includes administration of purified proteins or extracts from house dust mite (HDM), chicken egg ovalbumin (OVA), *Alternaria alternata* (*AA*), cockroach or ragweed to the airways of mice [196,197]. These allergens induce type-2 AAI in mice with treatment schedules ranging from 1 to 8-weeks to model an acute reaction [197,198]. Chronic reactions require month long treatments or involve transgenic animals that over express Th2 related cytokines, such as IL-9 or IL-13 [199]. An alternative mouse model uses adoptive transfer or intraperitoneal injection of allergen primed dendritic cells, which act as antigen presenting cells and lead to both Th2 and Th17 inflammation [172,200]. The intraperitoneal injection model is advantageous since it does not require anesthetization for treatment, which may reduce stress and variation of dosage between animals.

Human bronchial epithelial cell lines and primary human bronchial epithelial cells (HBECs) are vital models for studying asthma. Bronchial epithelial cell lines, such as BEAS-2Bs or A549s, stimulated with allergens can model the Th2 inflammatory response [201]. While these submerged cell culture systems are readily available and easily maintained, they lack the physical characteristics of the airway (i.e. exposure to air), prior disease history of asthma and have altered responses to allergens when compared to primary HBECs [93,201,202]. Alternatively, primary HBECs isolated from asthma patients via bronchial brushings, biopsies or transplanted lung tissue have distinct cytokine and epigenetic profiles when compared to healthy controls, which may explain their difference to their cell line counterparts [203,204]. Primary epithelial cells can also be cultured on air-liquid interface (ALI) culture systems. This allows for their differentiation into a pseudostratified monolayer that possess beating cilia and goblet cells [92]. More complex culture

systems use three-dimensional scaffolds and co-culture of several primary epithelial cells types [93,205]. Though, since primary HBECs are hard to come by, several groups are studying embryonic development of the lung to differentiate human induced pluripotent stem cells (hiPSCs) into bronchial or alveolar epithelial cells [94,206–208]. These cells can then be seeded into three-dimensional lung scaffolds or developed into organoids possessing secretory, basal and ciliated epithelial cells [95,209]. Thus, while primary airway epithelial cells are a highly translatable model to study asthma, the future of airway disease modeling lies in the development of hiPSCs into nearly identical structures as the lung.

2.0 The Receptor for Advanced Glycation Endproducts (RAGE) regulates mucus production & airway inflammation in models of Cystic Fibrosis

2.1 RAGE

2.1.1 RAGE structure and isoforms

There are multiple RAGE isoforms produced by alternative splice sites within the RAGE gene (*AGER*). These isoforms are conserved across mammalian species and are differentially distributed within tissues and cell types [210–213]. To date, greater than 20 human and 17 murine isoforms have been classified in various tissues including the lung, brain and heart [214–216]. While many human variations exist, approximately 50% of these transcripts contain a premature stop codon and are not stably expressed due to nonsense-mediated decay [214].

The most predominantly expressed transcript across species results in membrane-bound RAGE (mRAGE), which was discovered by Neeper et al. in bovine lung [210,217]. Posttranslational modifications produce a 45 kDa transmembrane protein with several domains, including a N-terminal signal sequence (aa1-22), a ligand binding V domain (aa22-116), two C-type domains C1(aa124-221) and C2(aa227-317), a transmembrane domain (343-363), and a C-terminal intracellular signaling domain (aa364-404) [110,210,214,218]. Interestingly, RAGE's c-terminal intracellular signaling domain does not contain a serine or threonine residue that can be phosphorylated [219].

The most common transcript variant other than mRAGE, results in the production of soluble RAGE or sRAGE that lacks the transmembrane domain [214,215]. sRAGE acts

extracellularly to sequester RAGE ligands and prevent canonical RAGE signaling pathways [220,221]. sRAGE may also be derived proteolytically from mRAGE rather than by alternative splicing mechanisms, and sRAGE itself can be enzymatically cleaved to produce endogenous secretory RAGE (esRAGE) and cleavage RAGE (cRAGE) [222,223]. Other mRAGE isoforms lack portions of the ligand binding V-domain and cannot transduce extracellular signals [110]. A newly discovered isoform of RAGE lacks the intracellular signaling domain and results in decreased downstream signaling [224].

While RAGE isoforms are numerous, derived by different mechanisms, and vary from tissue to tissue, it is important to note mRAGE is highly expressed in the lung [211,217]. This has led to the implication of RAGE and its isoforms as regulators of inflammation in several lung diseases such as idiopathic fibrosis [220,225,226], cystic fibrosis (CF) [227,228], chronic obstructive pulmonary disorder (COPD) [229–232] and asthma [113,114,233,234]. Within the human lung, percentages of the two main isoform transcripts, mRAGE and sRAGE, have been estimated (80%; 7% respectively) [214]. Ratios of these two key isoforms change in the disease state and may serve as novel biomarkers in several lung diseases [230,235,236].

2.1.2 RAGE ligands

RAGE ligands include a diverse set of biomacromolecules, where increases in their concentration can induce RAGE expression and multimerization. This positive feedback-loop indicates RAGE is an amplifier in response to inflammatory signals [110,237,238]. Advanced glycation end products (AGEs) were the first ligands identified for the receptor, which are found in food, tobacco smoke and are produced endogenously in the body [210]. Endogenous AGEs accumulate over long periods of time through reactions between free amine groups on

biomacromolecules and reducing sugars. Alternatively, AGEs in food or cigarette smoke are thought to form quickly by thermal heating [239,240]. While RAGE can transduce AGE related signals, many other AGE receptors have since been identified [110].

Most RAGE ligands can be classified as damage associated molecular patterns (DAMPs), including HMGB1, S100 proteins, amyloid-β and nucleic acids [111]. DAMPs are molecular mediators of immune responses that target innate immune effectors like RAGE, Toll-like receptors and inflammasomes [241]. HMGB1 or amphoterin was first found to bind RAGE in the brain and regulates neuronal projections during cortical development [242,243]. It is now understood HMGB1 is a chromatin-binding protein released as a DAMP by activated immune cells or through cellular necrosis [237,244,245]. HMGB1 was first found to bind to RAGE, but also binds Toll-like receptors (TLR2 and TLR4) due to shared motifs in the receptors' N-terminal signaling domains [246]. The S100 family of proteins are intracellular calcium signaling peptides also associated with neuronal outgrowth like HMGB1, but are also implicated in inflammatory diseases due to their secretion by innate inflammatory cells [246–248]. S100A12 was the first isoform of the family found to bind RAGE and it mediates immune cell recruitment [243]. Many additional S100 family members, including S100B, S100A1, S100A6 and S100A12, have also been identified as RAGE ligands [218,248–250].

Amyloid-β is yet another peptide DAMP recognized by RAGE. Amyloid-B acts as a neurotoxin in neurodegenerative diseases, such as Alzheimer's disease [251]. Upon binding to the receptor, amyloid-β has been found to activate microglia in the brain, a key indicator of Alzheimer's progression [252,253], and RAGE expressed in endothelial cells at the blood-brain barrier may contribute to amyloid-β transfer into the central nervous system [254]. RAGE isoforms have also been hypothesized to bind extracellular matrix (ECM) proteins from studies showing

RAGE overexpression in HEK293 cells promotes cellular extension on various ECM protein coated plates [255]. Indeed, RAGE has been shown to bind a diverse set of ECM proteins, including collagen I, IV and laminin, without additional scaffold proteins [256]. These direct interactions with the ECM may serve to regulate cell-to-matrix adhesion, though RAGE has been found to regulate cell-to-cell adhesion through binding β2 integrin protein (Mac-1) expressed on leukocytes [257]. These protein-protein interactions play an important role in immune cell migration to sites of inflammation. RAGE has also been shown to participate in protein-nucleic acid interactions during the inflammatory response. By binding both RNA and DNA, RAGE facilitates their uptake into endosomes in response to cell damage [238]. Even while there are many identified RAGE ligands, new molecules continue to be discovered, including pyridinoline, a molecule responsible for crosslinking collagen fibers [258].

2.1.3 RAGE signaling pathways

Due to the receptor's diverse ligands and expressional patterns, RAGE can induce an array of signaling cascades regulating inflammation, cellular differentiation, cell proliferation, migration and even cell death. The first evidence of RAGE inducing intracellular changes used AGE-albumin as a ligand, which increased the presence of proinflammatory reactive oxygen species (ROS), and led to the expression of the transcription factor nuclear factor kappa-light-chain-enhancer of activated B cells (NF-κB) [259,260]. The activation of NF-κB was found to be triggered by ROS oxidation of $p21^{RAS}$, which induced the mitogen activated protein kinases' (MAPKs), ERK1 and ERK2 [260,261]. These pathways directly regulate the activation of NF-κB by inhibiting the

inhibitor of κB (IκB), which allows the transcription factor to enter the nucleus, bind to the RAGE promoter and activate RAGE transcription [110,262].

MAP kinases were the first kinase family found to be activated by RAGE ligands, and share the Cdc42/Rac1 upstream pathway, which has been shown to be activated through Diaphanous-1 (Dia-1) binding to the receptor's C-terminal signaling domain [263]. Specific ligands, such as HMGB1, stimulate p38MAPK activation leading to muscle cell differentiation [264], and RAGE stimulated with S100B triggers MAP kinase kinases MKK4/7, which leads to c-Jun N-terminal kinase (JNK) induction of vascular cell adhesion molecule-1 (VCAM-1) found in aortic endothelial cells [265]. Our studies have also shown expression of VACM-1 is RAGE dependent in lung endothelial cells using RAGE knockout mice, which implicates RAGE as a mediator of immune cell recruitment in multiple tissues [113,266,267]. These MAP kinases have also been found to regulate metastatic glioma cell proliferation and migration through RAGE dependent mechanisms [268].

Other kinase cascades can regulate cell proliferation and migration and have been identified as targets of RAGE signaling. One pathway discovered in kidney cells showed AGEs can induce the activation of cyclin-D1 and cyclin-dependent kinase (Cdk) 4, which allows the cell to enter S-phase. This was transduced through the receptor tyrosine kinase, janus kinase (JAK) 2, and signal transducers and activators of transcription (STAT) 5 pathway, which promotes cell survival and proliferation by avoiding apoptosis [269–271]. STAT3 is another transcription factor that leads to cell proliferation through the oncogenic protein Moloney murine leukemia virus (Pim1) in vascular smoother muscle cells, where its activation was shown to be RAGE dependent using RAGE targeting small interfering RNA (siRNA) [272]. These findings suggest RAGE signaling affects the cell cycle through JAK/STAT pathways, which transforming growth factor-

β (TGF-β) may concomitantly regulate with RAGE [273]. This axis between RAGE signaling and TGF-β has also been shown to promote cell migration through MAPKs ERK and p38 phosphorylation of Smad 2/3 [274,275].

The phosphatidylinositol-3 kinase (PI3K)-AKT pathway is also activated by RAGE ligand binding. It stimulates NF-κB, inducing expression of proinflammatory cytokines like TNF-α and IL-6 [276]. AGEs have been shown to activate the PI3K-AKT pathway by studies utilizing RAGE inhibitors such as FPS-ZM1 in murine kidneys [277]. Through NF-κB, the inflammatory response is set, activating the expression of TGF-β, IL-6, and promoting the accumulation of ROS, which are all dampened by RAGE antagonists [277,278]. These responses to ligand binding can then perpetuate the inflammatory response through the activation of NF-κB via ROS, inducing further RAGE expression [260,279].

NF-κB activity is also increased when S100B proteins bind to RAGE, which has a pro-survival effect by increasing the expression of Bcl-2. Though, higher concentrations of this RAGE ligand can induce cytochrome-c release from mitochondria, and thus apoptosis through activation of caspase-3 [247]. Indeed, RAGE may play a role in both anti-apoptotic and pro-apoptotic signaling depending on the species and concentration of the ligand present [280,281]. In total, the diverse effects of RAGE ligands on intracellular signaling begin to shed light on the receptor's potential role as a co-receptor. Since RAGE shares pathways with other growth factor receptors, has the ability to multimerize, and leads to multiple cascades shared by some of its ligands, it has been hypothesized that RAGE is a co-receptor with serval other receptor families [246,273,274,282].

2.1.4 RAGE in CF type-2 airway inflammation

Cystic fibrosis is a chronic autosomal recessive genetic disorder that leads to progressive loss of lung function due to mutations in the cystic fibrosis transmembrane conductance regulator (CFTR) [283,284]. While patients experience a range of morbidities due to mutations in CFTR, including diabetes, malnutrition and liver disorders, respiratory failure and lung transplantation remain the main causes of death [8,11]. Patient lung function is frequently measured by the forced expiratory volume in one second (FEV_1) and is associated with infection status and mucus viscosity [34,285].

In the lung, CFTR resides in the apical membrane of HBECs and regulates the airway surface liquid (ASL) volume, mucus viscosity and mucociliary transport [286]. Loss of these homeostatic functions due to CFTR mutations cause CF patients to experience recurrent infections, which increases mucus production, mucus plugging and pulmonary morbidity [34,287–289]. Recent studies have shown CFTR modulators that enhance channel presence and function decrease some types of infections, though therapies directly targeting mucus production, mucus plugging and airway inflammation are an active area of investigation to develop new therapeutics for CF patients [41,287,290].

Recent studies have revealed RAGE as a mediator of the type-2 airway inflammation by regulating mucus production and eosinophilic inflammation in both murine and human models [112,114,233]. RAGE knock-out mice stimulated with allergens or IL-33 have reduced accumulation of group-2 innate lymphoid cells (ILC2s) in the lungs [114]. These cells when activated produce type-2 proinflammatory cytokines Interleukin-5 (IL-5) and Interleukin-13 (IL-13), which are key drivers of mucus production and eosinophilic airway inflammation

[138,291,292]. Thus, loss of RAGE prevents IL-13 driven mucus production and IL-5 driven recruitment of eosinophils to the lungs.

Notably, both the type-2 immune response and RAGE are elevated in CF patients when compared to Non-CF controls [37,228]. In patients with CF, IL-13 and IL-5 are associated with the development of bronchiectasis, *P. Aeruginosa* infection and are elevated in the bronchoalveolar lavage fluid (BALF) when compared to Non-CF controls [37]. IL-13 and IL-5 are also found in viscous *P. Aeruginosa* mucus biofilms that approximately 80% of patients with CF develop [90]. Intriguingly, CF patient sputum shows increased levels of full-length RAGE protein and mRNA [228]. A single nucleotide polymorphism (SNP) in RAGE's promoter region (rs1800625) identified in CF patients leads to increased expression of the receptor *in vitro*, and is associated with decreased FEV_1% predicted in a cohort of 967 CF patients [293]. The proinflammatory RAGE ligand, S100A12 or enRGAE, is also found at high levels in CF airways, while anti-inflammatory soluble RAGE (sRAGE) is found in low levels [227,249]. In addition, an increased ratio of enRAGE to sRAGE is correlated with decreased FEV_1% predicted in CF patients [228].

While RAGE regulates type-2 airway inflammation, and both are elevated in CF patients, studies inhibiting the type-2 immune response through RAGE in models of CF are lacking [287,290]. This led to the investigation of the role of RAGE in IL-13 induced mucus production and mucous hyperplasia in CF and Non-CF HBECs. Inhibition of RAGE signaling using the small molecule inhibitor FPS-ZM1 during IL-13 treatment blocks mucin gene expression, mucous hyperplasia, expression of mucous metaplasia transcription factors and the production of the chemoattractant eotaxin-2. Furthermore, knock-down of RAGE expression using dicer substrate siRNA (dsiRNA) in CF HBECs shows RAGE controls these various processes through activation of the signal transducer and activator of transcription-6 (STAT6). This study also investigated

RAGE's role in an *in vivo* mouse model of *P. Aeruginosa* induced type-2 airway inflammation. After one week of intranasal treatment with *P. Aeruginosa* derived exotoxin, RAGE-/- had reduced mucus production when compared to WT treated mice. These studies indicate RAGE modulates a common form of airway inflammation associated with CF pathology.

2.2 Materials and Methods

2.2.1 Animals and reagents

Twelve (6 female, 6 male) wild-type (WT) C57BL/6 mice were ordered from Taconic (Hudson, NY). An additional twelve age and gender matched RAGE-/- congenic C57BL/6 mice were obtained from an established breeding colony maintained under the University of Pittsburgh Department of Laboratory Animal Resources. All animals were aged to 7-weeks prior to experimentation. Animal studies were subsequently carried out under the National Research Council's guidelines in the ''Guide for the care and use of laboratory animals,'' with oversight by the University of Pittsburgh's Institutional Animal Care and Use Committee.

2.2.2 Modeling type-2 airway inflammation *in vivo*

Exotoxin derived from *P. aeruginosa* bacteria was used to model type-2 airway inflammation *in vivo* based on several published protocols [88,89,294]. WT and RAGE-/- animals were treated every day for 1-week intranasally with 50 μl of 1 mg/ml exotoxin dissolved in 10% ethanol in water (experimental group) or 50 μl of 10% ethanol in water (control group). Mice were

then sacrificed 24 hours after the seventh treatment and the bronchoalveolar lavage fluid (BALF), whole lung homogenates and whole lung sections were harvested. BALF was obtained by perfusion and withdraw of 0.8 mL of 0.9% saline to both lungs through the trachea. The left lung was flash frozen using liquid nitrogen to obtain whole lung homogenates, and the right lung was inflated with 0.6 ml of 4% paraformaldehyde (PFA, Electron Microscopy Sciences) to obtain whole lung sections.

2.2.3 Culture of primary human bronchial epithelial cells (HBECs)

Primary HBECs were obtained from excess lung tissue under a protocol approved by the University of Pittsburgh Investigational Review Board (IRB). Random samples of both Non-CF and CF tissues were used for subsequent pharmacological and genetic knock-down experiments. Specific CFTR mutations and previous diseases states in CF and Non-CF samples, respectively can be found in table 1 of the appendix.

To obtain HBEC cultures, bronchi were dissected, rinsed and incubated overnight at 4°C in MEM containing 0.1% type XIV protease (Sigma). The epithelial cells were isolated by centrifugation and washed in 5% FBS-MEM. After centrifugation, the cells were resuspended in serum-free bronchial epithelial growth medium (BEGM, Clonetics) and plated into collagen type IV coated t-25 flasks. After cells reached 80–90% confluence, they were trypsinized and resuspended in 5% FBS-MEM and seeded onto collagen type IV coated transwell filters for differentiation or onto 24-well plates to maintain their undifferentiated state (12 mm, Costar) at a density of $2x10^6$ cells/cm^2. After 24 hours, the medium was changed to DMEM-F-12 (1:1 volume) plus 2% Ultroser G (BioSepra). Apical media is removed to create an air-liquid interface (ALI) [92]. Media in the basolateral surface was then changed every 48 hours for 2-4 weeks until cells

were differentiated to polarized, ciliated cells. Differentiated cells were then used for pharmacological inhibition and imaging experiments, while cells in the undifferentiated state were used for genetic knockdown experiments. In both cases, Non-CF and CF HBEC samples were paired randomly for experiments based on what samples were available at the Lung Tissue Core at the University of Pittsburgh.

2.2.4 Modeling airway mucus production *in vitro*

To induce mucus production *in vitro*, human recombinant IL-13 (rIL-13, Biolegend) was used to stimulate induction of mucin gene expression, eotaxin production and mucous hyperplasia in HBECs [291,292]. Before rIL-13 stimulation, HBECs were differentiated in air liquid interface (ALI), which mimics the native condition of epithelial cells within the bronchus [295]. Cells exhibit moving cilia and produced a layer of mucus, both indicators of successful differentiation [92].

2.2.5 Pharmacological Inhibition of RAGE

RAGE singling was inhibited by adding FPS-ZM1 (Millipore), which targets RAGE's ligand binding V-type domain [296]. FPS-ZM1 was solubilized in DMSO (Sigma Aldrich) and added to fresh basolateral media of differentiated Non-CF and CF HBECs (50 μM). An equal volume of DMSO was dissolved in fresh basolateral media to act as the vehicle control in half of the samples. After one or three hours, rIL-13 (Biolegend) dissolved in 0.9% saline was added to the basolateral media of both RAGE inhibited and control HBECs (10 or 25 ng/ml). Control samples were treated with only 0.9% saline (2-5 μl) as the control for IL-13 treatment. After 48

hours, RNA, cell lysates and media supernatants were harvested. In extended experiments, RAGE inhibition and rIL-13 treatment were repeated at the 48-hour time-point. After 48 hours (96 hours from first treatment), RNA, cell lysates and media supernatants were harvested.

2.2.6 Knockdown of RAGE expression using dicer substrate siRNA (dsiRNA)

For knockdown of RAGE expression, Non-CF and CF HBECs were in an undifferentiated state to limit mucus production and enhance transfection efficiency [297]. HBECs were cultured in serum and antibiotic-free bronchial epithelial growth medium (BEGM, Clonetics). Cells were then transfected with RAGE targeted or control scramble dsiRNA (Integrated DNA Technologies) for 6 hours using Lipofectamine RNAi Max (Thermo). At 6 hours, media was changed to serum and antibiotic-free BEGM. After 20 hours post-transfection, cells were stimulated with rIL-13 in 0.9% saline dissolved in the media at 10 ng/ml for 4 hours. Control samples were treated with only 0.9% saline (5 μl) as the control for IL-13 treatment. Subsequently, cell lysates were harvested at 24 hours using difference gel electrophoresis (DIGE) buffer (7 M urea, 2 M thiourea, 30 mM Tris, and 4% CHAPS) with 1X of the Halt protease and phosphatase inhibitor cocktail (100X, Thermo) on ice. Cell lysates as well as RNA were harvested to verify adequate knockdown of RAGE using RT-qPCR and western blot analysis. Samples were stored at -80°C until use.

2.2.7 Quantitative RT-PCR

HBEC RNA extraction after pharmacological or dsiRNA knock-down of RAGE expression was conducted using the RNeasy Mini Kit per the manufacturer's instructions (QIAGEN). Primers used included human *AGER* (Hs00542584_g1), *MUC5AC*

(Hs01365616_m1), *SPDEF* (Hs00171942_m1), *FOXA3* (Hs00270130_m1), *CLCA1* (Hs00976287_m1) and glyceraldehyde3-phosphate dehydrogenase (*GAPDH*) control (Hs02758991_g1) (Applied Biosystems, Foster City, Calif). Reverse transcription was performed with Moloney murine leukemia virus reverse transcriptase (Applied Biosystems, Foster City, CA) in a Techne thermal cycler (Bibby Scientific US, Burlington, NJ). Quantitative polymerase chain reaction (qPCR) was performed with universal PCR buffer and TaqMan primer/probe assay reagent (Applied Biosystems). The following cycling protocol was followed on an ABI Prism 7300 machine (Applied Biosystems): 50°C (2 minutes), 95°C (10 minutes), and then 40 cycles of 95°C (15 seconds) followed by 60°C (1 minute). Fold change was then calculated compared with *GAPDH* mRNA control using the ΔΔCt method.

2.2.8 Western blot analysis

HBECs were lysed using DIGE Buffer with 1X of the Halt protease and phosphatase inhibitor cocktail (100X, Thermo) on ice. Total protein content was determined using a Bradford assay with bovine serum albumin (BSA, Fisher Scientific) and Coomassie protein assay (Thermo) or by the absorbance at 280 nm using a Nanodrop (Thermo). For gel loading, a mixture of 4X sample buffer (BIORAD) and 500 mM dithiothreitol (DTT) was prepared at a ratio of 9:1 and was subsequently mixed with 20-40 μg of HBEC protein at 1:3 ratio. Samples were then analyzed by SDS-PAGE on a 10% acrylamide gel (BIORAD) and subjected to immunoblotting. After blocking in 5% BSA-PBS, membranes were incubated in 1:1000 of primary rabbit anti-RAGE (Abcam, 35-45 kDa), rabbit anti-STAT6 (Cell Signaling, 100-110 kDa), rabbit anti-pSTAT6 (Cell Signaling, 100-110 kDa), and 1:5000 of primary mouse anti-β-Actin (Cell Signaling, 42 kDa) in 5% BSA-PBS. This was followed by three 15-minute wash steps in tris buffer with 0.1% tween (T-BST)

and incubation for 1 hour in 1:5000 secondary horseradish peroxidase anti-rabbit or anti-mouse antibody (Jackson ImmunoResearch) in 3% milk. Membranes were washed as stated above and finally developed with chemiluminescent detection using ECL Plus Reagent (Thermo) before imaging (LI-COR Odyssey Fc). Densitometry was analyzed using Image Studio software (LI-COR Biosciences).

2.2.9 Periodic-acid Schiff (PAS) Stain

HBEC cultures and mouse whole lung sections were fixed with 4% paraformaldehyde (PFA, Electron Microscopy Sciences), paraffin embedded and cut into sections 4 μm thick (Pitt Biospecimen Core, University of Pittsburgh). Slides were then deparaffinized using xylene (Fisher Scientific) and rehydrated using decreasing ethanol (Fisher Scientific) concentrations (100%, 90% to 70% in MilliQ water). Slides were treated with periodic-acid solution, washed with MilliQ water and stained with Schiff's regent before mounting with Permount media (Fisher). All slides were then examined by light microscopy. For PAS+ bronchial epithelial cells, total cell counts were recorded and the number of PAS+ cells or cells above the basal layer of cells where then divided by the total number of cells. The percentage of PAS+ airways was calculated by first counting all airways larger than 10 μm for each animal per treatment group. The number of PAS+ airways for each animal was then divided by the total airways in each animal and multiplied by 100% (n=5 per treatment group).

2.2.10 Immunofluorescence (IF) imaging

HBEC cultures were fixed with 4% paraformaldehyde (PFA, Electron Microscopy Sciences), paraffin embedded and cut into 4 μm thick sections (Pitt Biospecimen Core, University of Pittsburgh). Cells were then permeabilized with 0.3% Triton X-100, in 1% BSA-PBS for 10 minutes at room temperature (RT). Between each step, 5 washes with 0.5% BSA-PBS were performed. Sections were blocked with 2% BSA-PBS for 45 minutes at RT. Primary antibodies were incubated at 4° C for 60 minutes, while secondary antibodies were incubated in the dark at RT for 60 minutes. RAGE and MUC5AC were labeled using primary rabbit anti-RAGE (Abcam) at 1:200 in 0.5% BSA-PBS and mouse anti-MUC5AC (Abcam) at 1:200 in 0.5% BSA-PBS. Fluorescent labeling was conducted using secondary goat anti-rabbit IgG at 1:500 (546 nm) and goat anti-mouse IgG1 1:500 (488 nm) dissolved in PBS. Slides were then washed 5 times in PBS and stained with DAPI at 2.5 μg/ml for 10 minutes (Thermo). Isotype controls were performed on separate slides using mouse IgG1, kappa monoclonal antibody and rabbit IgG monoclonal antibody (Abcam) with previously mentioned species-matched secondary antibodies. Sections were mounted with Prolong Diamond mounting agent (Thermo) and examined by an Olympus IX71 inverted microscope (Olympus, Tokyo, Japan). All images were processed with ImageJ software (NIH). In all cases a rolling ball radius of 50.0 pixels was used.

2.2.11 ELISA for Eotaxin-2

HBEC media supernatants were harvested after bulk media was pelleted at 4° C for 10 minutes at 10,000 RPM. Subsequently, 100 μl of supernatant from each treatment group was loaded onto a 96-well plate and incubated with human Eotaxin-2 capture antibody per the

manufacturer's instructions (R&D Systems). Absorbance was then measured after following the manufactures protocol with a plate reader at 450 nm to determine the concentration of Eotaxin-2 in the media supernatant (Molecular Devices).

2.2.12 Statistical Analysis

Statistics were performed with GraphPad Prism 8 software (GraphPad Software, La Jolla, CA). Results are expressed as means of three to four HBEC trans-well filters from the same patient sample. For RT-qPCR, each trans-well (three to four replicates) was ran in duplicate before calculating the fold change and conducting the statistical analysis. For immunoblots, cell lysates were run in duplicate or triplicate and expression was quantified using densitometry (Image Studio). Statistical significance was determined using Student's T-test or 2-way ANOVA/3-way ANOVA followed by Bonferroni's multiple comparisons test based on the number of independent and dependent variables compared in each experiment ($p<0.05$ was considered significant). For the 3-way ANOVA used to look at gene expression from HBECs (Fig. 3, 6), a Brown-Forsythe test conducted in the GraphPad Prism 8 software was used to test for equal variance (Fig. 30-32). The Brown-Forsythe test showed significant differences in variance for several groups. This finding indicates a Tukey post-hoc test could not be used. Thus, a Bonferroni's multiple comparison test was used as a post-hoc test after 3-way ANOVA to analyze the three effects studied: CF, IL13 and RAGE inhibitor.

Power analyses were conducted in Minitab (Trialware, State College, PA) to determine if there was adequate statistical power for the *RAGE* expression analysis (Fig. 2, 29 A), and to determine the sample size required for future RAGE inhibition experiments looking at phosphorylation of STAT6 (Fig. 9, 29 B). The biological difference used in the power analysis for

RAGE expression was determined to be a 50% difference in RAGE expression or a difference of .5-fold change normalized to *GAPDH*. For determining the sample size for RAGE inhibition experiments looking at pSTAT6, the biological difference was obtained from dsiRNA experiments, where a change of approximately 350-fold change of pSTAT6 normalized to β-Actin was found to be significant when RAGE expression was blocked using dsiRNA during rIL-13 treatment (Fig. 10). For all figures and analyses, N is defined as the number of total samples, whereas n is defined as the number of samples in a particular treatment or conditional group.

2.3 Results

2.3.1 RAGE expression in CF vs. Non-CF HBECs

RAGE mRNA and full-length protein are elevated in CF patient sputum, and a SNP found in the promoter region of *RAGE* (-429T/C) in CF patients leads to increased expression of RAGE *in vitro* [228,293]. This led to the hypothesis that CF HBECs may have increased *RAGE* expression compared to Non-CF HBECs. Using RT-qPCR, RAGE expression was analyzed in six different Non-CF and CF HBEC cultures. *RAGE* expression in primary CF HBECs is similar to Non-CF controls (Fig. 2). However, it was unknown if any of these samples contained the SNP found in the promoter region of *RAGE* associated with increased expression. *RAGE* expression also did not appear to be dependent on the CFTR mutation class or prior disease state of the Non-CF HBECs (Appendix table 1).

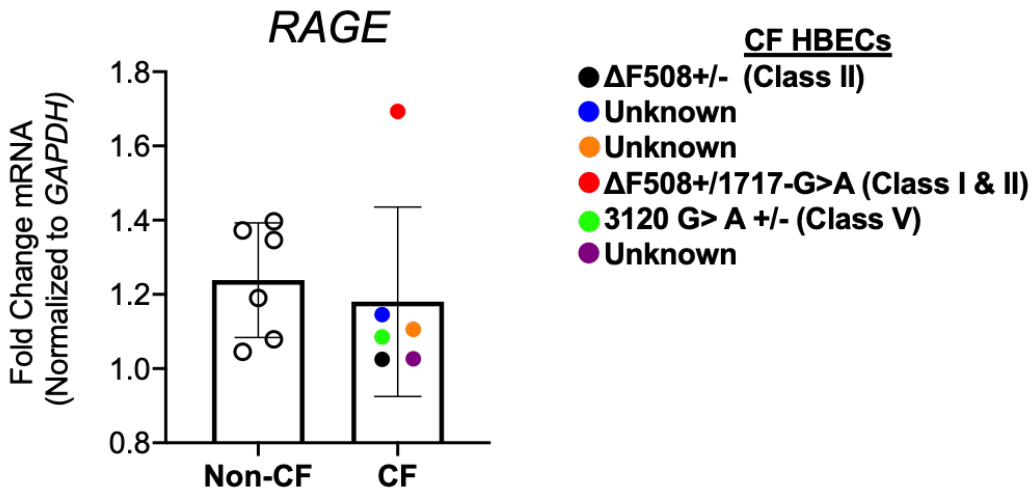

Figure 2: *RAGE* expression in differentiated HBECs

Fold change of *RAGE* expression was normalized to expression of *GAPDH* in Non-CF (n=6) and CF HBECs (n=6) using the ΔΔCt method. Colors represent the specific CFTR mutation(s) of the CF HBEC sample labeled in the figure, if known. Results for each HBEC sample are expressed as means of three to four replicates from the same patient. Statistical significance was determined using an Unpaired Student's T-test, $p<0.05$ was considered significant, N=12, n=6.

2.3.2 Pharmacological inhibition of RAGE blocks mucus production and CF HBEC hyperplasia

Prior studies have shown RAGE regulates the effects of IL-13, which induces mucin gene expression in mice and in primary HBECs [112,114,138]. While RAGE expression was not found to be elevated in CF HBECs, CF patients have increased levels of mucus and type-2 proinflammatory cytokine IL-13 [37,288]. To understand the role of RAGE in IL-13 induced mucus production in CF, Non-CF and CF HBECs were stimulated with recombinant human IL-13 (rIL-13) for 48 and 96 hours (Fig. 3 A).

Stimulation with rIL-13 significantly increased expression of *MUC5AC* at both 48 and 96 hours. In several cases, CF HBECs were hyperresponsive to rIL-13 stimulation compared to Non-CF HBECs (Fig. 3 B, D). In order to see if RAGE regulates rIL-13 induced mucus production, the small molecule inhibitor of RAGE, FPS-ZM1, was used to block the receptor's ligand binding V-domain [296]. Treatment with FPS-ZM1 before rIL-13 stimulation significantly decreased expression of *MUC5AC* at both 48 and 96 hours in CF HBECs (Fig. 3 B-E). This suggests RAGE plays a significant role in mucin gene expression in CF HBECs and RAGE inhibition blocks their excessive response to IL-13 stimulation.

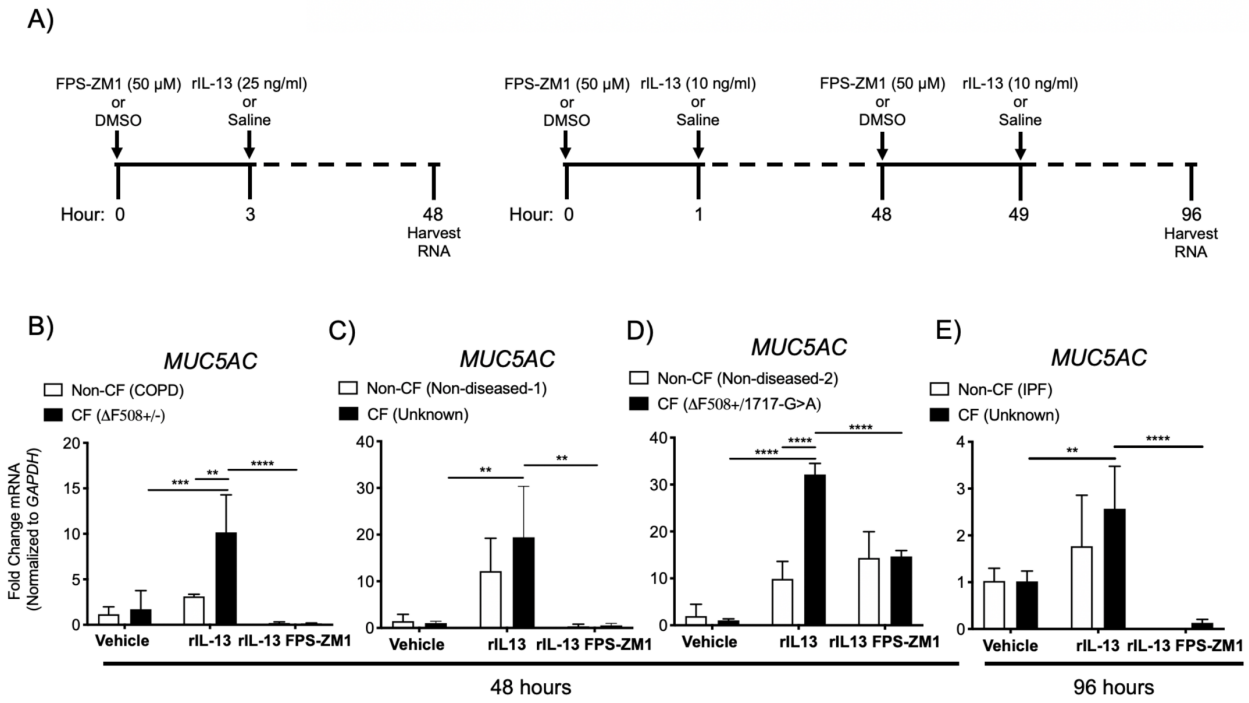

Figure 3: Mucin gene expression in differentiated HBECs

Fold change *MUC5AC* expression was normalized to the expression of GAPDH in Non-CF (n=4) and CF HBECs (n=4) 48 or 96 hours post the first treatment. HBECs were treated with FPS-ZM1 dissolved in DMSO (50 μM in basolateral media) or DMSO as the vehicle control. One to three hours later, HBECs were stimulated with rIL-13 dissolved in saline (10 or 25 ng/ml in basolateral media) or saline as the vehicle control. At the 48-hour time point, RNA was harvested (A, B-D) or HBECs were re-stimulated with FPS-ZM1 and rIL-13 and later harvested at the 96-hour time point (A, E). Results for each HBEC sample are expressed as means of three to four replicates per one patient. Statistical significance was determined using a 3-way ANOVA, followed by Bonferroni's Multiple Comparisons test, $p<0.05$ was considered significant, N=8, n=4. $p<0.0332$ (*), 0.0021 (**), 0.0002 (***), 0.0001 (****).

Mucus production was further assessed using Periodic-Acid Schiff (PAS) and immunofluorescent (IF) staining of Non-CF and CF HBEC cross-sections. HBEC cultures were first washed with PBS to eliminate any mucus present on the apical surface before conducting the 96-hour treatment schedule (Fig. 3 A). Under control conditions, PAS staining revealed CF

HBECs produced dehydrated mucus whereas Non-CF HBECs had minimal apical mucus secretions (Fig. 4 A, D). After rIL-13 stimulation, Non-CF HBECs produced a significant amount of mucus compared to the control (Fig. 4 B). Though unlike the Non-CF cells, CF HBECs displayed a proliferative response to rIL-13 treatment developing gland like structures above the apical surface (Fig. 4 E). Indeed, prior studies have found IL-13 induces proliferation in both mouse and human primary airway cells [298,299]. Mucous hyperplasia in CF HBECs was quantified by the percentage of PAS+ cells and cells present above the apical surface (Fig. 4 G, H). Subsequent RAGE inhibition with FPS-ZM1 blocked the increase of PAS+ cells in the CF HBECs (Fig. 4 E-H), indicating RAGE also mediates CF mucous hyperplasia.

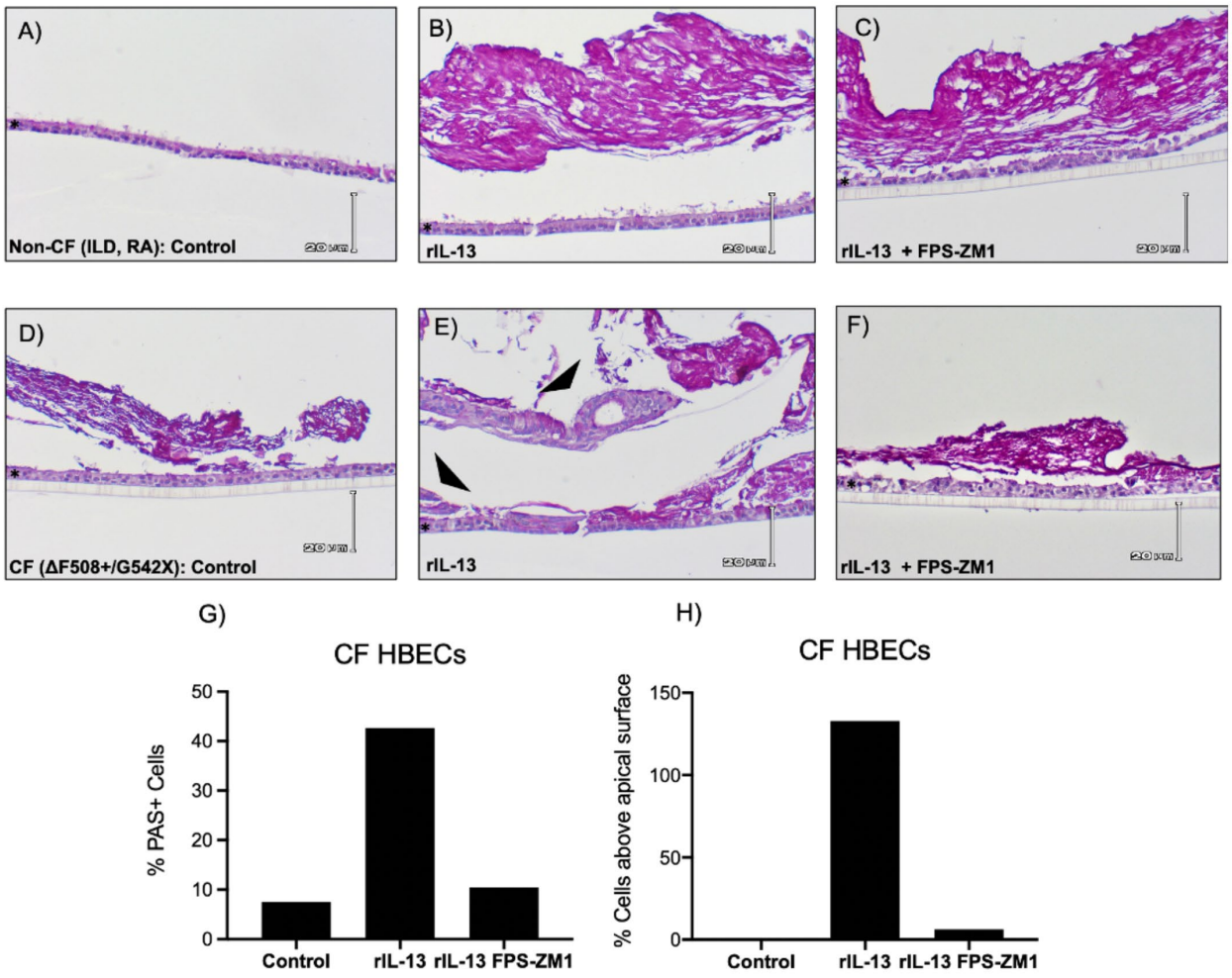

Figure 4: PAS stains of differentiated HBECs

PAS stains of Non-CF and CF HBECs cross-sections during control conditions (A,D) rIL-13 stimulation (10 ng/ml) (B,E) and RAGE inhibition with FPS-ZM1 (50 μM in basolateral media) (C,F). Mucins stain in dark magenta and black arrows indicate mucous hyperplasia (E). Prior disease states of the Non-CF HBECs were interstitial lung disease (ILD) and rheumatoid arthritis (RA) (A). CFTR mutations for the CF HBECs were of class I (G542X) and II (ΔF508+) (D). The percentages of PAS+ cells (G) and cells above the apical surface (H) in CF HBECs were quantified by diving the total amount of PAS+ cells or total amount of cells above the apical surface by the total amount cells from each individual image shown in D-F. These percentages were then graphed using GraphPad. Images were taken at 200X magnification. Scale bars = 20 μm. N=2, n=1.

RAGE, MUC5AC and nuclei (DAPI) were then stained in the same Non-CF and CF HBECs cross sections under control conditions or rIL-13 stimulation with or without RAGE inhibition (Fig. 5). Images were taken separately of Non-CF and CF HBECs using fluorescence microscopy before merging DAPI, RAGE and MUC5AC images, respectively (Fig. 26, 27). In control conditions, RAGE was found to be expressed in the apical surface of the cells and within the mucus on CF HBECs (Fig. 5 A, D). This is supported by previous studies finding RAGE mRNA and protein levels are elevated in CF patients' sputum when compared to Non-CF controls [228]. Upon rIL-13 stimulation, MUC5AC expression increased in Non-CF HBECs (Fig. 5 B). Nuclear staining of CF HBECs shows an increase in cell number during rIL-13 treatment with cells forming gland like structures that express RAGE (Fig. 5 E). RAGE inhibition eliminated the presence of these structures in the CF HBECs and decreased MUC5AC staining in the Non-CF HBECs (Fig. 5 C, F). Together, these images show RAGE is expressed within the apical surface of the bronchial epithelium, is present within mucus secretions, and may play a role in inducing mucous hyperplasia in CF HBECs.

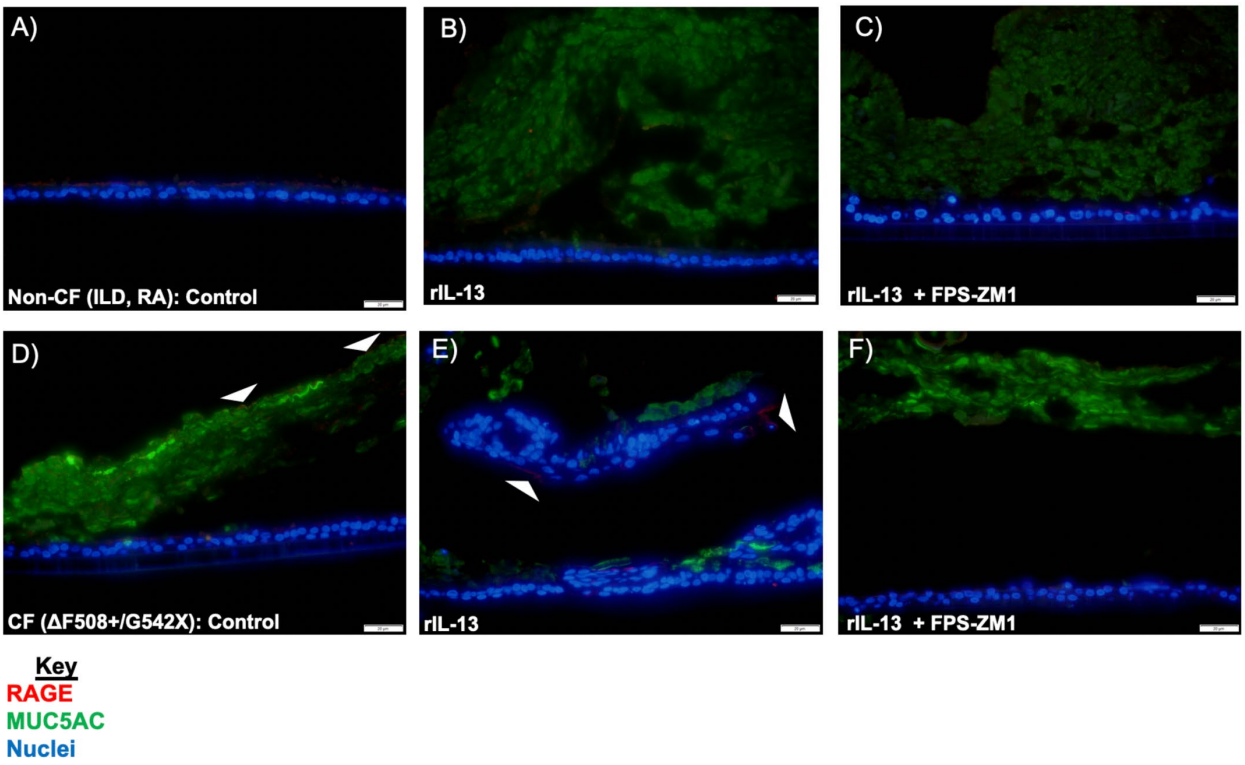

Figure 5: IF images of differentiated HBECs

IF images of Non-CF and CF HBECs cross-sections during control conditions (A,D) rIL-13 stimulation (10 ng/ml) (B,E) and RAGE inhibition with FPS-ZM1 (50 μM in basolateral media) (C,F). Primary antibodies used to target RAGE (red) and MUC5AC (green) were diluted at 1:100 ratio. Secondary antibodies, goat anti-rabbit IgG (546 nm) and goat anti-mouse IgG1 (488 nm) were dissolved in PBS at a 1:500 ratio. Nuclei were stained using DAPI (2.5 μg/ml). White arrows indicate RAGE expression in mucus and in cell structures formed in CF HBECs after rIL-13 stimulation. Prior disease states of the Non-CF HBECs were interstitial lung disease (ILD) and rheumatoid arthritis (RA) (A). CFTR mutations for the CF HBECs were of class I (G542X) and II (ΔF508+) (D). Images were taken at 200X magnification. Scale bars = 20 μm. N=2, n=1.

2.3.3 RAGE regulates expression of mucous metaplasia transcription factors

IL-13 induced mucous hyperplasia and metaplasia are regulated by secreted factors and transcription factors (TFs). The induction of mucous metaplasia begins by secretion of CLCA1

from the cell, which leads to activation of MAP kinase [292]. MAP kinase then activates expression of TFs SPDEF and FOXA3, which both positively regulate mucous hyperplasia and metaplasia in mice exposed to IL-13 [173,300–302]. In order to understand how RAGE regulates the increase of PAS+ cells seen in CF HBECs in response to rIL-13 (Fig. 4 E), RT-qPCR was used to analyze the expression of genes regulating mucous metaplasia during rIL-13 treatment and RAGE inhibition. This included the expression of upstream signaling protein *CLCA1* and the TFs *SPDEF* and *FOXA3* (Fig. 6).

For Non-CF HBECs, only *SPDEF* and *FOXA3* were upregulated during rIL-13 treatment (Fig. 6 A-C). When RAGE was inhibited during rIL-13 stimulation, expression of these TFs was significantly diminished. In only one experiment did Non-CF HBECs have significantly greater expression of *SPDEF* compared to CF HBECs during rIL-13 treatment (Fig. 6 B). In contrast, rIL-13 significantly upregulated *CLCA1* and *FOXA3* in CF HBECs when compared to Non-CF HBECs (Fig. 6 A-C). Whether Non-CF or CF, when expression of these factors was upregulated during rIL-13 treatment, RAGE inhibition with FPS-ZM1 was able to significantly down regulate their expression. These results support our previous finding that rIL-13 induces an increase in PAS+ cells in CF HBECs (Fig. 4 F, G) and begin to uncover how RAGE may regulate mucous hyperplasia through the activation of TF expression. This led us to further investigate other factors RAGE may regulate during rIL-13 treatment in CF HBECs.

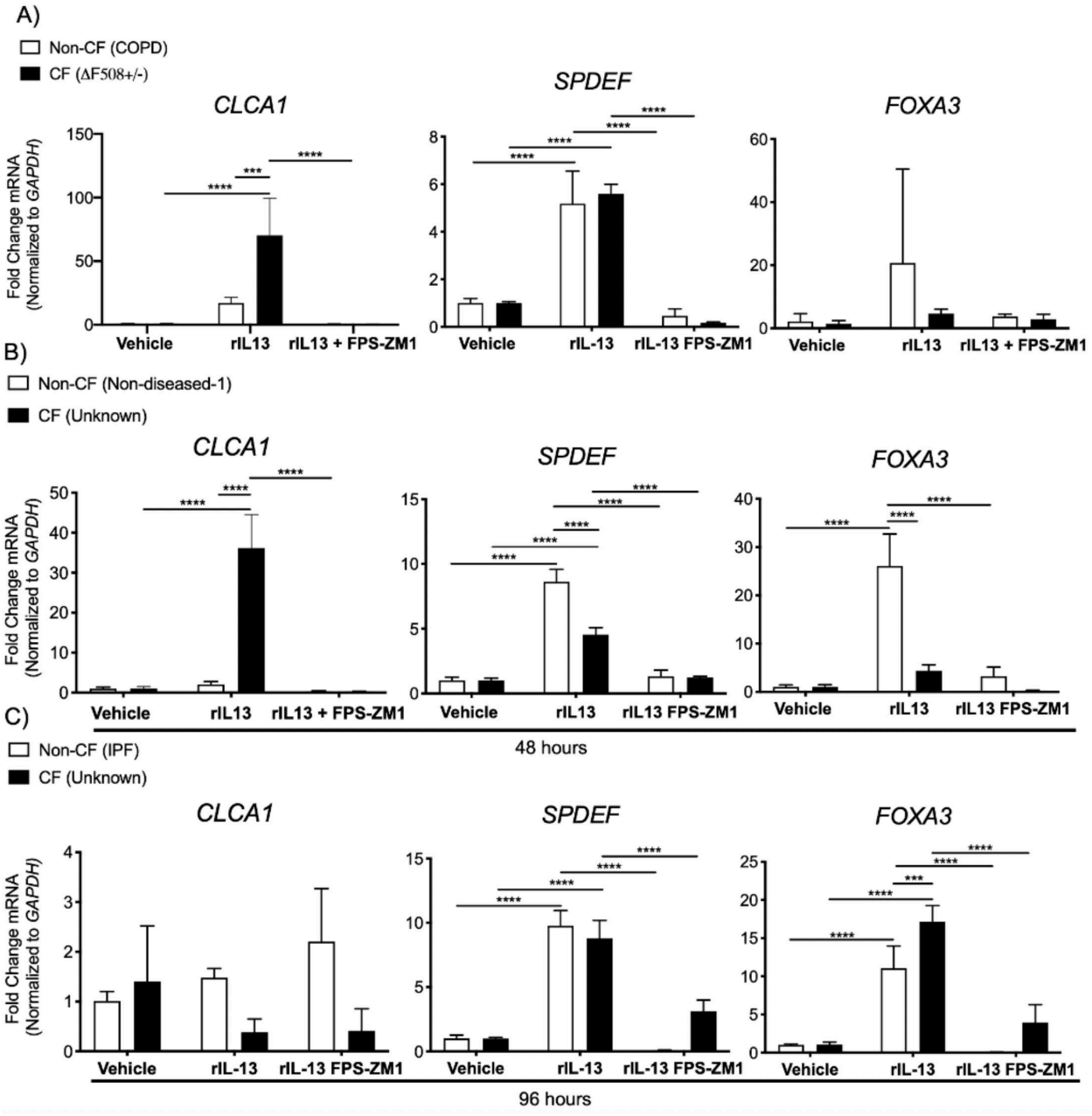

Figure 6: Expression of TFs regulating mucous metaplasia in differentiated HBECs

Fold change of *CLCA1*, *SPDEF* and *FOXA3* expression was normalized to the expression of *GAPDH* in Non-CF (n=3 patients) and CF HBECs (n=3 patients) 48 (A, B) or 96 hours (C) post the first treatment (see Fig. 2A). HBECs were treated with FPS-ZM1 dissolved in DMSO (50 μM in basolateral media) or DMSO as the vehicle control. One hour later, HBECs were stimulated with rIL-13 dissolved in saline (10 or 25 ng/ml in basolateral media) or saline as the vehicle control. At the 48-hour time point, RNA was harvested or HBECs were re-stimulated with FPS-ZM1 and rIL-13 and later harvested at the 96-hour time point. Results for each HBEC sample are expressed as means of three to

four replicates. Statistical significance was determined using a 3-way ANOVA, followed by Bonferroni's Multiple Comparisons test, $p<0.05$ was considered significant, N=6, n=3. $p<0.0332$ (*), 0.0021 (**), 0.0002 (***), 0.0001 (****).

2.3.4 Inhibition of RAGE reduces production of an eosinophil chemoattractant

Signaling of IL-13 is not limited to the induction of mucus production and metaplasia. In models of asthma using allergens or IL-13 as a surrogate, bronchial epithelial cells respond by secreting high amounts of eotaxin-2 (CCL24) in the airway in response to IL-13 [233,291,303]. Prior studies show that RAGE inhibition with FPS-ZM1 significantly reduces levels of eotaxin-2 in mice and primary human airway cells treated with IL-13 [112]. This chemoattractant recruits eosinophils into the lung, where they play a role in allergic inflammation by releasing reactive oxygen species (ROS) and inducing mucus production through release of IL-13 within the airways [304–306]. Intriguingly, CF patients have elevated levels of eosinophils and IL-13 within the airways during *Pseudomonas aeruginosa* infection or when compared to non-diseased control patients [36,37,90,307].

ELISA was used to detect eotaxin-2 production in the extracellular media supernatants of Non-CF and CF HBECs treated with FPS-ZM1 and rIL-13. In response to rIL-13 treatment, Non-CF and CF HBECs secreted eotaxin-2 into the extracellular media (Fig. 7). Notably, both CF patient samples secreted higher levels of the chemoattractant than either Non-CF sample (Fig. 7 B, D). When RAGE was inhibited during rIL-13 treatment, Non-CF HBECs significantly reduced their production of eotaxin-2. In contrast, only one CF sample showed reduced eotaxin-2 production during RAGE inhibition (Fig. 7 B). This shows RAGE regulates other IL-13 mediated eotaxin-2 production in the bronchial epithelium in addition to mucus production and hyperplasia.

These data again suggest CF HBECs are more responsive to rIL-13 treatment, enabling their ability to maintain secretion of eotaxin-2 during RAGE inhibition.

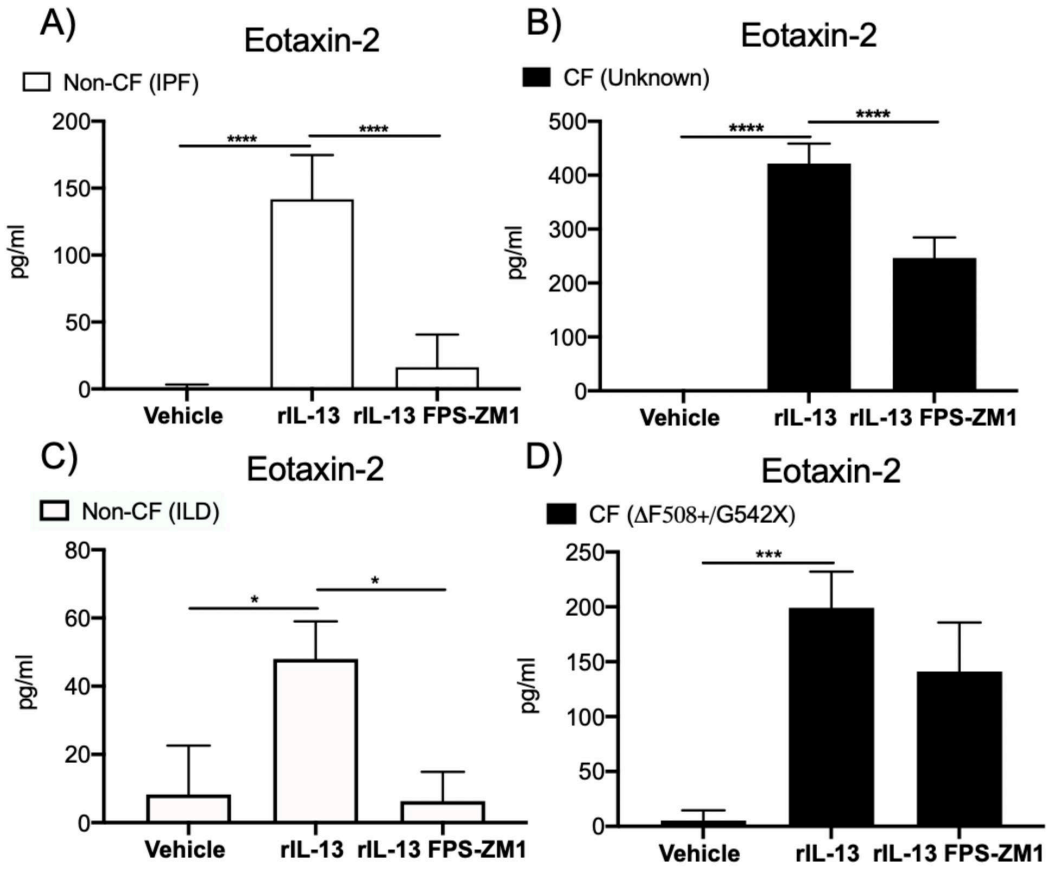

Figure 7: Eotaxin-2 production in differentiated HBECs

ELISA analysis of media supernatants from Non-CF (A, C) and CF (B, D) HBECs at 96 hours (N=4). HBECs were treated with FPS-ZM1 dissolved in DMSO (50 μM in basolateral media) or DMSO as the vehicle control. One hour later, HBECs were stimulated with rIL-13 dissolved in saline (10 ng/ml in basolateral media) or saline as the vehicle control. At the 48-hour time point, cells were again treated with FPS-ZM1 and rIL-13. Media supernatants were then harvested at the 96-hour time point. Results for each HBEC sample are expressed as means of four replicates. Statistical significance was determined using a 2-way ANOVA, followed by Bonferroni's Multiple Comparisons test, $p<0.05$ was considered significant, N=4, n=3. $p<0.0332$ (*), 0.0021 (**), 0.0002 (***), 0.0001 (****).

2.3.5 Inhibition of RAGE reduces STAT6 phosphorylation

To determine the signaling pathway involved in RAGE mediated mucus production, activation of the transcription factor (TF) known as the signal transducer and activator of transcription-6 (STAT6) was evaluated in Non-CF and CF HBECs. Activation via phosphorylation of STAT6 leads to the expression of *MUC5AC*, mucous metaplasia TFs and eotaxin-2 in models of type-2 airway inflammation [112,138,303]. Prior to activation of STAT6, IL-13 binds to the IL-13Rα1 and IL-4Rα receptor complex leading to phosphorylation and Jak kinase activation. Jak kinase then phosphorylates STAT6, which enters the nucleus to induce the expression of its downstream targets including *SPDEF*, *FOXA3*, *MUC5AC* and *CCL24* (eotaxin-2) [173,292,303] (Fig. 8). To understand if RAGE regulates phosphorylation of STAT6, Non-CF and CF HBECs were treated with rIL-13 or rIL-13 with the RAGE inhibitor FPS-ZM1 and whole cell lysates were harvested at 96 hours (Fig. 3 A).

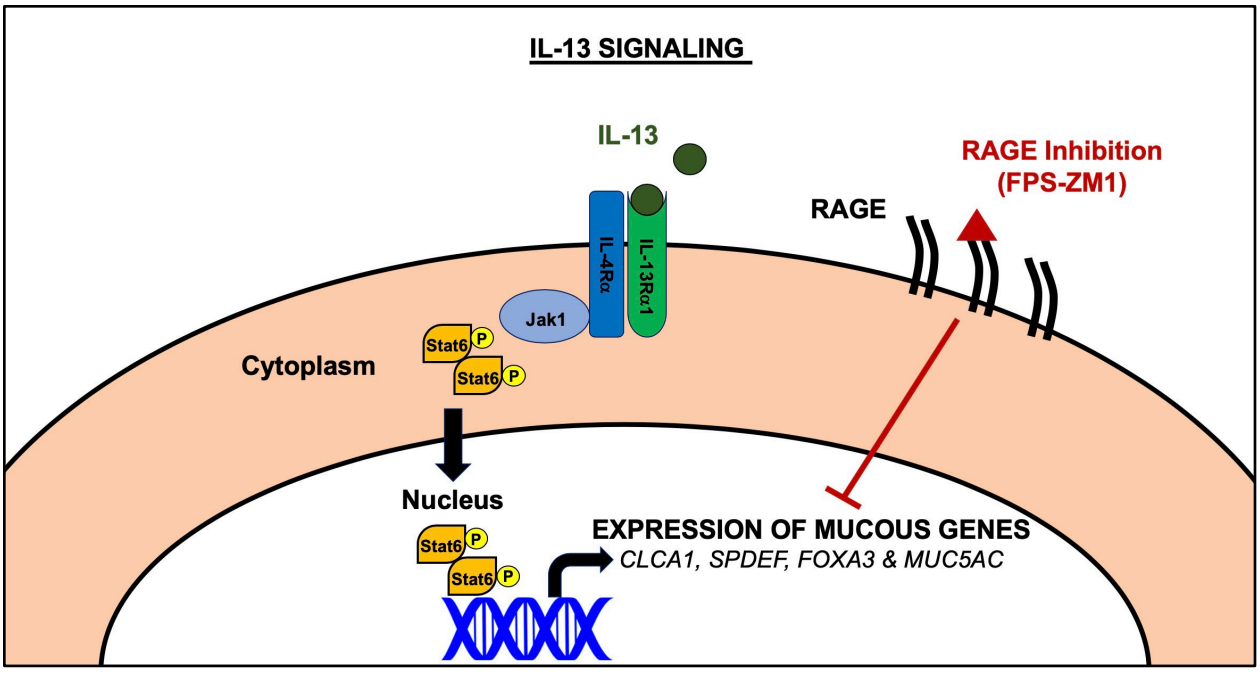

Figure 8: IL-13 signaling pathway

IL-13 binds to the IL-13Rα1 and IL-4Rα receptor complex leading to phosphorylation and Jak kinase activation. Jak kinase then phosphorylates STAT6, which enters the nucleus to induce the expression of its downstream targets. FPS-ZM1 acts on RAGE and inhibits intracellular signaling, affecting STAT6 responsive gene expression.

While there was STAT6 total protein in the vehicle control samples, no phospho-STAT6 (pSTAT6) was detected in Non-CF and CF HBECs controls (Fig. 9 A). Upon treatment with rIL-13, pSTAT6 was induced in Non-CF and CF HBECs. Using β-actin as a loading control, pSTAT6 was then quantified in all three conditions (Fig. 9 B, C). Treatment with rIL-13 and the RAGE inhibitor, FPS-ZM1, results in a trend of reduced pSTAT6 in CF HBECs (Fig. 9 C). Conversely, no noticeable difference in pSTAT6 was seen in the Non-CF samples treated with rIL-13 and FPS-ZM1 (Fig. 9 B). These results begin to suggest RAGE regulates mucus production, mucous metaplasia TFs and eotaxin-2 production in CF HBECs through phosphorylation and activation of STAT6. Several mouse studies modeling type-2 airway inflammation have showed STAT6 plays a key role in IL-13 induced mucus production and airway inflammation [88,89,294]. As well, a

prior study shows wildtype mice have sustained activation of STAT6 when compared to RAGE-/- mice treated with intranasal rIL-13 [112].

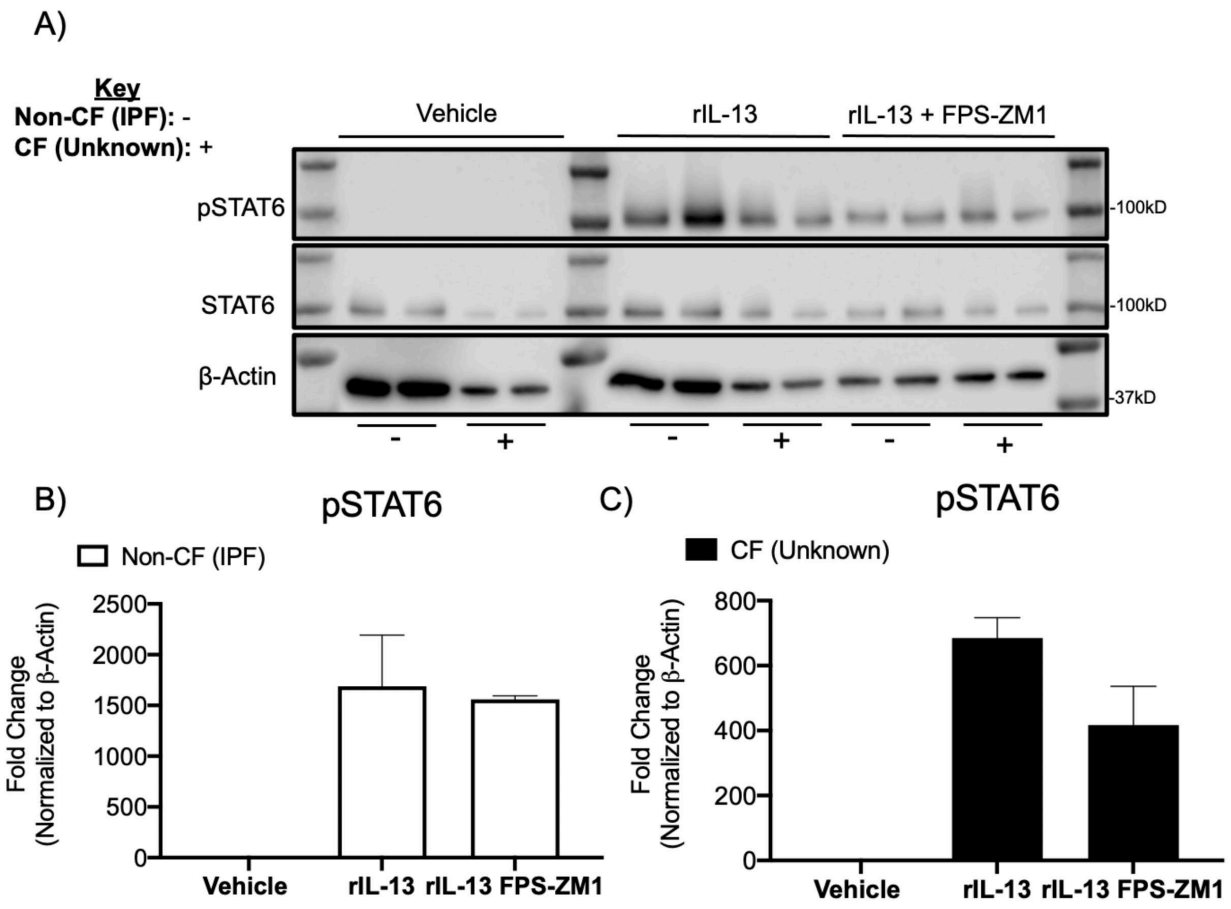

Figure 9: STAT6 phosphorylation in differentiated HBECs

Differentiated Non-CF and CF HBECs were treated with FPS-ZM1 dissolved in DMSO (50 μM in basolateral media) or DMSO as the vehicle control. One hour later, HBECs were stimulated with rIL-13 dissolved in saline (10 ng/ml in basolateral media) or saline as the vehicle control. At the 48-hour time point, cells were re-stimulated with FPS-ZM1 and rIL-13. Cell lysates were then harvested at the 96-hour time point using phosphatase inhibitors to observe activation of STAT6. Gel electrophoresis and immunoblot were then conducted using primary antibodies for pSTAT6, STAT6 and β-Actin (A). Error bars represent the maximum value from the two replicate cell lysates per condition in the western blot. Densitometry was used to calculate the fold change for pSTAT6 normalized to β-Actin (B, C). Results for each condition are expressed as means of two replicates. N=2, n=1.

2.3.6 Knock-down of RAGE expression reduces STAT6 phosphorylation

To further interrogate the role of RAGE in phosphorylation of STAT6, dicer substrate interfering RNA (dsiRNA) was used to genetically knock-down RAGE expression in undifferentiated primary HBECs. dsiRNA constructs were chosen to post transcriptionally silence RAGE expression due to their enhanced integration with the RNA induced silencing complex (RISC) and knock-down compared to traditional siRNA [308]. In addition, undifferentiated primary HBECs were used over differentiated cultures due to their enhanced transfection efficiency and absence of airway secretions that inhibit transfection of oligonucleotides [297]. Both Non-CF and CF primary cells were transfected with a non-targeted control dsiRNA (dsiCON) or a pool of three dsiRNA constructs to knock-down RAGE expression (dsiRAGE). Subsequently, these cells were treated with rIL-13 and cell lysates were harvested to see the effect of RAGE knock-down on phosphorylation of STAT6 (Fig. 10 A).

Expression of *RAGE* was significantly downregulated in undifferentiated primary Non-CF HBECs when transfected with the pooled dsiRAGE constructs in undifferentiated primary Non-CF HBECs (Fig. 10 B). These results were further confirmed by looking at RAGE protein abundance after transfection with dsiRAGE (Fig. 10 C, F). Quantification of RAGE protein abundance was normalized to β-Actin using densitometry and showed RAGE was significantly decreased in both Non-CF and CF HBECs using dsiRAGE (Fig. 10 D, G). To understand how loss of RAGE would affect phosphorylation of STAT6 in CF HBECs, dsiRNA transfected cells were treated with rIL-13 (Fig. 10 A). While rIL-13 induced phosphorylation of STAT6 in both Non-CF and CF dsiCON transfected cells, only CF HBECs treated with rIL-13 had significantly less pSTAT6 when RAGE protein was depleted (Fig. 10 E, H). These results support the previous finding that RAGE may regulate phosphorylation of STAT6 primarily in CF HBECs, which leads

to the induction of mucin gene expression, mucous hyperplasia and eotaxin-2 production (Fig. 9 C) [292,303].

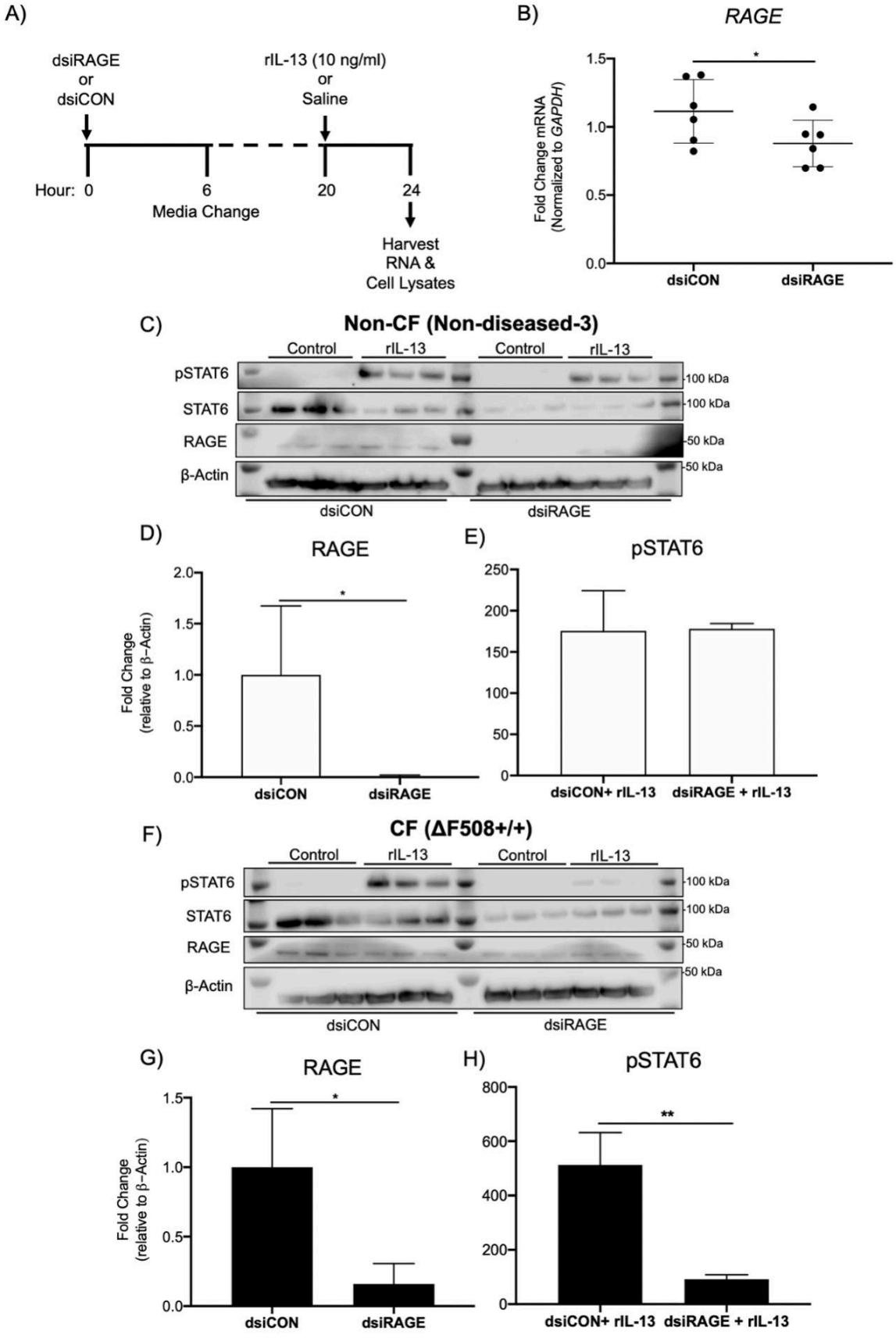
A)
dsiRAGE
or
dsiCON
rIL-13 (10 ng/ml)
or
Saline
Hour: 0
6
Media Change
20
24
Harvest
RNA &
Cell Lysates
B)
RAGE
Fold Change mRNA
(Normalized to GAPDH)
1.5
1.0
0.5
0.0
*
dsiCON
dsiRAGE
C)
Non-CF (Non-diseased-3)
Control
rIL-13
Control
rIL-13
pSTAT6
STAT6
RAGE
β-Actin
100 kDa
100 kDa
50 kDa
50 kDa
dsiCON
dsiRAGE
D)
RAGE
Fold Change
(relative to β−Actin)
2.0
1.5
1.0
0.5
0.0
*
dsiCON
dsiRAGE
E)
pSTAT6
250
200
150
100
50
0
dsiCON+ rIL-13
dsiRAGE + rIL-13
F)
CF (ΔF508+/+)
Control
rIL-13
Control
rIL-13
pSTAT6
STAT6
RAGE
β-Actin
100 kDa
100 kDa
50 kDa
50 kDa
dsiCON
dsiRAGE
G)
RAGE
Fold Change
(relative to β−Actin)
1.5
1.0
0.5
0.0
*
dsiCON
dsiRAGE
H)
pSTAT6
800
600
400
200
0
**
dsiCON+ rIL-13
dsiRAGE + rIL-13

Figure 10: dsiRNA knock-down of RAGE expression in undifferentiated HBECs

Undifferentiated primary Non-CF and CF HBECs were first transfected with either a non-targeted dsiRNA (dsiCON, 100 nM) construct or a pool of three dsiRNA constructs targeted to RAGE expression (dsiRAGE, 100 nM). Transfection was carried out using RNAiMax in antibiotic free media for six hours, after which the media was changed (A). Cells were then treated with rIL-13 dissolved in saline (10 ng/ml in media) or saline as the vehicle control for four hours before RNA or cell lysates were harvested at 24 hours (A). RAGE mRNA expression analysis was conducted at this time point using RT-qPCR in non-diseased Non-CF HBECs and means represent six replicates (B). Cell lysates from Non-CF and CF HBECs were subjected to gel electrophoresis and immuno-blotting to detect protein abundance of RAGE, STAT6, pSTAT6 and β-Actin (C, F). Fold change expression of RAGE and pSTAT6 for Non-CF (white, D, E) and CF HBECs (black, G, H) were calculated using Image Studio densitometry software and means represent three replicates for each culture condition. Error bars represent the standard deviation from the three replicate cell lysates per condition in the western blot. Statistical significance was determined using an Unpaired Student's T-test, $p<0.05$ was considered significant, N=2. $p<0.0332$ (*), 0.0021 (**), 0.0002 (***), 0.0001 (****).

2.3.7 RAGE-/- mice have reduced mucus production in response to exotoxin derived from *P. aeruginosa*

Since it is known RAGE modulates the effects of type-2 cytokines in the airway and a SNP in *RAGE* is associated with lung function indices (FEV_1%) in patients with CF, it was hypothesized RAGE may regulate type-2 airway inflammation in response to exotoxin derived from *P. aeruginosa* [112,114,293]. In order to test this hypothesis, WT and RAGE-/- mice were treated with intranasal exotoxin, the primary immunogenic antigen present on *P. aeruginosa.* The bronchoalveolar lavage fluid (BALF) and lungs from these animals were analyzed for several markers of type-2 airway inflammation to determine if RAGE plays a role in exotoxin induced inflammation.

Control treated WT or RAGE-/- animals did not have a significant induction in mucus production or airway inflammation using PAS staining of whole lung sections (Fig. 11 A-H). Exotoxin treatment caused a significant increase in the percentage of PAS+ airways in WT animals, indicating mucus production (Fig. 11 Q). In several animals, there were significant signs of type-2 airway inflammation including large accumulations of mucus in the airway (Fig. 11 I), mucous hyperplasia (Fig. 11 J) and even bronchiolitis obliterans in one animal (Fig. 11 L). There were no PAS+ airways in the lungs of any RAGE-/- mice treated with exotoxin (Fig. 11 M-P, Q). Intriguingly, prior studies using exotoxin to induce airway inflammation found similar results in STAT6-/- mice. Even after intranasal treatment with exotoxin for three weeks, they found no airway inflammation in these animals [88]. These results support our findings in CF HBECs that RAGE contributes to the regulation of mucus production and the expression of mucus metaplasia TFs through activation of STAT6 (Fig. 9, 10).

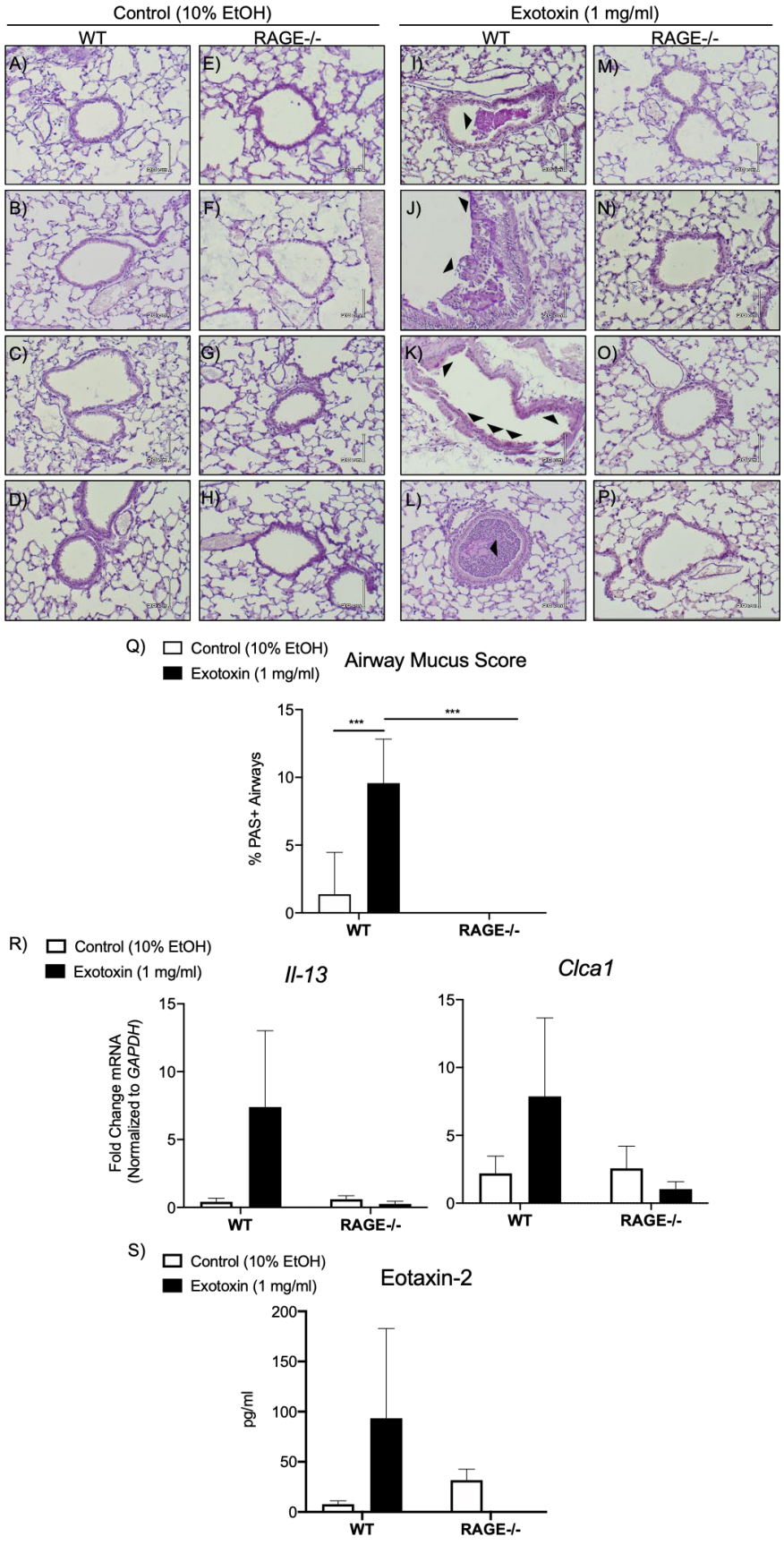
Control (10% EtOH)
Exotoxin (1 mg/ml)
WT
RAGE-/-
WT
RAGE-/-
A)
B)
C)
D)
E)
F)
G)
H)
I)
J)
K)
L)
M)
N)
O)
P)
Q)
Control (10% EtOH)
Exotoxin (1 mg/ml)
Airway Mucus Score
% PAS+ Airways
15
10
5
0
***
***
WT
RAGE-/-
R)
Control (10% EtOH)
Exotoxin (1 mg/ml)
Il-13
Clca1
Fold Change mRNA (Normalized to GAPDH)
15
10
5
0
WT
RAGE-/-
15
10
5
0
WT
RAGE-/-
S)
Control (10% EtOH)
Exotoxin (1 mg/ml)
Eotaxin-2
pg/ml
200
150
100
50
0
WT
RAGE-/-

Figure 11: Exotoxin treated WT and RAGE-/- mice

Control WT and RAGE-/- animals were treated with 10% EtOH intranasally as the vehicle control following the same treatment schedule (N=20, n=5). Whole lung sections were then fixed and embedded in paraffin for PAS staining to detect inflammation and mucus production in the airways (A-P). Each image is from one animals and black arrows indicate sites of PAS positivity in the animals (dark magenta) (I-L). An airway mucus score was then developed by calculating the percentage of PAS+ airways in each animal per the total amount of airways in each section (Q). Whole lung homogenates were collected to obtain RNA and subjected to RT-qPCR analysis to detect expression of *Il-13* and *Clca1* (R). The BALF from these animals was also collected to detect eotaxin-2 accumulation in the airways (S). Results for each treatment group are expressed as means of five animals. Statistical significance was determined using a 2-way ANOVA, followed by Bonnferoni's Multiple Comparisons test, $p<0.05$ was considered significant, N=20, n=5. $p<0.0332$ (*), 0.0021 (**), 0.0002 (***), 0.0001 (****).

Since *P. aeruginosa* infection is associated with elevated levels of IL-13 in the airways of CF patients, whole lung RNA was obtained to assess *Il-13* expression in WT and RAGE-/- mice treated with exotoxin [36,37]. While *Il-13* expression trended to increase in WT mice treated with exotoxin, RAGE-/- mice had no elevated expression of the proinflammatory cytokine (Fig. 11 R). Downstream, IL-13 signaling leads to expression of *Clca1,* a critical factor for the expression of mucus metaplasia TFs [292]. There was a similar trend of increased *Clca1* expression in WT mice treated with exotoxin, though this was not found in RAGE-/- mice (Fig. 11 R). To further characterize the degree of airway inflammation in response to exotoxin, levels of the innate immune cell chemoattractant eoxtain-2 were analyzed in the BALF of WT and RAGE-/- mice treated with exotoxin. Eotaxin-2 production is induced by IL-13 signaling through activation of STAT6 [303]. There was no increase in eotaxin-2 production in the airways of RAGE-/- mice treated with exotoxin (Fig. 11 S). Combined, these results suggest RAGE may play a role in inducing the type-2 inflammatory response during *P. aeruginosa* infection.

2.4 Discussion

In CF patients, RAGE mRNA and protein are elevated in the sputum when compared to Non-CF patients, and a SNP in RAGE is associated with decreased FEV1% predicted in CF patients [228,293]. Concomitantly, levels of type-2 proinflammatory cytokines IL-5 and IL-13 are elevated in CF patient airways and during *P. aeruginosa* infection [36,37]. This increases mucus production and airway inflammation in CF patients, which contributes to declining lung function over time [288,290,309]. While RAGE is known to regulate key steps of type-2 airway inflammation and is associated with CF, studies investigating how RAGE regulates this immunity in models of CF have not been conducted [112,114]. In this study, Non-CF and CF human bronchial epithelial cells (HBECs) were used to address how RAGE regulates the direct effects of the type-2 immune response using recombinant human IL-13 (rIL-13). In addition, we address if RAGE regulates type-2 immunity *in vivo* in response to *P. aeruginosa* derived exotoxin using WT and RAGE-/- mice.

Based on our prior studies showing internasal treatment with IL-13 does not lead to mucus production in the airways of RAGE-/- mice, this study hypothesized RAGE may regulate the direct effects of IL-13, including mucus production and mucous hyperplasia in the bronchial epithelium. [112]. CF HBECs expressed significantly more *MUC5AC* than Non- CF HBECs and RAGE inhibition blocked this expression (Fig. 3). Concomitantly, PAS staining of HBEC cultures showed CF HBECs were hyperresponsive to rIL-13 treatment compared to Non-CF cells (Fig. 4, 5). While the CF bronchial epithelium is more responsive, there was no significant difference in *RAGE* expression between Non-CF and CF HBECs (Fig. 2).

This suggests while RAGE may not be elevated in CF HBECs, RAGE still contributes to mucin gene expression and mucous hyperplasia during rIL-13 stimulation. However, one CF HBEC sample (7, Appendix Table 1) possessing both severe classes of CFTR mutations (class I and class II) had the highest level of *RAGE* expression (Fig. 2; 1.69-fold change normalized to *GAPDH*) [8]. It would be interesting to investigate CFTR mutation effect on *RAGE* expression, though since there was only an N=1 for the CF sample with both severe classes of CFTR mutations, the specific CFTR class effect on *RAGE* could not be analyzed. With a sample size of only six, it is possible the two-sample Student's T-test was not adequately powered to detect a significant difference between Non-CF and CF HBEC *RAGE* expression. Using a two-sample T-test based power analysis on these data (s=0.2048, α=0.05, n=6 per treatment group, biological difference=0.5-fold change normalized to *GAPDH* or a 50% difference in fold change), the power (1-β) was found to be 0.967 (Fig. 29 A). This indicates that while the sample size was low, the two-sample Student's T-test was adequately powered to correctly reject the null hypothesis if the alternative hypothesis is true. Since the two-sample Student's T-test determined the null hypothesis is true (there is no statistical significance between the two groups), it can be concluded there is no significant difference in *RAGE* expression between Non-CF and CF HBECs.

In addition, this study found RAGE regulates the expression of key factors involved in mucous metaplasia in CF HBECs. CF HBECs significantly expressed more *CLCA1* and *FOXA3* than Non-CF HBECs when treated with rIL-13 (Fig. 6 A-C). CLCA1 is critical for the expression of *FOXA3* and both are activated by the transcription factor STAT6 [173,292]. CF cells also consistently induced expression of *SPDEF* in response to rIL-13, suggesting *SPDEF* plays a key role in the induction of mucus hyperplasia and metaplasia in CF [300,301]. Upon RAGE inhibition, the expression of *CLCA1*, *SPDEF* and *FOXA3* were significantly down regulated. While RAGE

may not be elevated in CF HBECs, these cells are hyperresponsive to effects of rIL-13 through increased activation of *CLCA1* and *FOXA3* in a RAGE dependent manner. Since phosphorylation of STAT6 is upstream from the expression of these factors, it is also possible CF HBECs have sustained activation of STAT6 when compared to Non-CF HBECs [88,112].

CF HBECs also produced more than double the amount of eotaxin-2 compared to Non-CF HBECs when treated with rIL-13 (Fig. 7). Inhibition of RAGE significantly reduced eotaxin-2 production in both Non-CF and CF HBECS, though to a lesser extent in CF HBECs (Fig. 7 B, D). This indicates CF HBECs are more sensitive to IL-13 induced production of eotaxin-2, and that other pattern recognition receptors present in the bronchial epithelium may regulate production of eotaxin-2 alongside RAGE. Indeed, absence of Toll-IL-1 receptor 8 (TIR-8) in mice reduces expression of *Il-13* and *Ccl24* (eotaxin-2) during stimulation with house dust mite (HDM) [310]. Since eotaxin-2 is also regulated by activated STAT6, this study sought to understand how RAGE modulates the expression of mucins, mucous metaplasia TFs and eotaxin-2 by investigating activation of the upstream transcription factor STAT6.

STAT6 is activated via phosphorylation by Jak kinases after IL-13 binds to the IL-13Rα1 and IL-4Rα receptor complex [292]. To interrogate the role of RAGE in phosphorylation of STAT6 in CF HBECs, both pharmacological inhibition and dicer substrate siRNA (dsiRNA) knock-down of RAGE expression were used to block RAGE signaling during rIL-13 treatment (Fig. 9, 10). In Non-CF and CF HBECs, rIL-13 treatment induced phosphorylation of STAT6 (pSTAT6) after 96 hours (Fig. 9 A). While Non-CF HBECs treated with rIL-13 and the RAGE small molecule inhibitor FPS-ZM1 maintained pSTAT6, a trend toward decreased pSTAT6 was seen in CF HBECs treated with rIL-13 and the RAGE inhibitor FPS-ZM1 (Fig. 9 C).

However, a statistical analysis could not be conducted on the decreased fold change of pSTAT6 normalized to β-Actin since there were only two samples per treatment group of CF HBECs. In order to determine how many samples would be required to correctly reject the null hypothesis (i.e. there is no significant difference between rIL-13 treated and rIL-13 with FPS-ZM1 treated CF HBECs), a two-sample T-test based power analysis was used (s=90.95, α=0.05, 1-β=0.85, biological difference=350-fold change normalized to β-Actin) (Fig. 29 B). This analysis found three samples (n=3) per treatment group are needed to correctly reject the null hypothesis and determine if RAGE inhibition with FPS-ZM1 blocks rIL-13 driven phosphorylation of STAT6. Thus, future studies should treat a minimum of three samples of CF HBECs with rIL-13 and rIL-13 with FPS-ZM1.

While this experiment was not adequately powered, it is interesting that Non-CF HBECs maintained rIL-13 driven pSTAT6 even during RAGE inhibition. This further supports the idea that bronchial epithelial cells may be reliant on other receptors than RAGE to activate STAT6 in response to IL-13, such as IL-4Rα or TIR-8 [292,310,311]. However, prior studies have shown Non-CF HBECs do rely on RAGE for activation of STAT6 [112]. This contradiction can be explained in part due to differences in the prior disease states or environments of patients where Non-CF HBEC samples were obtained, which have been shown alter expression of RAGE, its isoforms or other pattern recognition receptors such as Toll-like receptors [228,236,312]. Changes in receptor presence may ultimately affect subsequent downstream signaling, leading to either maintained phosphorylation of STAT6 or a decreased reliance on RAGE signaling for phosphorylation of STAT6.

Phosphorylation of STAT6 was also assessed after confirming dsiRNA knock-down of RAGE expression was significant at the mRNA and protein level (dsiRAGE). Only in CF HBECs

did genetic knock-down of RAGE expression significantly deplete levels of pSTAT6 during rIL-13 treatment (Fig. 10 B, F-H). It is worthwhile to note total STAT6 trended to decrease in response to dsiRAGE treatment (Fig. 10 C, F). However, this was not found to be a significant decrease using an unpaired Students T-test (Fig. 28). As well, in dsiRNA experiments carried out to 48 hours, there was no noticeable trend of decreasing total STAT6 in response to dsiRAGE treatment (Fig. 25 B, C). dsiRNA experiments carried out until 48 hours also show CF HBECs do have sustained activation of STAT6 in response to rIL-13 treatment when compared to Non-CF HBECs (Fig. 25). Together, these results indicate CF HBECs may be more dependent on pSTAT6 than Non-CF HBECs signaling to induce the activation of mucin gene synthesis, mucous metaplasia TFs and eotaxin-2. This could be due to chronic activation of STAT6 since CF patients develop frequent lung infections and have elevated levels of IL-13 in their airways [36,37]. These data further corroborate CF HBECs hyperresponsiveness to rIL-13 treatment.

To better link decreased STAT6 activation in CF HBECs with the effects of rIL-13, including mucin gene expression, expression of mucous metaplasia TFs and production of eotaxin-2, it would be interesting to analyze these effects in CF HBECs treated with RAGE targeted dsiRNA. In this study, undifferentiated primary HBECs were used to enhance transfection efficiency [297]. Though to see how reduced RAGE expression affects mucin gene expression, the expression of mucous metaplasia TFs and the production of eotaxin-2, it would be necessary to knock-down RAGE expression in differentiated HBECs during rIL-13 treatment. This may require viral transduction of short-hairpin RNA (shRNA) to sustain knock-down of RAGE expression during the differentiation of HBEC cultures [92,313].

The role of RAGE in inducing the type-2 immune response was also investigated during treatment with *P. aeruginosa* exotoxin. *P. aeruginosa* infection in CF patients is associated with

pulmonary exacerbations, decreased lung function and elevated levels of type-2 proinflammatory cytokines in the BALF [36,37,90,309]. Prior studies using intratracheal inoculation with *P. aeruginosa* in mice show RAGE-/- animals have reduced airway inflammation and cytokine production in the BALF, though they did not investigate type-2 cytokines or mucus production in these animals [314].

Exotoxin is a tricyclic phenazine present on the *P. aeruginosa* membrane, which is elevated in mucus biofilms and CF patient sputum [88]. When strains of *P. aeruginosa* lack the ability to produce exotoxin, administrations with these species greatly reduces their ability to induce inflammation and pneumonia in the lungs of mice [88,315,316]. Since these and other studies have shown treatment with exotoxin alone in bronchial epithelial cells and in mice can induce the type-2 immune response, WT and RAGE-/- mice were intranasally administered exotoxin for seven days [88,89].

While exotoxin treatment in WT mice induced significant mucus production, mucous hyperplasia and even bronchiolitis obliterans, no signs of inflammation or mucus production were found in any of the lung sections from RAGE-/- mice treated with exotoxin (Fig. 11 I-Q). This is further supported by a lack of *Il-13* and *Clca1* expression in exotoxin treated RAGE-/- mice whole lungs (Fig. 11 R). RAGE-/- mice treated with exotoxin also trended to have depleted levels of eotaxin-2 in the BALF when compared to WT treated mice (Fig. 11 S). This suggest RAGE not only modulates the direct effects of IL-13 on the bronchial epithelium, but also plays a role in the most common infection CF patients develop. Importantly, studies using intranasal administration of exotoxin show STAT6-/- mice are protected from the proinflammatory effects of exotoxin [88]. Concomitantly, prior studies show RAGE-/- mice treated with IL-13 have reduced activation of STAT6 [112]. These previous finding along with this study further support the role of RAGE and

STAT6 in CF lung pathology. However, it would be valuable to extend the exotoxin treatment and determine if pSTAT6 is reduced in RAGE-/- animals.

This study illuminates how RAGE plays a direct role in type-2 airway inflammation seen in CF. This is through modulation of the effects of IL-13 induced mucus production, mucous hyperplasia, mucous metaplasia TFs and eotaxin-2 production in CF HBECs. RAGE also facilitates mucus production in mice treated with intranasal exotoxin derived from *P. aeruginosa*. Both of these effects are likely modulated through activation of STAT6, though further RAGE inhibition experiments and shRNA knock-down of RAGE expression in differentiated HBECs are needed. However, prior studies have shown absence of RAGE reduces IL-13 induced activation of STAT6 over time in HBECs and mice, and absence of STAT6 reduces lung inflammation during exotoxin treatment [88,112]. In summary, RAGE may serve as a viable target for CF patients with an elevated type-2 immune response through direct regulation of STAT6.

3.0 IL-33 is not released from murine Type-1 Alveolar Epithelial Cells or Human Alveolar Organoids *in vitro*

3.1 Interlukin-33 (IL-33)

3.1.1 IL-33 structure and function

IL-33 is a part of the interleukin-1 family of proteins and is a tissue derived nuclear cytokine expressed in multiple human tissues, including the lung [317]. It is translated as a 31-kDa protein (pro-IL-33, 270 aa) containing the IL-1 family consensus sequence (A-X-D) [318]. Full length IL-33 is biologically active and binds to the IL-1 receptor ST2 expressed on mast cells, endothelial cells and type-2 innate lymphoid cells (ILC2s) upon its release [317,319]. In the nucleus, IL-33 has been shown to bind heterochromatin and mitotic chromosomes in multiple human cell lines through its N-terminal helix-turn-helix domain [320]. IL-33 can regulate transcription in the nucleus, though upon its release during cell necrosis or allergen stimulation, IL-33 acts as a cytokine alarmin activating inflammation [202,321,322]. Interestingly, removal of IL-33's N-terminal chromatin binding domain results in severe inflammation in both lymphoid and non-lymphoid organs in mice [323]. Thus, harboring IL-33 within the nucleus also acts to suppress inflammatory responses.

When released, IL-33 drives type-2 allergic airway inflammation (AAI) in mucosal organs and induces eosinophilia and production of type-2 proinflammatory cytokines, such as IL-5, IL-13 and IL-4 [114,317,324]. This is through activation of ILC2s that produce these cytokines [165,325]. While other alarmins such as IL-25 can induce type-2 AAI, IL-33 is a more potent

inducer of immune cell proliferation and production of proinflammatory cytokines in models of asthma and chronic obstructive pulmonary disorder (COPD) [150,167,317]. This is corroborated by a single nucleotide polymorphism (SNP) flanking IL-33 (rs1342326) being associated with multiple subgroups of asthma patients, including child-onset, occupational, severe and adult-onset asthma [326].

Several studies have indicated released IL-33 is cleaved into different products depending on the initial stimuli. IL-33 has been shown to be cleaved by caspase-3 during apoptosis in both human and mouse cell lines. Though in comparison to models of necrosis, most of the cytokine remains inside the cell during apoptosis [321]. While prior studies showed IL-33 could be cleaved by inflammatory caspase-1, induction of inflammation did not result in cleavage of IL-33 by caspase-1 [317,321]. Allergen stimulation also induces cleavage of IL-33 into multiple products based on proteases present within the specific allergen [327,328]. While these cleavage products varied in length and amino acid composition, all induced higher levels of type-2 AAI *in vitro* and *in vivo* when compared to full length IL-33 [327].

Since IL-33 and its cleavage products are potent inducers of type-2 AAI, it is imperative to understand how and in which cells IL-33 is released [167,327,328]. While some studies have shown allergens stimulate IL-33 release from human lung epithelial cells through an ATP dependent mechanism, it is still unknown how and where IL-33 is released in response to allergic stimuli [202,329]. This led to the investigation of which lung epithelial cell types are responsible for IL-33 release during allergen stimulation.

3.1.2 RAGE regulation of IL-33 in type-2 allergic airway inflammation

RAGE is a member of the immunoglobulin superfamily and acts as a pattern recognition receptor by recognizing damaged associated molecular patterns (DAMPs) [110,210]. It recognizes DAMPS through its ligand binding V-domain, such as HMGB1, S100A12 and nucleic acids [250,330,331]. Since RAGE is most highly expressed within the lung epithelium, its ligands have been found to play a role in multiple lung inflammatory diseases, including asthma, COPD and cystic fibrosis [211,228,229].

Pulmonary function measures, such as the forced expiratory volume in 1 second (FEV_1), are crucial tools to predict the severity and survival of individuals with lung disease, including asthma [99]. Importantly, a meta-analysis of three genome-wide association studies (approx. 75,000 individuals) found a SNP in RAGE (rs2070600) associated with a measure of airway obstruction or the ratio of FEV_1 to forced vital capacity (FEV_1/FVC) [97,98,332]. This SNP leads to an amino acid substitution (G82S) in RAGE's ligand-binding domain and enhances the binding affinity of the RAGE ligand S100A12, which induces mucus production in airway epithelial cells [109,250]. Moreover, S100A12 stimulation of primary human cells heterozygous for the G82S SNP enhances their production of proinflammatory cytokines, such as TNF-α and IL-6 [109].

Importantly, our studies found the receptor for advanced glycation end-products (RAGE) is required for IL-33 induced type-2 AAI in response to allergens house dust mite (HDM) and *Alternaria alternata* (*AA*) [114]. In WT mice treated with intranasal *AA*, production of IL-33 is significantly increased in the whole lung homogenates. Conversely, global RAGE-/- mice treated with *AA* do not upregulate production of IL-33. In allergen stimulated WT mice, IL-33 then induces proliferation and recruitment of ILC2s to the lung [167,325,333]. In subsequent studies, RAGE was found to be required for ILC2 recruitment to the lung through upregulation of vascular

adhesion factor 1 (VCAM1) [113,114]. ILC2s can then migrate to the lung from the vasculature and secrete proinflammatory type-2 cytokines, IL-5 and IL-13 [334]. These cytokines are known to play a critical role in the development of type-2 AAI by promoting mucus production, recruitment of eosinophils and mucous metaplasia [173,335–337]. While IL-33 and type-2 AAI are absent in the lungs of RAGE-/- mice, it is unknown how RAGE regulates IL-33 release and in what cell types this process occurs in. This led to the investigation of which lung cell types express RAGE and may release IL-33.

3.1.3 Cellular localization of IL-33 release in the lung

While many lung epithelial cells have been identified as IL-33 producing, type-1 alveolar epithelial cells (ATIs) neighbor the vasculature and highly express RAGE [338–340]. Our preliminary studies indicate primary mouse ATIs stably express RAGE in culture and release IL-33 in response to *Alternaria alternate* (*AA*) (data not shown). Other lung cell types, such as human bronchial epithelial cells (HBECs), have been shown to harbor IL-33 within the nucleus and release it extracellularly in response to allergens [202]. Using *AA* stimulation, Kouzaki et al. showed IL-33 is released extracellularly from HBECs after four hours.

Contradicting these studies, other groups have not detected IL-33 in bronchial epithelial supernatants after allergen stimulation [201]. Using multiple allergens, including house dust mite (HDM), *AA*, *Acetosella vulgaris* (buckwheat) and *Betula pendula* (silver birch) Ramu et al. was not able to detect any IL-33 in the media supernatants. Further studies have identified lung basal cells, serous cells and type-2 alveolar epithelial cells (ATIIs) to harbor IL-33. These cells have been shown to upregulate IL-33 in models of influenza, COPD and aspirin-exacerbated respiratory disease (AERD), though not in models of asthma [150,151,341]. Though, while these cells may

express IL-33 in models of type-2 airway inflammation, these studies have not deduced if IL-33 was released from these lung epithelial cells.

It remains unclear which lung cell type both expresses RAGE and releases IL-33 in response to allergen stimulation. ATIs highly express RAGE and are positioned to induce type-2 AAI by neighboring the vasculature for recruitment of ILC2s [340]. Concomitantly, variants of RAGE are associated with measures of airway obstruction and RAGE is required for allergen induced IL-33 production in the lung [97,109,114]. These studies have led to the hypothesis that RAGE mediates allergen induced IL-33 release from ATIs. To test this, primary murine ATIs isolated from WT and RAGE-/- mice were treated with *AA* to induce IL-33 release. In a second model, human induced pluripotent stem cell (hiPSC) derived alveolar organoids were treated with *AA* and IL-33 release was analyzed using ELISA.

3.2 Materials and Methods

3.2.1 Isolation of primary murine type-1 alveolar epithelial cells (ATIs)

3.2.1.1 Lung perfusion and digestion

Primary murine ATIs were isolated from both WT and RAGE-/- mice (N=12, n=6). Animals were first euthanized with 150 µl Pentobarbital (Henry Shein INC.) in PBS at a ratio of 1:8. After opening the abdominal and thoracic cavities exposed the heart and lungs for perfusion, mice were exsanguinated by severing the vena cava, and lungs were perfused with 10 ml PBS. A 20-gauge luer stub adapter was secured in the trachea with a suture, and lungs were inflated with

1.5 ml 37° C Solution B (40 ml RPMI (Gibco), 1ml of 1 M HEPES (Gibco), 4 g Dextran (Sigma) and 72 mg Elastase (Worthington)). Lungs were then separated from chest cavity and incubated by shaking in 3ml Solution B at 37° C. In a sterile hood, lungs were dissected using forceps into small pieces on TPP sterile plates (Sigma) for the cutting surface. Next, 3ml of DNAse Solution (40 ml RPMI, 1ml of 1 M HEPES, 2ml FBS and 4.5 µl DNAse-1 (Invitrogen)) was added before series filtration through 100, 70, 40 and 20 µm filters (Fisher Scientific). Filtrates were then pelleted at 350 RCF for 10 minutes at 4° C before being incubated for 5 minutes at room temperature (RT) in 3 ml Ammonium-Chloride-Potassium (ACK) red blood cell lysis buffer (Gibco). After lysis, 20 ml of 20% FBS-PBS was added to wash away the lysis buffer. Cells were then pelleted at 350 RCF for 10 minutes at 4° C and resuspended in 1 ml of 20% FBS-PBS and keep on ice before antibody labeling.

3.2.1.2 Fluorescence-activated cell sorting (FACS)

Ultra-Comp Bead (Invitrogen) single stain controls were used to compensate for spectral overlap during isolation of primary murine ATIs. Approximately 50 µl (one drop) of beads were incubated with 0.2 µg of each selection antibody, including BUV395 rat anti-Mouse CD45 (BD Biosciences), APC750 anti-mouse CD31 (BioLegend), Pacific Blue anti-mouse I-A/I-E or MHC class II (BioLegend) and APC anti-mouse Podoplanin or T1-α (BioLegend). Bead mixtures were then pulse vortexed and incubated on ice for 15 minutes, washed with 1 ml of 20% FBS-PBS and spun at 600 RCF for 4 minutes. Labeled beads were then resuspended in 200 µl of 20% FBS-PBS and kept on ice until the murine samples were labeled.

From the main sample, two 50 µl aliquots were pulled for an unstained and dead cell control. Next, 10 µl of rat anti-mouse CD16/32 (BD Biosciences) was added to the main sample

and incubated on ice in the dark for 10 minutes. After washing in 10 ml of 20% FBS-PBS, the main sample was resuspended in 1 ml of 20% FBS-PBS and a third 50 µl aliquot was pulled for the fluorescence minus one (FMO) control. Cells were then counted in the main sample and FMO control before incubating with proper antibodies at a 0.25 µg/10^6 cells concentration. The main sample was incubated with all selection antibodies, whereas the FMO control was only incubated with negative selection antibodies (CD31, CD45 and MHC-class 11). Cells were then incubated on ice in the dark for one hour before washing and resuspension in with 1ml of 20% FBS-PBS. Lastly, 5 µl of 7-AAD Ghost Dye (TONBO Biosciences) was added to the main sample, FMO and dead cell controls before FACS isolation (United Flow Core, University of Pittsburgh).

3.2.1.3 Culture of primary murine ATIs

One day before isolation, a 24-well plate was coated with matrigel matrix at 0.768 mg/ml (Corning) in a 1:5 ratio with ATI media (40 ml DMEM (Gibco), 10 ml FBS and 0.5 ml 100X penicillin-streptomycin (Gibco)) and 0.03 mg/ml rat type-1 collagen (Corning). After FACS, murine ATIs were then seeded onto matrigel coated plates at 5x10^6 cells/well. ATI media was changed every 48 hours and cells were expanded for 6-8 days before experimentation.

3.2.2 Culture of human induced pluripotent stem cells (hiPSCs) and alveolar organoids

The BU3 NKX2-1^{GFP} hiPSC line, received from the Kotton lab, was derived from peripheral blood mononuclear cells (PBMCs) from a female donor [342,343]. This line was previously characterized and showed a normal karyotype [208]. BU3 NKX2-1^{GFP} hiPSCs were maintained in feeder-free conditions using matrigel (Corning) coated 6-well tissue culture dishes (Costar). Cells were fed every 24 hours using in mTeSR1 medium (StemCell Technologies) until

they reached confluence. Sites of colony differentiation were dissociated using autoclaved pipet tips (Fisher Scientific) and washed with 1 ml PBS before being aspirated. Colonies were then passaged using gentle cell dissociation reagent (StemCell Technologies).

Alveolar organoids were differentiated from the SPC2 hiPSC line derived from dermal fibroblasts (Kotton Lab, Boston University, Center for Regenerative Medicine (CReM)). Organoids were shipped live from the Kotton lab in four 75 µl 3D matrigel (Corning) droplets suspended in CK+DCI media. CK+DCI media was formulated using IMDM (Thermo), Ham's 12 (Cellgro), B-27 supplement (Invitrogen), N-2 supplement (Invitrogen), BSA (Fisher Scientific), Primocin (Invivogen), GlutaMAX (Thermo), ascorbic acid (Sigma), MTG (1-thioglycerol, Sigma), CHIR99021 (Wnt activator, Tocris), rKGF (R&D Systems), dexamethasone (Sigma), cyclic-AMP (8-bromoadenosine 3',5'-cyclic monophosphate, Sigma) and IBMX (3-isobutyl-1-methylxanthine, Sigma) (Kotton Lab, Boston University, CReM). Upon receipt, alveolar organoids in 3D matrigel were centrifugated at 150 RCF for 2 minutes and resuspended in Dispase (Thermo) dissolved in DMEM (Gibco) at 2 mg/ml. Alveolar organoids were then incubated at 37°C for 30 minutes, and spun down at 200 RCF for 4 minutes. After removal of dispase, organoids were resuspended in 1 ml of 0.05% trypsin (Gibco) in DMEM and transferred to a 12-well plate for incubation at 37°C for 5 minutes. The single cell suspension was then added to 1.5 ml conical vials and pelleted at 300 RCF for 5 minutes. Cells were resuspended in CK+DCI with 10 µM Y-27632 (Rho-associated kinase inhibitor, Tocris) to inhibit apoptosis, centrifuged at 300 RCF for 5 minutes, resuspend in 3D matrigel and plated in a 12 well plate. After 72 hours of culture, Y-27632 was removed from CK+DCI media. After eight days of culture, cells were characterized and subjected to allergen exposure.

3.2.3 Modeling allergen exposure *in vitro*

To model type-2 AAI induction in primary murine ATIs and alveolar organoids, cells were exposed to the fungal allergen *Alternaria alternata* (*AA*) (GREER Laboratories INC). For primary murine ATIs, cells were treated with 50 μg/ml in ATI media for 6 hours. This is based on our own studies and others finding *Alternaria* is correlated with human asthma attacks, induces IL-33 release from lung epithelial cells at 50 μg/ml between 2-8 hours, and increases IL-33 within the whole lung [114,202]. When considering alveolar organoids cannot reach confluency like primary alveolar cells due to their 3D culture conditions, a lower range of concentrations were used for type-2 AAI induction (0, 1, 5 and 10 μg/ml of *AA* dissolved in organoid differentiation media (CK+DCI) for 6 hours).

3.2.4 Western blot analysis

After murine ATIs were treated with *AA*, media supernatants were harvested after bulk media was centrifuged at 4° C for 10 minutes at 10,000 RPM. These supernatants were then concentrated using 0.5 ml, 3 kDa Pierce concentrators (Thermo) per the manufacturer's protocol. Murine ATIs were then lysed using DIGE Buffer (7 M urea, 2 M thiourea, 30 mM Tris, and 4% CHAPS) with 1X of the Halt protease and phosphatase inhibitor cocktail (100X, Thermo) on ice. Samples were then stored at -80° C until analysis. Total protein content was determined for media supernatants and cell lysates using a Bradford assay with bovine serum albumin (BSA, Fisher Scientific) and Coomassie protein assay (Thermo). A mixture of 4X sample buffer (BIORAD) and 500 mM dithiothreitol (DTT) was prepared at a ratio of 9:1 and was subsequently mixed with 10-20 μg of murine ATI protein at 1:3. Samples were then analyzed by SDS-PAGE on a 10%

acrylamide gel (BIORAD) and subjected to immunoblotting. After blocking in 5% BSA-PBS, membranes were incubated in 1:1000 of primary antibodies, including mouse anti-IL-33 (Enzo Life Sciences, 30 kDa), rabbit anti-RAGE (Abcam, 35-45 kDa), rabbit anti-Auqaporin-5 (AQP5, Millipore Sigma, 28 kDa), rabbit anti-pro-Surfactant protein-C (proSPC, Millipore Sigma), mouse anti-Vimentin (Abcam, 54 kDa) and 1:5000 of primary mouse anti-β-Actin (Cell Signaling, 42 kDa) in 5% BSA-PBS. This was followed by three 15 minute wash steps in tris buffer with 0.1% tween (T-BST) and incubation for 1 hour in 1:5000 secondary horseradish peroxidase anti-rabbit or anti-mouse antibody (Jackson ImmunoResearch) in 3% milk. Membranes were washed as stated above and finally developed with chemiluminescent detection using ECL Plus Reagent (Thermo) before imaging (LI-COR Odyssey Fc).

3.2.5 Immunofluorescence (IF) and fluorescence microscopy

3.2.5.1 IF: hiPSC characterization

Human iPSC (hiPSC) were first cultured on matrigel (Corning) in a 12-well plate (Costar) on top of UV sterilized glass cover slips (Fisher Scientific) for seven days. Cultures were then fixed with 4% paraformaldehyde (PFA, Electron Microscopy Sciences) and permeabilized with 1 ml of 0.3% Triton X-100 in PBS for 10 minutes at room temperature (RT). Between each step, three 5 minute washes were conducted using tris buffer with 01% tween (T-BST). hiPSCs were blocked with 4% goat serum-PBS for 30 minutes at RT (Vector Labs). Primary antibodies including mouse anti-cell-surface stage specific antigens (SSEA-1 and SSEA-4) and mouse anti-keratin sulfate associated antigen (TRA-1-81) were incubated at 1:50 in 4% goat serum-PBS for one hour at RT (Millipore Sigma). Secondary antibodies including goat anti-mouse IgG (AF546 nm) and goat anti-mouse IgM (AF488 nm) were incubated at 1:100 in PBS for one hour at RT

(Life Technologies). Slides were then washed as stated above and stained with DAPI at 2.5 µg/ml (Thermo). Cover slips were then mounted with gelvatol (Sigma) and imaged by an Olympus IX71 inverted microscope (Olympus, Tokyo, Japan).

3.2.5.2 Fluorescence microscopy: Alveolar organoid characterization

hiPSC derived alveolar organoids were differentiated from hiPSC surfactant protein-C (SPC) cell line from Dr. Darrell Kotton (Boston University, MA). The SPC line expresses a tdTomato reporter allele before exon-1 of SPC to verify their differentiation to type-2 alveolar epithelial cells [208]. Alveolar organoids were then cultured in 75 µl droplets of 3D Matrigel (Corning) for 8 days before imaging by an Olympus IX71 inverted microscope (Olympus, Tokyo, Japan) under the tetramethylrhodamine (TRITC) channel to verify expression of SPC.

3.2.6 ELISA for murine and human IL-33

3.2.6.1 Murine IL-33 ELISA: Murine ATI media and lysates

After murine ATIs were treated with *AA*, media supernatants were harvested after bulk media was centrifuged at 4° C for 10 minutes at 10,000 RPM. Murine ATIs were then lysed using DIGE Buffer as stated above. Subsequently, volumes of media supernatants and lysates from each treatment group were loaded onto a 96-well plate incubated with murine IL-33 capture antibody per the manufacturer's instructions (R&D Systems). Following the manufactures protocol, absorbance was measured with a plate reader at 490 nm to determine the concentration of IL-33 in the media supernatants and lysates (Molecular Devices).

3.2.6.2 Human IL-33 ELISA: Alveolar organoid media, matrigel supernatant and lysates

After hiPSC derived alveolar organoids were treated with *AA* (50 μg/ml) for 6 hours, media supernatants were harvested after bulk media was spun down at 4° C for 10 minutes at 10,000 RPM. 3D Matrigel droplets with alveolar organoids were washed three times with warm PBS and dissolved using Cell Recovery Solution (Corning) at 10X the volume of gel droplet for one hour on ice. Samples were then spun at 20 RCF for 5 minutes at 4° C. Matrigel was harvested from this supernatant, while organoids were washed twice in PBS at 20 RCF for 5 minutes at 4° C. The final cell pellets were lysed using DIGE Buffer (7 M urea, 2 M thiourea, 30 mM Tris, and 4% CHAPS) with 1X of the Halt protease and phosphatase inhibitor cocktail (100X, Thermo) on ice. Subsequently, undiluted volumes of media, Matrigel supernatant and organoid lysates were loaded onto a 96-well plate incubated with human IL-33 capture antibody per the manufacturer's instructions (R&D Systems). Following the manufactures protocol, absorbance was measured with a plate reader at 490 nm to determine the concentration of IL-33 (Molecular Devices).

3.2.7 Statistics

Statistics were performed with GraphPad Prism 8 software (GraphPad Software, La Jolla, CA) for ELISA of murine and human IL-33. Means were determined from six to eight biological replicates per treatment group. Statistical significance was finally determined by using Student's T-test or a One-way/2-way ANOVA followed by Bonferroni's multiple comparisons test. A p-value of less than 0.05 was considered significant from the multiple comparisons test where each treatment group was considered within the analysis. N is defined as the number of total samples, whereas n is defined as the number of samples in a particular conditional group.

3.3 Results

3.3.1 Isolated primary WT and RAGE KO murine ATIs do not release IL-33 in response to *Alternaria alternata*

Primary murine lung epithelial cells were isolated from WT mice to test the hypothesis that ATIs are responsible for RAGE dependent IL-33 release. After lung dissection and digestion, cells positive for T1-α were sorted (Fig. 12, pink). T1-α is a 40 kDa glycoprotein expressed in both humans and rodents [344]. This marker was used to sort murine ATIs since rodent *in vivo* studies have shown T1-α acts as a specific developmental biomarker for ATIs [345]. Approximately $1x10^6$ cells were sorted using T1-α (Fig. 12).

After culturing these cells on matrigel containing rat type-1 collagen, they were then characterized using immunoblot for ATI specific markers. Interestingly, both control and *AA* treated cells expressed markers of ATIs, including aquaporin-5 (AQP5) and RAGE (Fig. 13) [255]. Though, these cells also expressed markers of type-2 alveolar epithelial cells (ATIIs) and mesenchymal cells, including pro-surfactant protein-C (proSPC) and vimentin respectively [339]. This was verified by looking at expression of these markers using whole lung homogenates (WLH) from WT and RAGE-/- (KO) mice (Fig. 13).

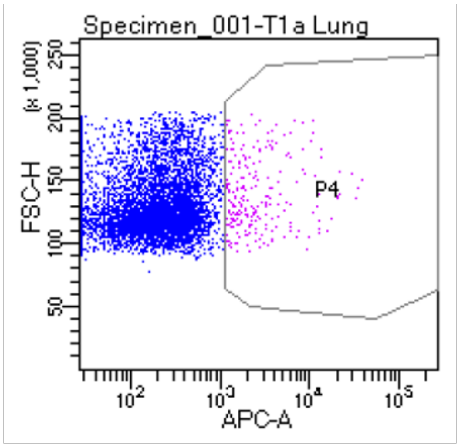

Figure 12: Initial FACS isolation protocol for primary murine ATIs

Flow cytometry analysis shows cells positive for T1-α (pink) and negative for T1-α (royal blue) isolated from WT murine lungs. Cells were stained using APC anti-T1-α (pink) after being blocked with anti-mouse CD16/32. Six WT mice were used for the isolation protocol. Approximately $1x10^6$ cells per total sample were isolated and cultured for further characterization.

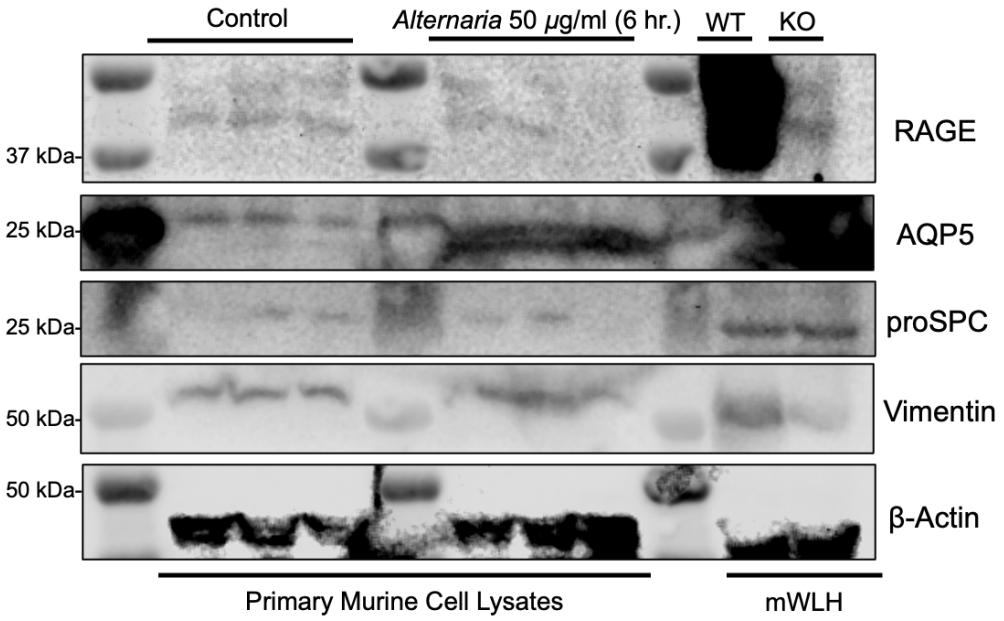

Figure 13: Western blot of murine ATI markers

T1-α isolated primary murine cells were cultured for seven days and treated with *Alternaria* (50 μg/ml) or control saline for 6 hours before cell lysates were harvested. Murine whole lung homogenates (mWLH) from WT and RAGE-/- mice (knock-out, KO) served as the positive and negative control for RAGE labeling. Immunoblot for ATI markers (RAGE, AQP5), an ATII marker (proSPC) and mesenchymal cell marker (Vimentin) shows T1-α isolated primary murine cells express markers of all these cells types.

The expression of vimentin and proSPC suggested the isolation protocol was not sufficient to isolate a pure population of murine ATIs. However, since other lung epithelial cells, such as ATIIs, increase IL-33 expression after exposure to influenza or Sedai virus, media supernatants from the mixed population of cells were analyzed for IL-33 [150,151]. While ELISA analysis showed a trend for the release of IL-33 after *AA* treatment, there was no statistically significant difference between the control and *AA* treated cell supernatants or lysates (Fig. 14 A, B)

After finding the isolated murine lung cells were not pure and did not release IL-33 after allergen exposure, a new FACS isolation protocol was evaluated in an attempt to obtain a pure

population of ATIs. Using methods developed by Nakano et al. to isolate multiple cell populations from murine lungs, including ATIs, ATIIs, bronchial epithelium and endothelial cells, the protocol was altered to negatively select for endothelial cells and ATIIs [346] (Fig. 15 A, B). Antibodies to CD31 and MHC-II were used to negatively select for endothelial cells and ATIIs, respectively, since both of these markers are highly expressed in these cell populations [347]. This was followed by positive selection of ATIs using T1-α (Fig. 15 C).

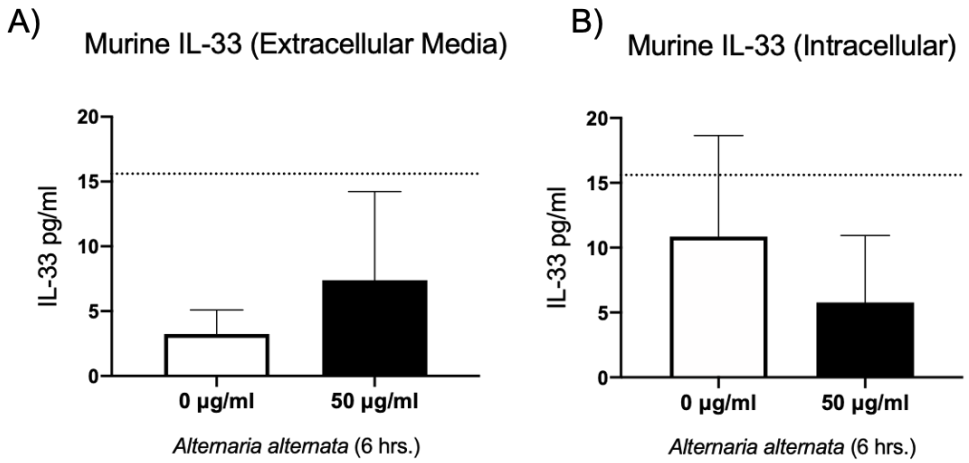

Figure 14: IL-33 release from primary murine lung cells

WT primary murine lung cells were stimulated with 0 and 50 µg/ml of *Alternaria* in ATI media for 6 hours at day 7 (D7) of their culture. Subsequently, extracellular media supernatants (A) and cells lysates (B) were harvested and subjected to ELISA for detection of murine IL-33 (n=3 for each sample). The dashed line at y=15.6 pg/ml indicates the detection limit. Statistical significance was determined using a Student's T-test, $p<0.05$ was considered significant.

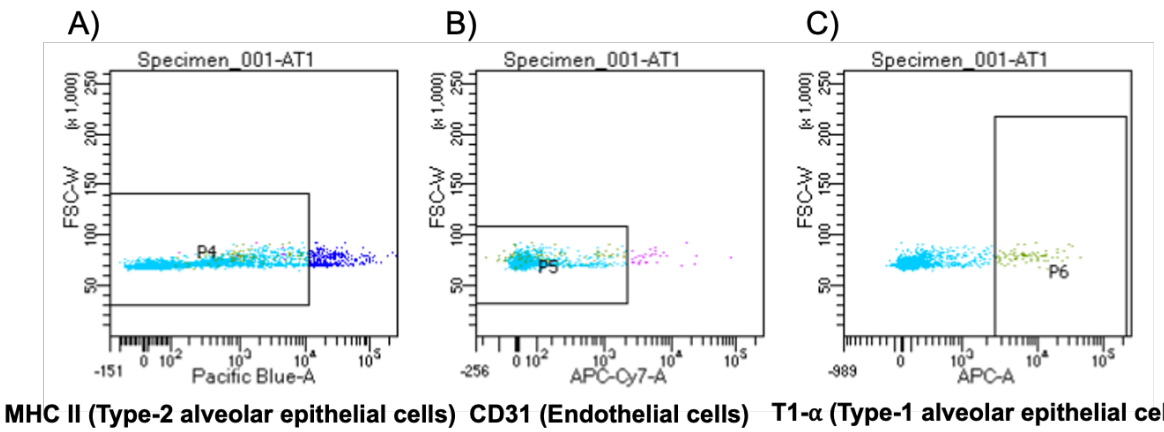

Figure 15: FACS isolation of WT primary murine ATIs

Flow cytometry analysis shows negative selection of cells positive for MHC-II (royal blue) (A) and CD31 (pink) (B), marking ATIIs and endothelial cells respectively, isolated from WT murine lung cells. Positive selection of cells expressing ATI marker T1-α (green) followed (C). Cells were stained with Pacific Blue anti-MHC-II, APC-Cy7 anti-CD31 and APC anti-T1-α after being blocked with anti-mouse CD16/32. Six WT mice were used for the isolation protocol. Approximately $0.5x10^6$ cells per total sample were isolated and cultured for further characterization.

After employing the new isolation protocol, isolated WT murine lung cells were cultured on matrigel containing rat collagen-1 (Fig. 16). Cells displayed a morphology typical of ATIs, with a wide cytoplasm distributed around the nucleus, which facilitates their gas exchange function *in vivo* [338]. At day seven, cell lysates were harvested to determine ATI marker expression (Fig. 17). Indeed, isolated murine lung cells expressed markers of ATIs, including AQP5 and RAGE, but do not express proSPC. This suggested the new isolation protocol was sufficient to obtain a pure population of ATIs.

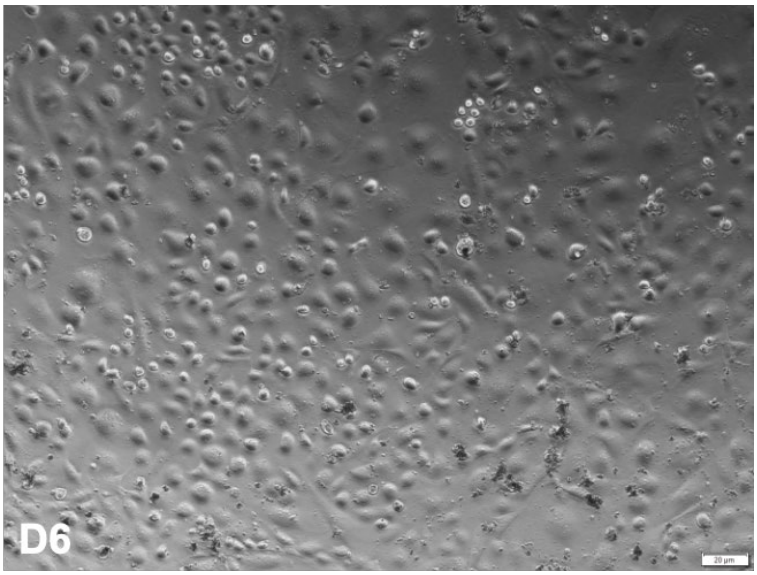

Figure 16: Culture of WT primary murine ATIs

After FACS isolation, WT primary murine ATIs were seeded onto matrigel coated plates at $5x10^6$ cells/well. ATI media was changed every 48 hours and cells were expanded for 6-8 days before experimentation. Cells exhibit a round and broad morphology, indicative of ATIs, by day 6 (D6).

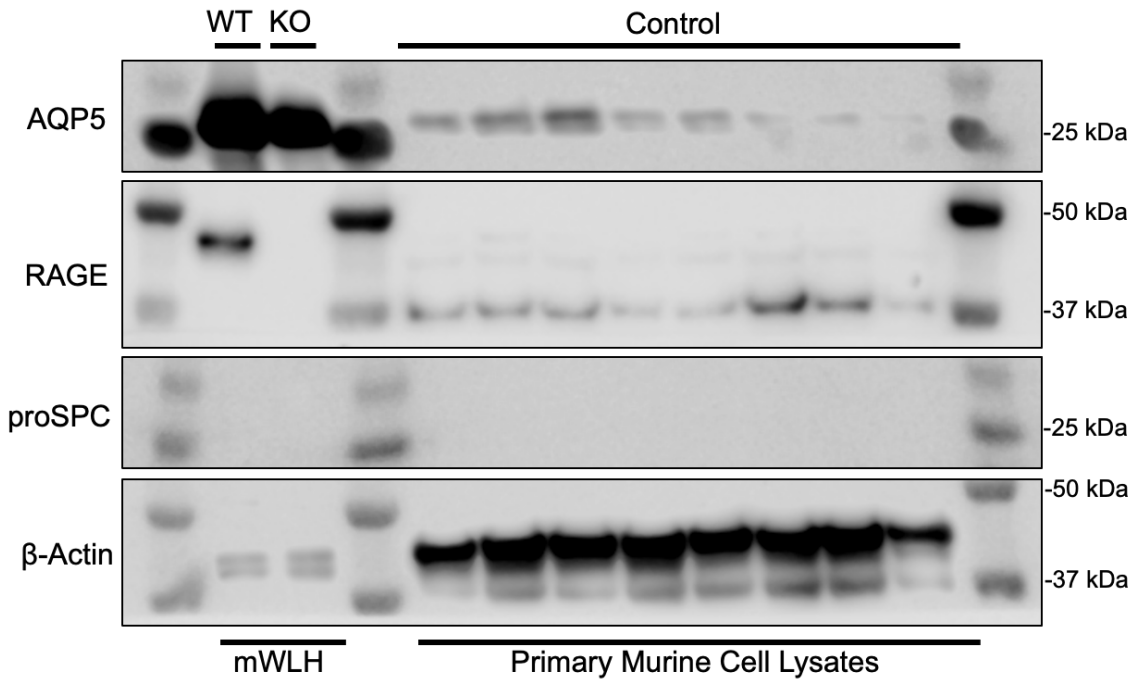

Figure 17: Western blot of murine ATI markers

Isolated primary murine cells were cultured for seven days before cell lysates were harvested. Only control primary murine cell lysates were subjected to immunoblot. Murine whole lung homogenates (mWLH) from WT and RAGE-/- (knock-out, KO) mice served as the positive and negative control for RAGE expression. Immunoblot for ATI markers (RAGE, AQP5), an ATII marker (proSPC) shows T1-α + isolated primary murine cells express markers of ATIs.

The new protocol was then used to isolate both WT and RAGE-/- murine ATIs to test the hypothesis that RAGE is required for allergen induced IL-33 release. WT and RAGE-/- murine ATIs were isolated by using an additional negative selection for CD45 (Leukocytes) to further enhance purity of our population (Fig. 18, B pink). Cells where then positively selected for using T1-α (Fig. 18, D sky blue). After culture for six days, there was a low cell density in both WT and RAGE-/- ATIs compared to the prior isolation (Fig. 19). This is likely due to having three negative selection antibodies compared to only two (Fig. 15, 16).

At day seven, WT and RAGE-/- murine ATIs were treated with 0, 25 or 50 μg/ml of *Alternaria* for 6 hours to test if RAGE was required for IL-33 release from these lung epithelial cells. Control treated cell lysates were used to determine ATI marker expression (Fig. 20). While adding a third negative selection antibody decreased cell confluency, isolated murine lung cells still expressed markers of ATIs, including AQP5 and RAGE, but not proSPC (Fig. 20). The extracellular media supernatants of WT and RAGE-/- ATIs treated with *Alternaria* were then analyzed for IL-33 release, but no detectable levels of murine IL-33 were found in either population (Fig. 21).

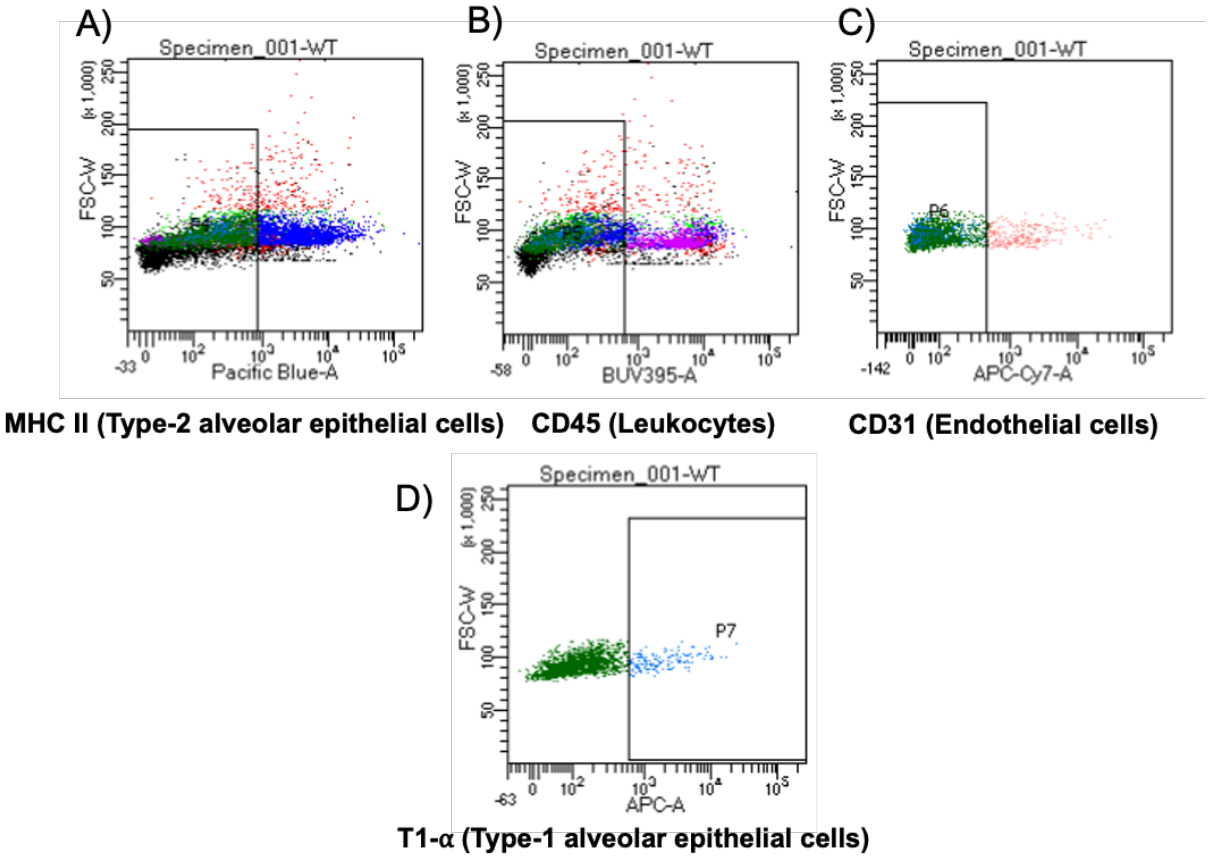

Figure 18: FACS isolation of WT primary murine ATIs

Flow cytometry analysis shows negative selection of cells positive for MHC-II (royal blue) (A), CD45 (pink) (B), and CD31 (red) (C) isolated from WT murine lungs and RAGE-/- murine lungs (data not shown). Positive selection of cells expressing ATI marker T1-α (sky blue) followed (D). Cells were stained with Pacific Blue anti-MHC-II, BUV395 rat anti-CD45, APC-Cy7 anti-CD31and APC anti-T1-α after being blocked with anti-mouse CD16/32. Six WT and RAGE-/- mice were used for the isolation (N=12, n=6). Approximately 0.25-0.35x10^6 cells per total sample were isolated and cultured for further characterization.

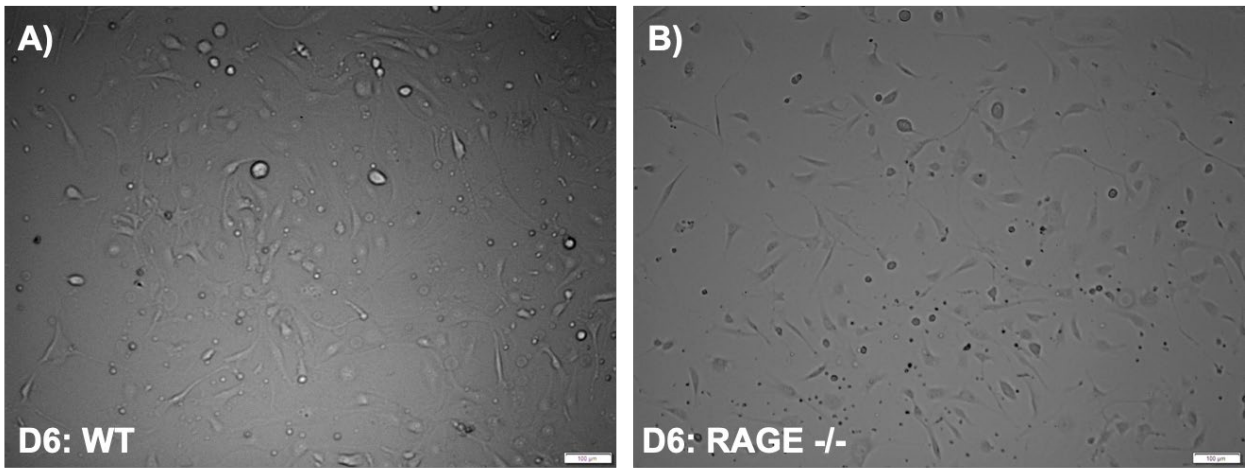

Figure 19: Culture of WT and RAGE-/- primary murine ATIs

After FACS isolation, WT (A) and RAGE-/- (B) primary murine ATIs were seeded onto matrigel coated plates at $5x10^6$ cells/well. ATI media was changed every 48 hours and cells were expanded for 7 days before experimentation. Most cells exhibit a round and broad morphology, indicative of ATIs, by day 6 (D6).

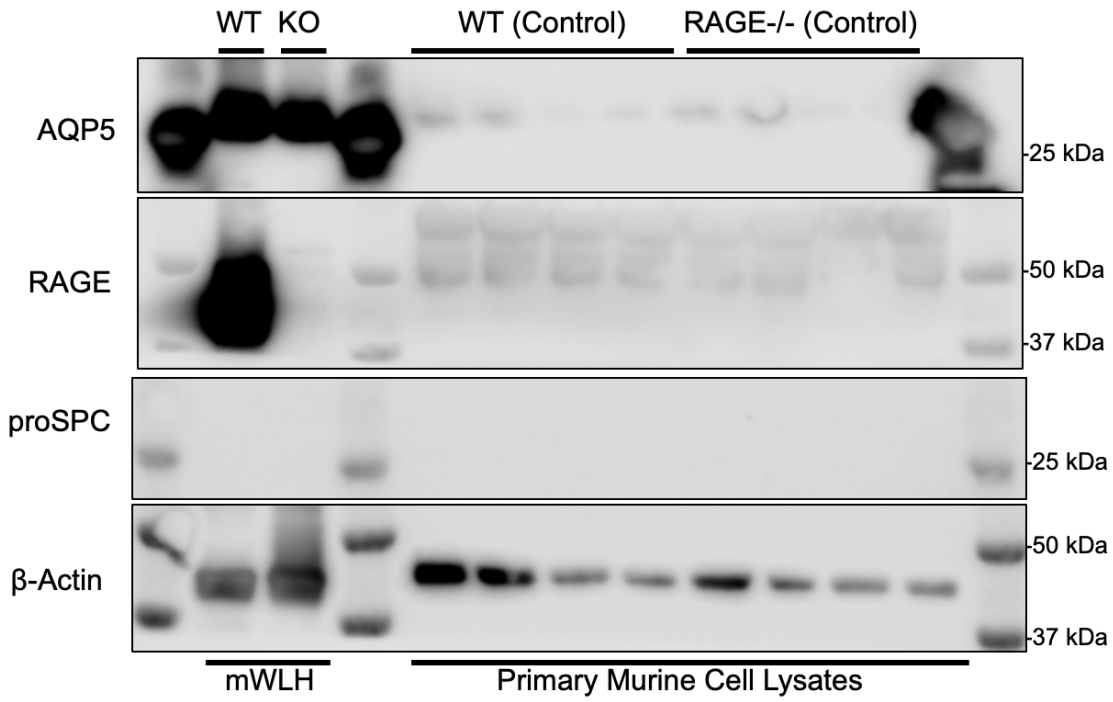

Figure 20: Immunoblot of WT and RAGE-/- murine ATI markers

Isolated primary murine cells were cultured for seven days and treated with *Alternaria* (50 μg/ml) or control saline for 6 hours before cell lysates were harvested. Only control primary WT and RAGE-/- murine cell lysates were subjected to immunoblot. Murine whole lung homogenates (mWLH) from WT and RAGE-/- (knock-out, KO) mice served as the positive and negative control for RAGE labeling. Immunoblot for ATI markers (RAGE, AQP5), an ATII marker (proSPC) shows T1-α isolated primary murine cells express markers of ATIs.

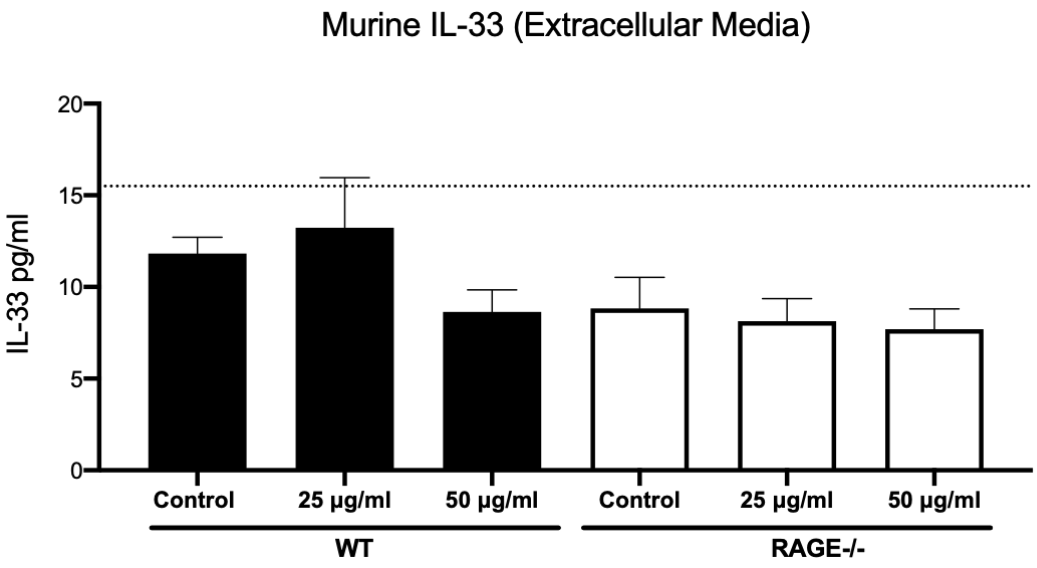

Figure 21: IL-33 release from WT and RAGE-/- primary murine lung cells

WT and RAGE-/- primary murine lung cells were stimulated with 0, 25 and 50 µg/ml of *Alternaria* in ATI media for 6 hours at day 7 of their culture. Subsequently, extracellular media supernatants were harvested and subjected to ELISA for detection of murine IL-33 (n=3 for each group). The dashed line at y=15.6 pg/ml indicates the detection limit. Statistical significance was determined using a 2-way ANOVA, followed by Bonferroni's Multiple Comparisons test, $p<0.05$ was considered significant.

Since IL-33 was not able to be detected from murine ATIs using multiple isolation protocols, it appears these cells alone are not responsible for IL-33 release. It is possible a relationship exists between ATIs and other lung epithelial cell types, such as ATIIs, which have been shown to express IL-33 during allergen exposure [151,348,349]. To further explore the potential role of alveolar epithelial cells in IL-33 release during allergen exposure, a human model was employed, using human induced pluripotent stem cell (hiPSC) derived alveolar organoids.

3.3.2 hiPSCs express human pluripotency markers

The hiPSC line NKX2.1-GFP were cultured and expanded to bank them for future differentiation to lung epithelial cell organoids using protocols developed by the Kotton Lab [95,342]. To verify these cells were still in their undifferentiated state, immunofluorescence (IF) studies were performed to assess the expression of pluripotency markers, including cell-surface stage specific antigens (SSEA-1 & SSEA-4) and keratin sulfate associated Antigen (TRA-1-81) (Fig. 22, A-C). Both SSEA-4 and TRA-1-81 are markers of pluripotency in human embryonic stem (ES) cells and human carcinoma cell lines, though SSEA-1 is only upregulated in mouse ES cells (Fig. 22 C) [350]. IF images for these markers showed that after seven days of culture NKX2.1-GFP hiPSCs were still in a pluripotent state since they only were positive for SSEA-4 and TRA-1-81 (Fig. 22 A, B).

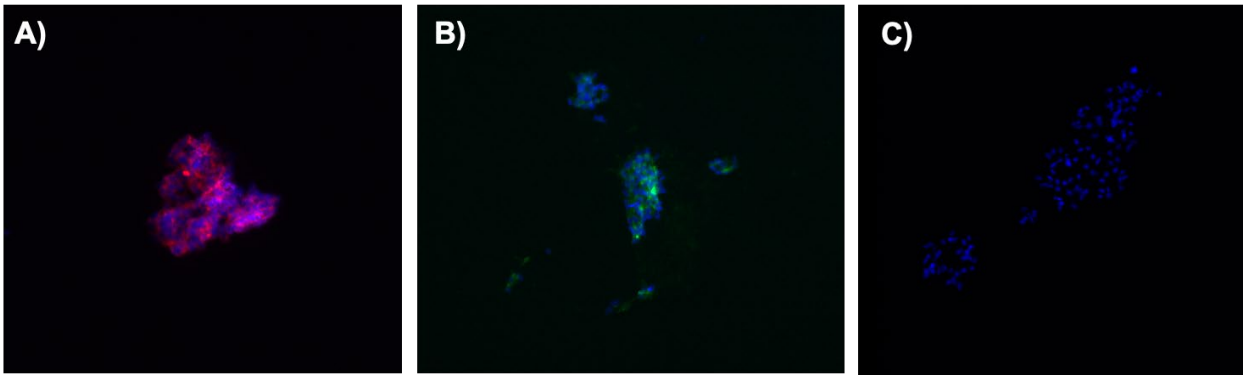

Figure 22: hiPSCs express pluripotency markers

hiPSCs were cultured for on matrigel coated glass cover slips. At day seven, these cells were then subjected to IF for imaging of SSEA-4 (546nm) (A), TRA-1-81 (488nm) (B) and SSEA-1 (488nm) (C). hiPSCs were positive for human pluripotency markers SSEA-4 and TRA-1-81, but not for the murine pluripotency marker SSEA-1 (C).

3.3.3 Organoids express marker of type-2 alveolar epithelial cells (ATIIs)

Alveolar organoids were differentiated from the hiPSC surfactant protein-C (SPC) cell line developed at the Kotton Lab. The hiPSC SPC cell line expresses a tdTomato reporter allele before exon-1 of SPC to verify their differentiation into type-2 alveolar epithelial cells (ATIIs) [208]. Upon receiving the sample from the Kotton Lab, alveolar organoids were cultured in 75 µl droplets of 3D Matrigel for 8 days (Fig. 23 A). To confirm alveolar organoids were still in their differentiated state, 3D cultures were subjected to fluorescence microscopy to verify expression of SPC (Fig. 23 B, C).

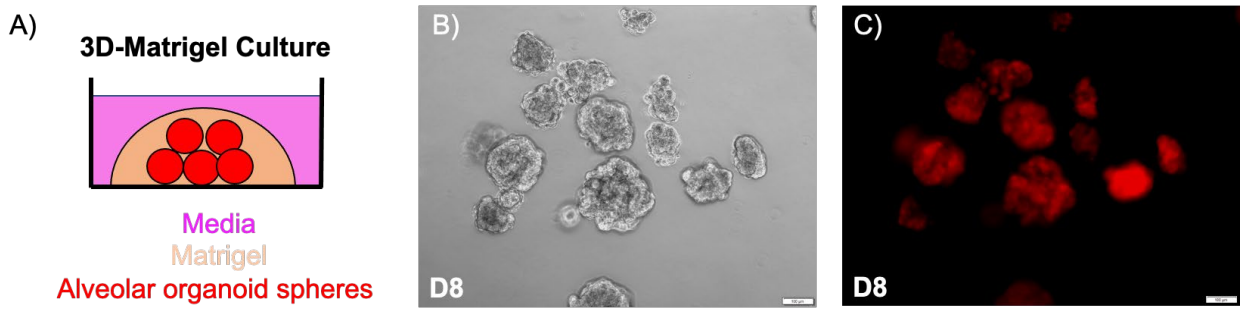

Figure 23: Alveolar organoid culture and characterization

Alveolar organoids were cultured in 75 µl droplets of 3D Matrigel in CK+DCI media. A graphical representation of the culture conditions (A) is followed by microscopic images in grey scale (B) and under the tetramethylrhodamine (TRITC) channel (C). This shows alveolar organoids after 8 days of culture were able to maintain their differentiated state as ATIIs shown by their expression of surfactant protein-C (SPC, red).

3.3.4 Organoids do not release IL-33 in response to *Alternaria alternata*

To test the hypothesis that alveolar organoids mainly comprised of ATIIs release IL-33 in response to allergens, alveolar organoids were treated with varying concentrations of *AA* (Fig. 24). Lower concentrations of *AA* (1, 5, 10 μg/ml) were used to stimulate alveolar organoids since the amount of cellular material in the 75 μl droplet was significantly less than isolated primary alveolar epithelial cells. After stimulation for 6 hours, extracellular media supernatants as well as matrigel supernatants and cell lysates were harvested and probed for human IL-33 (Fig. 24 A-C). Using ELISA, no detectable levels of IL-33 were found in any of the treatment group samples.

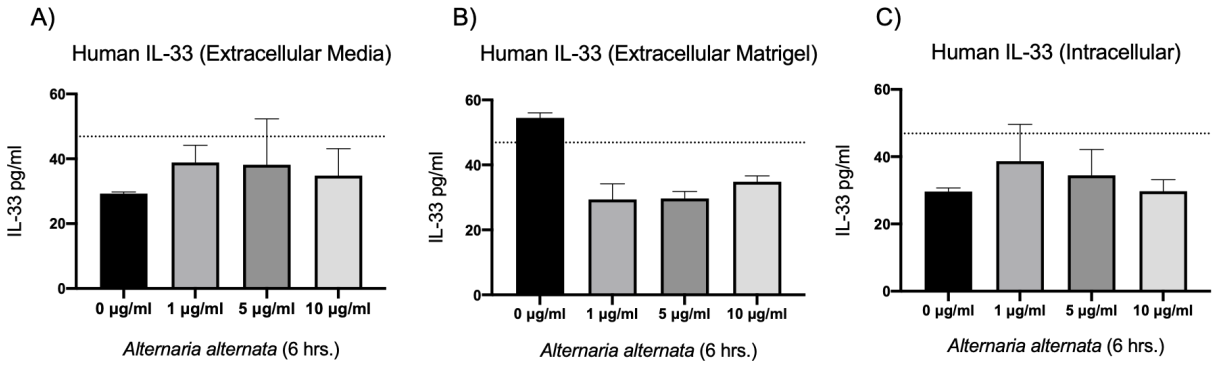

Figure 24: Human IL-33 release from alveolar organoids

Alveolar organoids were stimulated with 0, 1, 5 and 10 μg/ml of *Alternaria* in CK+DCI media for 6 hours at D8 of their culture. Subsequently, extracellular media supernatants (A), matrigel aggregates (B) and cells lysates (C) were harvested and subjected to ELISA for detection of human IL-33. The dashed line at y=46.9 pg/ml indicates the detection limit. Statistical significance was determined using a One-way ANOVA, followed by Bonferroni's Multiple Comparisons test, $p<0.05$ was considered significant.

3.4 Discussion

Allergen induced IL-33 release from lung epithelial cells is a complex process, which may involve potentially multiple cell types. Prior studies found no increased levels of murine IL-33 within the whole lung homogenates of RAGE-/- mice after stimulation with *Alternaria alternata* (*AA*) [114].Yet, it remains unknown which RAGE expressing lung epithelial cell type releases IL-33 in response to allergens in a RAGE dependent manner. This led to the hypothesis that type-1 alveolar epithelial cells (ATIs), which express the highest levels of RAGE in the lung, could be the primary cell that releases IL-33 in response to allergens [338,339]. Conversely, treating primary lung epithelial cells isolated from murine lung tissue using the ATI specific marker T1-α with high concentrations of *AA* did not induce IL-33 release into the extracellular media (Fig. 14). After assessing the purity of these cells using immunoblotting, markers of mesenchymal cells and type-2 alveolar epithelial cells (ATIIs) were found (Fig. 13).

To increase the purity of primary murine ATIs, multiple negative selection antibodies targeting endothelial cells and ATIIs were added to the gating strategy using protocols developed in the literature (Fig. 15, 18) [346]. After confirming the primary murine lung epithelial cells were indeed ATIs, these cells were stimulated with *AA*. Though no detectable IL-33 were found in the media supernatants (Fig. 21). This was true for cells isolated from either WT or RAGE-/- mice. The major limitation of these experiments is the lack of the immune system and presence of only one lung epithelial cell type. During type-2 airway inflammation, alveolar macrophages and dendritic cells sequester allergen antigens and present them to CD4+ T-cells, while barrier epithelial cells in the lung (bronchial epithelial cells, or alveolar epithelial cells) exposed to allergen antigens produced cytokine alarmins IL-33, TSLP and IL-25 [154]. The release of these cytokine alarmins is thought to occur by recognition by pattern recognition receptors, such as

RAGE and Toll-like receptors [114,166]. These cytokine alarmins then activate ILC2s and further perpetuate the activation of type-2 airway inflammation, dendritic cells and CD4+ T-cells [154,167].

Intriguingly, lung epithelial cells found to express or release IL-33 in models of allergen driven type-2 airway inflammation, such as ATIIs and HBECs, have also been found to express MHC-II [150,202,341,351]. In this study, antibodies targeted to MHC-II were used to selectively isolate ATIIs from murine lung tissue (Fig. 15, 18) [346]. Thus, it is possible ATIIs or HBECs may act to further perpetuate type-2 airway inflammation via presentation of allergen antigens to the immune system. Indeed, studies have shown ATIIs expressing surfactant protein-C (SPC) in mice present influenza antigens to CD4+ T-cells *in vivo* [352]. While studies have not shown MHC-II is required for IL-33 expression or release from lung epithelial cells, MHC-II recognition of allergen antigens may be a critical mechanism for lung epithelial cells to communicate to the immune system, leading to further release of cytokine alarmins, such as IL-33, from lung epithelial cells [353]. In summary, properly investigating how IL-33 is upregulated in the lung epithelium requires identification of lung epithelial cell types *in vivo* that upregulate IL-33 in response to allergens in the presence of the immune system. These future experiments will be further considered in the following chapter.

In this study, methods were adapted to model human embryonic developmental cues *in vitro* to produce stable alveolar organoids from human induced pluripotent stem cells (hiPSCs) [95,208]. To employ these models, hiPSCs were cultured in an undifferentiated state for expansion and future differentiation experiments (Fig. 22). Since ATIIs have been shown to express IL-33 in models of type-2 AAI, hiPSC derived alveolar organoids mainly comprised of ATIIs were used to investigate their role in IL-33 release in response to the allergen *AA* [150]. After verifying alveolar

organoids were in their differentiated state by assessing expression of surfactant protein-C (SPC), alveolar organoids were treated with varying concentrations of *AA* (Fig. 23). While multiple studies have shown ATIIs express IL-33 in the context of type-2 AAI, IL-33 was not detected in the media, cell lysates or matrigel supernatants in response to *AA* stimulation [150,151] (Fig. 24). However, alveolar organoids were cultured in a miniscule 75 µl 3-D matrigel droplet that greatly reduces the totally amount of cellular material in the culture compared to a 2-D culture system. Thus, it is plausible the limited number of alveolar organoids in each well resulted in low IL-33 production, which was not detected using a human IL-33 ELISA (Fig. 24).

Many lung epithelial cell types have been identified to express or harbor IL-33 in models of type-2 AAI, including ATIIs, serous (clara) cells, bronchial and basal epithelial cells [150,202,340,348]. Even though RAGE is required for IL-33 upregulation in the whole lung and ATIs express RAGE more than any other lung epithelial cell, multiple lung epithelial cells may be involved in IL-33 release [114]. In one experiment, we showed a population of murine lung epithelial cells had both markers of ATIs and ATIIs, RAGE and pro-surfactant protein C (pro-SPC) (Fig. 13). Even with both populations of alveolar epithelial cells, *AA* treatment did not induce a significant amount IL-33 release in comparison to the control treated cells (Fig. 14). Since mesenchymal cells expressing vimentin were also present within this population, it is possible they may have inhibited release of IL-33 from other lung epithelial cells in the culture (Fig. 13). This study also shows RAGE expression did not affect IL-33 release from lung epithelial cells that only expressed markers of ATIs (Fig. 20, 21).

An assumption of this work is that IL-33 is already present within the cell and is subsequently released upon allergen stimulation. However, prior studies found no detectable IL-33 present in control treated WT or RAGE-/- animal whole lung homogenates [114,202]. This

suggest IL-33 does not reside in the nucleus of lung epithelial cells *in vivo* and is actually transcribed upon allergen stimulation. Indeed, other studies detected low levels of IL-33 in lung epithelial cells in control treated animals where IL-33 was found to significantly increase in animals treated with viruses or allergens [150,151,341].

For future studies, murine *in vivo* experiments would allow specific labeling of lung epithelial cells and IL-33 simultaneously to determine which cell types play a role in allergen induced IL-33 expression. These experiments could then inform *in vitro* experiments to test the direct role of RAGE in IL-33 release or expression from epithelial cells found to upregulate IL-33 *in vivo*. It would also be interesting to see how coculture of lung epithelial cells, such as ATIs, ATIIs, basal and bronchial epithelial cells affect IL-33 release. Since we also did not see a definitive response from the alveolar organoid cultures, further development or larger cultures of hiPSC derived lung epithelial cell organoids would serve as a more useful human model to elucidate where IL-33 is released in response to allergens. These future experiments will be further explored in the following chapter.

3.5 Final Conclusions: Chapter 2 & 3

The studies presented in this work addressed two key questions related to how RAGE plays a role in the development of type-2 airway inflammation in cystic fibrosis (CF) and asthma (Fig. 1, H1 and H2). In patients with CF, type-2 proinflammatory cytokines IL-13 and IL-5 are associated with the development of bronchiectasis, *P. Aeruginosa* infection and are elevated in the bronchoalveolar lavage fluid (BALF) when compared to Non-CF controls [37]. IL-13 and IL-5 are also found in *P. Aeruginosa* mucus biofilms that approximately 80% of patients with CF develop

[90]. Whereas in asthma patients, IL-13 and IL-5 are two key biomarkers that establish the main endotypes of asthma, Th2 “high” and Th2 “low” [149,170]. Consequences of elevated type-2 airway inflammation ultimately lead to declined lung function measured by the forced expiratory volume in one second (FEV_1) in both CF and asthma patients, which is associated with mortality in both patient populations [37,177,283].

In the first study presented in chapter 2, RAGE was found to regulate the direct effects of IL-13 on the bronchial epithelium using human bronchial epithelial cells (HBECs). This included the expression of the mucin gene *MUC5AC*, transcriptions factors known to induce mucus metaplasia in mice and the production of eotaxin-2, a chemoattractant for eosinophils (Fig. 3, 6, 7). Mucus production, mucus plugging and eosinophilia are clinical features in asthma and CF patients, indicating RAGE inhibition may block these phenomena in patients with elevated levels of type-2 proinflammatory cytokines [36,37,290,354]. Indeed, clinical studies looking to block type-2 airway inflammation using monoclonal antibodies targeted to IL-5 (mepolizumab and reslizumab) and the IL-4Rα/IL-13Rα complex (depilumab) reduce pulmonary exacerbations, eosinophilia and the need to use corticosteroids in asthma patients [187–189]. In addition, this study showed using WT and RAGE-/- mice that RAGE regulates mucus production in response to exotoxin derived from *P. Aeruginosa* (Fig. 11). Infection with *P. Aeruginosa* seen in both CF and asthma patients and increases the risk of developing a pulmonary exacerbation in both disease states [34,36,37,355]. Thus, RAGE inhibition may also reduce mucus production and pulmonary exacerbations associated with *P. Aeruginosa* infection in CF and asthma patients. Though, further *in vivo* studies investigating *P. Aeruginosa* infection in WT and RAGE-/- animals should be conducted.

The study presented in chapter 3 sought to identify the RAGE expressing lung epithelial cell type responsible for IL-33 release in response to allergen stimulation. This is based on prior work showing RAGE is required for IL-33 upregulation in the lung in response to stimulation with the allergen *Alternaria alternata* (*AA*) [114]. Initially, it was hypothesized type-1 alveolar epithelial cells may be the RAGE expressing lung cell type responsible for IL-33 release. However, isolation and culture of ATIs from mice show ATIs are not solely responsible for IL-33 release in response to stimulation with *AA* (Fig. 14-21). This was also true when using a human alveolar organoid model, which is mainly comprised of type-2 alveolar epithelial cells (ATIIs) where no IL-33 was found to be released after stimulation with *AA* (Fig. 24, 25).

While this study was unable to uncover the exact cell type(s) responsible for IL-33 release, prior work showing RAGE regulates IL-33 upregulation in the lung is a critical finding related to the pathogenesis of both asthma and CF. Single nucleotide polymorphisms in IL-33 are associated with asthma diagnosis, while IL-33 is found to be upregulated in basal epithelial cells in CF patient lung explants [326,356]. The latter finding may also inform future experiments to investigate how RAGE regulates IL-33 release in basal epithelial cells in models of CF.

Interestingly, when CF HBECs are exposed to *P. Aeruginosa* expression of IL-33 increases through regulation by toll-like receptors, which have significant structural similarity to RAGE [282,357]. Since *P. Aeruginosa* infection is seen in both asthma and CF patients, and is associated with pulmonary function in both patient populations, RAGE inhibition may deplete IL-33 production in models of *P. Aeruginosa* infection. This may lead to novel treatments for patients with asthma or CF presenting with a *P. Aeruginosa* infection [36,355].

Depletion of IL-33 through RAGE inhibition has also been shown *in vivo* to reduce the activation of group-2 innate lymphoid cells (ILC2s), which produce IL-13 [114]. Concomitantly,

this study and others show RAGE plays a role in the direct effects of IL-13 induction of mucus production through activation of STAT6 in the bronchial epithelium (Fig. 10) [112]. This indicates RAGE inhibition in asthma and CF patients could target IL-13 induced mucus production and eosinophilia in the bronchial epithelium through reduced activation of STAT6, as well as through reduction of IL-33 expression in the lung that leads to the production of IL-13 from ILC2s [112,114,292]. In summary, RAGE plays a multifaceted role in type-2 airway inflammation seen in asthma and CF by regulating the production of IL-33 in the lung, the direct effects of IL-13 on the bronchial epithelium, and mucus production in response to exotoxin derived from *P. Aeruginosa*.

4.0 Future Directions

4.1 Rage regulation of mucus production in Cystic Fibrosis

4.1.1 Role of RAGE in CF

While RAGE expression, protein abundance and its mutations have been found to be associated with CF, prior studies have not addressed how RAGE may modulate lung inflammation in models of CF. This study asked how RAGE regulates type-2 airway inflammation using *in vitro* and *in vivo* models of CF. Prior work found RAGE mRNA and protein levels are elevated in the sputum of CF patients, while the anti-inflammatory RAGE isoform sRAGE was decreased in CF sputum compared to Non-CF patients [228]. Other studies have found RAGE single nucleotide polymorphisms (SNPs) are associated with decreased lung function in CF patients [293]. Since prior work implicated RAGE in multiple steps of type-2 airway inflammation, and since CF patients have higher levels of type-2 proinflammatory cytokines, increased mucus production and eosinophilia, we hypothesized RAGE may regulate type-2 airway inflammation in CF [37,112,114,288,307].

Recombinant human IL-13 (rIL-13) was used to induce mucus production in Non-CF and CF primary HBECs. Using the small molecule inhibitor of RAGE (FPS-ZM1), this study found RAGE regulates mucin gene expression, mucous hyperplasia, the expression of mucous metaplasia transcription factors and the production eotaxin-2 (Fig. 3-7). To understand how RAGE can modulate all these processes within CF HBECs, phosphorylation of STAT6 was analyzed using immunoblotting. STAT6 is a critical transcription factor required for mucin gene expression,

mucous metaplasia and transcription of eotaxin-2 [173,292,303]. Inhibition of RAGE using either FPS-ZM1 or dicer substrate siRNA (dsiRNA) targeted to RAGE was able to block phosphorylation of STAT6 during rIL-13 stimulation in CF HBECs (Fig. 9, 10). These studies are the first to mechanistically link previous associations between RAGE and CF lung function.

While this study shows RAGE may modulate these processes through activation of STAT6, this was only shown at 24 hours post transfection (Fig. 10 A). As well, it is not clear why knock-down of RAGE expression in Non-CF HBECs during rIL-13 stimulation did not block activation of STAT6 (Fig. 10 C, E). In order to address these unanswered question, future *in vitro* experiments will be proposed herein. Alternative experiments will also be proposed to better understand how RAGE and its isoforms may play a role in CF type-2 airway inflammation.

4.1.2 *Pseudomonas aeruginosa* driven type-2 airway inflammation in CF

To induce type-2 airway inflammation *in vivo,* exotoxin derived from *P. aeruginosa* was administered intranasally to WT and RAGE-/- mice. *P. aeruginosa* is the most common lung infection in adult CF patients [358]. Concomitantly, infection with *P. aeruginosa* is associated with decreased lung function and increased mortality in CF patients [90,309]. These infections are particularly troublesome since the gram-negative bacteria develop viscous mucus biofilms, which aid in the development of antibiotic resistant strains of *P. aeruginosa* and limit antibiotic effectiveness [38]. In order to model this infection *in vivo*, researchers utilize exotoxin, the most potent antigen present on the cell wall of the bacteria [315]. Since studies have found type-2 proinflammatory cytokines are associated with *P. aeruginosa* infection in CF patients, we hypothesized RAGE may regulate exotoxin induced type-2 airway inflammation *in vivo* [36,37].

The exotoxin treatment schedule based on prior work using this model [88]. After intranasal treatment of WT and RAGE-/- C57BL/6 mice with exotoxin (50 μg) for seven days, whole lung sections, RNA and the bronchoalveolar lavage fluid (BALF) were harvested. Intriguingly, RAGE-/- mice were protected from exotoxin driven type-2 airway inflammation using PAS staining of whole lung sections (Fig. 11 M-Q). RT-qPCR analysis of whole lung RNA showed increases in *Il-13* and *Clca1* expression in WT mice treated with exotoxin, though this was absent in RAGE-/- mice (Fig. 11 R). Using ELISA analysis of the BALF, we found a similar increase in the production of eotaxin-2 in WT mice treated with exotoxin, which was absent in the RAGE-/- animals (Fig. 11 S).

Intriguingly, STAT6-/- mice are also protected from type-2 airway inflammation during exotoxin treatment [88]. Pairing these results with our *in vitro* data indicates RAGE may modulate type-2 airway inflammation through phosphorylation of STAT6 (Fig. 9, 10). Importantly, prior studies show RAGE-/- have reduced activation of STAT6 over time after stimulation with IL-13. While RAGE-/- mice were protected from type-2 airway inflammation using PAS staining, there were no significant increases in expression of *Il-13*, *Clca1* or eotaxin-2 production (Fig. 11 R, S). This indicates exotoxin treatment for one-week was not sufficient to induce a robust type-2 immune response in these animals. Conversely, prior studies indicate treatment for one-week with exotoxin increases mucus production in the airways, while at 16 hours post treatment mice develop small airway constriction and neutrophil influx [315,359]. In the future, it will be pertinent to increase exotoxin exposure and to verify if RAGE-/- mice treated with exotoxin have reduced activation of STAT6 when compared to WT treated animals. To address these unanswered questions, future experiments are proposed herein.

4.1.3 Future investigations: Regulation of type-2 airway inflammation in CF

4.1.3.1 Extended dsiRNA *in vitro* experiments

To further explore RAGE regulation of pSTAT6, it would be useful to carry out longer term dsiRNA knock-down experiments. Non-CF and CF HBECs could first be transfected with the same control or RAGE targeted dsiRNA constructs for six hours. After 20 hours post transfection, cells could then be stimulated with rIL-13 for four hours to induce phosphorylation of STAT6 (Fig. 25 A). Preliminary data show dsiRNA knock-down is present at 48 hours and CF HBECs maintain activation of STAT6 longer than Non-CF HBECs (Fig. 25 B, C). Indeed, Non-CF HBECs treated with rIL-13 had no pSTAT6 present at 48 hours using western blot analysis (Fig. 25 B). This further supports CF HBECs are hyperresponsive to rIL-13 treatment and that RAGE regulates this sustained phosphorylation of STAT6.

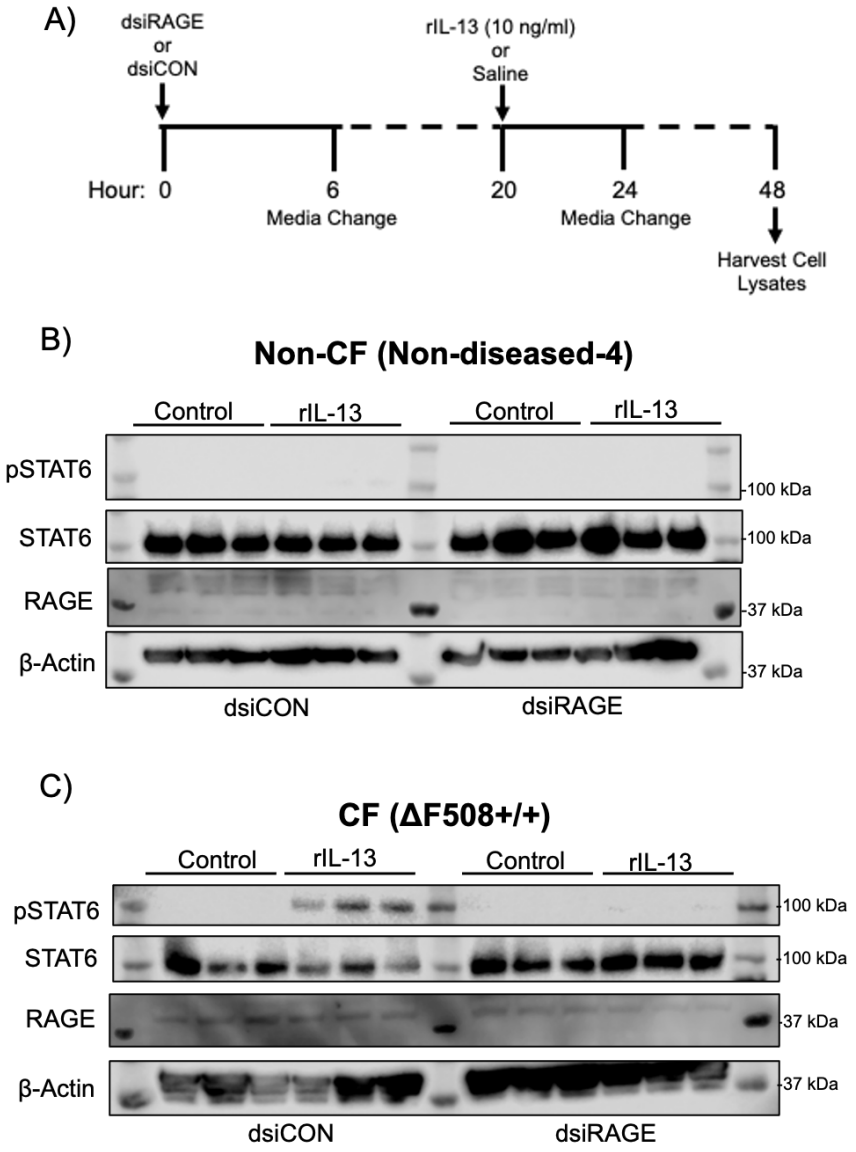

Figure 25: CF HBECs have sustained activation of STAT6

Undifferentiated primary Non-CF and CF HBECs were first transfected with either a non-targeted dsiRNA (dsiCON, 100 nM) construct or a pool of three dsiRNA constructs targeted to RAGE expression (dsiRAGE, 100 nM). Transfection was carried out using RNAiMax in antibiotic free media for six hours, after which the media was changed (A). Cells were then treated with rIL-13 dissolved in saline (10 ng/ml in media) or saline as the vehicle control for four hours before RNA or cell lysates were harvested at 48 hours (A). Cell lysates from Non-CF and CF HBECs were subjected to gel electrophoresis and immuno-blotting to detect protein abundance of RAGE, STAT6, pSTAT6 and β-Actin (B, C). N=2.

4.1.3.2 Exotoxin *in vitro* experiments

It would also be valuable to investigate if RAGE regulates mucus production and mucous hyperplasia in response to *P. aeruginosa* exotoxin. RAGE-/- mice have lower grades of mucus production when compared to WT mice treated with exotoxin derived from *P. aeruginosa* (Fig. 11 M-Q). This was based on prior studies using exotoxin as a model to induce typ-2 airway inflammation in mice. These studies also treated human bronchial epithelial cell lines with exotoxin and found exotoxin induced mucous hyperplasia and increased expression of mucin genes *MUC5B* and *MUC5AC* [89,294]. To see if RAGE may regulate the direct effects of exotoxin on the bronchial epithelium, Non-CF and CF HBECs could be treated with FPS-ZM1 and exotoxin (12.5 μg/ml) for 48 and 96 hours. In order to test RAGE's role in this process, experimental groups of HBECs would be treated with FPS-ZM1 one hour before exotoxin stimulation. Upon harvesting cell lysates for RNA, mucin gene expression and the expression of mucous metaplasia transcription factors could be analyzed using RT-qPCR. Since RAGE regulates the direct of IL-13, and since P. aeruginosa infection increases IL-13 levels, it is plausible that RAGE inhibition with FPS-ZM1 may block mucus production and the transcription of mucous metaplasia transcription factors in CF HBECs.

4.1.3.3 sRAGE in vitro experiments

Another avenue of investigation should study the relationship of CF and the RAGE isoform sRAGE. The most common transcript variant of membranous RAGE is soluble RAGE or sRAGE, which lacks the transmembrane domain [214,215]. This variant is released extracellularly and acts to sequester RAGE ligands and prevent canonical RAGE signaling pathways [220,221]. Thus, sRAGE could be used as a way to block RAGE signaling *in vitro*. Intriguingly, CF patients have reduced levels of sRAGE within their sputum [228]. Absence of sRAGE may then perpetuate

RAGE singling and subsequent inflammation since it is no longer present to act as a "decoy receptor".

In order to test if sRAGE could block IL-13 or exotoxin induced mucus production in CF HBECs, human sRAGE must first be purified. Human sRAGE could be purified from human lung tissue using similar methods described for purification of sRAGE from murine lung tissue [360]. Briefly, homogenized human lung tissue would first be mixed with A-Sepharose-4B before column compaction. The bulk eluate from this column would then be subjected to heparin-Sepharose chromatography and fractionization. Fractions containing sRAGE would be analyzed using SDS-PAGE gel electrophoresis followed by immunoblotting for human sRAGE. Pooled sRAGE fractions would then be dialyzed before anion-exchange chromatography. Final sRAGE containing fractions would then be lyophilized to obtain purified sRAGE, which could be confirmed using mass spectrometry.

Using a similar protocol as shown in Fig. 3 A, sRAGE could be administered to Non-CF and CF HBECs one hour before stimulation with rIL-13 or exotoxin. After 48 hours, cell lysates could be harvested for RNA or total protein. Conversely, at 48 hours HBECs could be given sRAGE again one hour before a second stimulation with rIL-13 or exotoxin. Cell lysates could be harvested at 96 hours post the first stimulation (Fig. 3 A). RT-qPCR analysis of RNA could then be used to see if sRAGE blocks mucin gene expression or the expression of mucous metaplasia transcription factors. Total protein could then be subjected to SDS-PAGE gel-electrophoresis and immunoblotting to see if sRAGE blocks activation of STAT6. Non-CF and CF HBECs treated with sRAGE and rIL-13 or exotoxin could also be fixed, and paraffin embedded for imaging analysis. PAS staining or IF staining of RAGE and MUC5AC could then illuminate if sRAGE reduces mucous hyperplasia or MUC5AC staining in CF HBECs (Fig. 4, 5). In summary, these

studies would begin to uncover if sRAGE would be a suitable treatment for CF patients lacking sRAGE.

4.1.3.4 G82S RAGE expression *in vitro*

Another avenue of investigation will be to investigate the RAGE single nucleotide polymorphism (rs2070600) associated with FEV1/FVC [98]. This SNP leads to an amino acid substitution (G82S) in RAGE's ligand-binding and enhances the binding affinity of the RAGE ligand S100A12, which stimulates mucus production and is associated with asthma [109,250]. Human phagocytes heterozygous for the G82S SNP enhances their production of proinflammatory cytokines, such as tumor necrosis factor-a (TNF-a) and IL-6, though increased phosphorylation of MEK and MAPK downstream of of STAT6 activation [109,292]. Thus, it could be hypothesized that G82S RAGE leads to increased phosphorylation of STAT6 in bronchial epithelial cells.

To express G82S in primary human bronchial epithelial cells (HBECs), clustered regulatory interspaced short-palindromic repeats (CRISPR) and the CRISPR associated peptide-9 (Cas9) endonuclease could be utilized. HBECs would first be transfected a plasmid containing Cas9 and a RAGE targeted single- stranded guide RNA (sgRNA) (5μg/5x106 cells) before cells undergo differentiation. The plasmid will also express red-fluorescent protein (RFP) with Cas9 to identify and isolate Cas9 expressing cells [208]. The experimental group of these cells will simultaneously receive a DNA olgio template containing the G82S RAGE SNP (5μg/5x106 cells). To integrate G82S RAGE into their genome, Cas9 will generate a double strand break (DSB) within the RAGE locus, and the G82S RAGE template will be integrated via homology dependent repair (HDR) [361]. Control cells will be transfected with a plasmid containing Cas9 with a non-targeting sgRNA, and a nonspecific DNA olgio template. The plasmids and oligos will be transfected into hiPSCs with a 4D-Nucleofector system via electroporation (Lonza). Transfected

HBECs will then be cultured for 48 hours and sorted of RFP+ cells using FACS. After 10 days, colonies of sufficient size will be chosen for clonal expansion and genetic screening using PCR primers for WT and G82S RAGE. Cells would then be treated with either rIL13 or exotoxin for 48 and 96 hours to determine if G82S RAGE increases phosphorylation of STAT6, which would be determined by SDS-PAGE gel electrophoresis and immunoblotting.

4.1.3.5 Extended exotoxin *in vivo* experiments

After intranasal stimulation of WT and RAGE-/- mice with exotoxin for seven days, *Il-13* expression and eotaxin-2 production in the BALF increased, but these were not significant. In order to create a more robust induction of type-2 airway inflammation in these animals, it would necessary to extend the exotoxin treatment in WT and RAGE-/- mice. Prior studies treated C57BL/6 mice intranasally with exotoxin isolated from *P. aeruginosa* for 1, 3, 6 and 12 weeks [88,89,294]. Schedules ranged from treating every day to treating every three days per week, where each treatment was 25 μg of exotoxin. To induce a more robust inflammatory response, WT and RAGE-/- should be intranasally administered 50 μg of exotoxin every day for 3-weeks. This will provide a greater challenge for RAGE-/- mice, since prior studies show 25 μg of exotoxin was able to induce mucous hyperplasia, increases in BALF type-2 proinflammatory cytokines and increases in immune cell recruitment to the lung [88,294]. To confirm the new treatment schedule induces robust type-2 airway inflammation and that RAGE modulates this response to exotoxin, similar analyses should be conducted, including PAS staining of whole lung sections, ELISA of BALF eotaxin-2 production and RT-qPCR of whole lung RNA for *Il-13* expression and other genes upregulated during type-2 airway inflammation. In addition, activation via phosphorylation of

STAT6 should be analyzed from whole lung homogenates using SDS-PAGE gel electrophoresis followed by immunoblotting for STAT6, pSTAT6, RAGE and β-Actin.

4.1.3.6 sRAGE *in vivo* experiments

To support the above proposed *in vitro* experiments using sRAGE to block RAGE signaling, *in vivo* experiments using the RAGE isoform should also be considered. As mentioned previously, sRAGE acts a "decoy receptor" for RAGE ligands and lacks the transmembrane domain [214,360]. Sputum sRAGE is decreased in CF patients and lower levels of sRAGE within plasma are associated with decreased lung function in idiopathic fibrosis and COPD patients [228,230,236]. In a murine model of chronic sepsis, intraperitoneal treatment with sRAGE (0.5 and 1 μg) one hour before cecal ligation significantly reduced lung inflammation and overall mortality [362]. Other studies have shown intraperitoneal administration of sRAGE in mice does not reach the lung, whereas intratracheal administration of sRAGE to mice significantly increases organ biodistribution to the lung [256]. Purification of sRAGE from murine lung tissue would be conducted based on a previously published protocol for administration to experimental mice [360].

Based on these studies, two groups of WT C57BL/6 mice could be established, where one is given an intratracheal administration of sRAGE (1 μg) and the other a vehicle control. After one hour, both groups of mice would receive an intranasal treatment with exotoxin (50 μg). Following a 3-week schedule, intratracheal administration with sRAGE would occur every day one-hour before intranasal administration with exotoxin. Subsequent harvesting of whole lung sections, whole lung RNA and the BALF would then allow for characterization of type-2 airway inflammation in these animals. Since reduced plasma sRAGE is associated with reduced lung function, it is possible sRAGE, by blocking RAGE signaling, may alleviate exotoxin induced type-

2 airway inflammation. This would be evidenced by decreased PAS stain positivity, decreased mucin gene expression and reduced BALF immune cell accumulation in sRAGE treated animals.

4.2 IL-33 release during allergic airway inflammation

4.2.1 Role of IL-33 in type-2 AAI

IL-33 is a potent initiator of type-2 allergic airway inflammation (AAI). This is based on *in vivo* studies showing the cytokine alarmin induces robust ILC2 proliferation and subsequent production of IL-5 and IL-13 when compared to other lung epithelial derived alarmins [141,167]. Concomitantly, variants in IL-33 are associated with asthma and IL-33 is elevated COPD versus Non-COPD human lung tissue [150,326,348]. Prior studies show RAGE regulates IL-33 accumulation in the lung during allergen exposure, but do not address which specific lung epithelial cell(s) is responsible for its release. IL-33 is upregulated in the whole lung homogenates of WT mice exposed to the allergen *Alternaria alternata* (*AA*), though is significantly depleted in RAGE-/- mice [114]. It is crucial to understand which lung epithelial cell(s) regulate this process to enhance our understanding of type-2 AAI and to develop cell specific therapeutics for the treatment of asthma.

The studies presented here began to address the question: Which RAGE expressing lung epithelial cell type is responsible for IL-33 release? Work done by Shirasawa et al. showed RAGE is a developmental biomarker for type-1 alveolar epithelial cells (ATIs) [338]. Since ATIs are adjacent to the vasculature, enabling IL-33 to signal immune cell activation, it was hypothesized ATIs could be the RAGE expressing lung epithelial cell responsible for IL-33 release. Though,

using primary murine ATIs and stem cell derived alveolar organoids, IL-33 was not detected in response to allergen stimulation with *AA* (Fig. 21, 24). In order to better elucidate this mechanism, it is important to understand which lung epithelial cells have been identified to express or release IL-33 in response to allergic stimuli. This information can then be used to develop novel experiments to uncover where IL-33 is released in the lung and how RAGE may regulate this process.

4.2.2 Lung epithelial cell type expression of IL-33

While many different lung epithelial cells have been identified to express IL-33 in models of airway inflammation, mainly human bronchial epithelial cells (HBECs) have been shown to release IL-33 extracellularly in response to allergic stimuli. This is an important distinction since upon its release during cell necrosis or allergen stimulation, IL-33 acts as a cytokine alarmin activating inflammation and airway remodeling [202,321–323]. Conversely, IL-33 expression itself does not fully describe how it regulates type-2 AAI during allergen exposure.

In vitro studies looking for IL-33 outside the cell have either used cell lines or primary HBECs. Primary HBECs exposed to *AA* were shown to release IL-33 from the nucleus after four hours [202]. Another group using the bronchial cell line Beas-2bs showed these cells do not release IL-33 after one hour of stimulation with either house dust mite (HDM), *AA*, *Acetosella vulgaris* (buckwheat) or *Betula pendula* (silver birch) [201]. Importantly, these studies differ in the methods used to detect IL-33 release. While Kouzaki et al. used immunofluorescencent labeling of IL-33 in fixed HBEC sections, Ramu et al. used ELISA to detect IL-33 in the media supernatants. These studies highlight the importance of what allergic stimuli was used, the exposure time, the cell type/line and the methods used to detect IL-33 release.

In vivo studies had identified even more lung cell types that express IL-33 in models of type-2 airway inflammation, including basal cells, serous cells and type-2 alveolar epithelial cells (ATIIs) [150,151,341]. Though, only ATIIs have also been implicated in IL-33 release *in vivo*. Mice stimulated with influenza virus for 72 hours had increased IL-33 labeling in ATIIs and had elevated IL-33 present within the bronchoalveolar lavage fluid (BALF) [151]. ATIIs have also been found to express IL-33 in murine models of COPD and aspirin-exacerbated respiratory disease (AERD) [150,341]. Other than ATIIs, serous cells have been identified to express IL-33 in a murine model of COPD, while only basal cells were found to express IL-33 in human COPD lung tissue [150]. This study found no IL-33 expression in basal cells, goblet cells or ciliated bronchial cells in the murine COPD model, while no IL-33 expression was found in goblet cells, serous cells or ciliated bronchial cells in the human COPD lung tissue [150].

Since these studies only looked at colocalization of IL-33 with a specific cell type marker and did not probe for IL-33 in the BALF, it remains unclear if these cells may release IL-33 after exposure to the inflammatory stimulus. In WT mice treated with intranasal *AA*, production of IL-33 is significantly increased in the whole lung homogenates. Conversely, global RAGE-/- mice treated with *AA* do not upregulate production of IL-33. Contrary to prior studies showing IL-33 is present in the nucleus and is released into the extracellular environment upon allergen stimulation, thus not upregulated through gene expression of *IL-33*, there was no detectible IL-33 within the control treated WT or RAGE-/- animal whole lung homogenates [114,202]. This suggest IL-33 does not reside in lung epithelial cells *in vivo* and is transcribed upon allergen stimulation. Indeed, other studies detected low levels of IL-33 in lung epithelial cells in control treated animals where IL-33 was found to significantly increase in animals treated with Sendai virus, influenza or HDM [150,151,341]. Considering the differences between these studies looking at IL-33 release or

expression in models of airway inflammation, new experimental designs are needed to elucidate the true mechanism of IL-33 release during allergen stimulation.

4.2.3 Future investigations: cell specific IL-33 release during type-2 AAI

4.2.3.1 Murine *in vivo* and *in vitro* experiments

The most efficient strategy to determine which lung epithelial cell(s) upregulate and release IL-33 in the context of allergen stimulation would be to first stimulate *IL-33* reporter mice with *AA*. Prior studies investigating localization of *IL-33* expression after stimulation with Sendai virus used heterozygous *IL-33* gene trap mice (*IL-33*$^{Wt/Gt}$), where IL-33 expression is maintained in one allele and blocked in the second allele due to insertion of a *LacZ* reporter in intron-1 of the *IL-33* gene locus [363]. This allows heterozygous *IL-33* gene trap mice to produce IL-33, inducing IL-13 accumulation and mucus production, while also labeling IL-33 expressing lung epithelial cell types through expression of the β-gal reporter [150]. After intranasal stimulation with Alternaria for 10 days every three days, whole lung sections would be obtained from these animals and stained for β-gal, DAPI and lung epithelial cell specific markers to determine which lung epithelial cell types express *IL-33* [114,150]. This experiment would then inform *in vitro* experiments testing the hypothesis that RAGE may regulate IL-33 release in response to allergen stimulation. Several *in vitro* models could be used, including 1) primary murine lung cells 2) primary human lung cells or 3) human induced pluripotent stem cells (hiPSCs) differentiated to specific lung cell types.

For primary murine lung cells, ATIIs and serous cells could be isolated from enzymatically digested mouse lung tissue using fluorescence activated cell sorting (FACS) for positive markers of ATIIs or serous cells, while also negatively sorting for other cell types, such as endothelial cells or leucocytes (see Fig. 15, 18). ATIIs have been shown in mice to express and release IL-33 during

stimulation with influenza or Sendai viruses, while serous cells have been shown to express IL-33 in mice treated with Sendai virus [151,167]. However, the proposed *in vivo* experiment using *AA* stimulation in *IL-33* reporter mice would uncover which lung epithelial cell types upregulate IL-33 in response to allergen stimulation.

To test the hypothesis that RAGE may regulate IL-33 release during allergen stimulation, cells found to upregulate *IL-33* should be isolated from WT and RAGE-/- mice. For example, WT and RAGE-/- cultures of ATIIs and serous cells could then be treated with an assortment of allergens including house dust mite (HDM), *AA*, *Acetosella vulgaris* (buckwheat) or *Betula pendula* (silver birch) for 4 hours. This is based on the *in vitro* studies showing IL-33 was released outside the cell after 4 hours using *AA* treatment, but was not seen after only one hour of *AA* treatment [201,202]. However, it would applicable to conduct a time course of 2, 4, 6- and 8-hour stimulations to determine the time required for IL-33 expression and release from these epithelial cells. IL-33 expression and release could then be quantified by RT-qPCR, ELISA or by fixing lung epithelial cell cultures for immunofluorescent labeling of IL-33. Coculture of these lung epithelial cells could also be treated with allergens to see if multiple cell types are required for IL-33 release. This is because multiple lung epithelial cells have been found to upregulate IL-33 in models of asthma, chronic obstructive pulmonary disorder and during viral infection [150,151,202]. Conversely, IL-33 release from a specific cell type may be dependent on the specific stimuli since these studies used different approaches to induce type-2 lung inflammation.

4.2.3.2 Human *in vitro* experiments

Experiments using primary human lung cells or hiPSC derived lung organoids could use either ATIIs or HBECs. This is based on studies showing ATIIs in COPD human lung tissue express high levels of IL-33, and HBEC cultures stimulated with the allergen *AA* have been found

to release IL-33 after 4 hours [150,202]. Though, cell type selection should be informed by *in vivo* experiments using heterozygous *IL-33* gene trap mice. For isolation of ATIIs or HBECs from human lung tissues, FACS could be used to select for cells expressing markers for these cell types while negatively selecting for other lung cells, endothelial cells or leukocytes. FACS gating strategies used in this study were adapted from Nakano et al. and could also be applied to enzymatically digested human lung tissue [346]. To test if RAGE regulates IL-33 release from these primary human lung cells, the small molecular inhibitor of RAGE, FPS-ZM1, could be administered one hour before allergen stimulation to block RAGE signaling. Multiple allergens should be used to see if RAGE may play a role during specific allergic stimuli.

Recent methods have been developed to differentiate hiPSCs into lung epithelial cells of the alveolus and the bronchus [95,208]. In the second study, hiPSC derived alveolar organoids mainly comprised of ATIIs were exposed to the allergen *AA* for 6 hours (Fig. 23). Though, ELISA analysis showed no IL-33 was present in the media or matrigel supernatants (Fig. 24). Previous studies have shown these organoids do not express RAGE, though other studies have shown ATIIs can express the pattern recognition receptor [208,364]. Further experiments should verify RAGE expression in the hiPSC derived ATIIs using RT-qPCR. If they do express RAGE, then FPS-ZM1 could be used to determine if RAGE plays a role in IL-33 release from hiPSC derived alveolar organoids.

hiPSC derived bronchial epithelial cell organoids have also been developed [95]. Since prior studies have shown primary HBECs can release IL-33, it would be of interest to see if bronchial organoids mimic the immunological functions seen in primary HBECs. In order to test RAGE's role in IL-33 release from bronchial organoid cultures, RAGE expression should be verified via RT-qPCR. If the HBEC organoid model indeed expresses RAGE, then two groups of

organoid cultures could be established, where one receives only the allergic stimuli and the other is treated with the RAGE inhibitor FPS-ZM1 before allergen stimulation. A time course of 2, 4, 6- and 8- hours should be used to determine the time required for IL-33 expression and release. As stated before, IL-33 release could be analyzed in the media and matrigel supernatants from these cultures using ELISA. In addition to inhibiting RAGE pharmacologically, it would be beneficial to knock-down RAGE expression. This could be done by transfecting siRNA targeted to RAGE in these organoid cultures before allergen stimulation and could be compared to cells given a scramble or non-targeted siRNA construct before allergen stimulation.

Appendix A

Multiple samples of CF and Non-CF HBECs were used for pharmacological inhibition and knock-down of RAGE expression experiments. Mutations and prior disease states of these samples are listed below if known.

Table 1: Non-CF and CF HBEC samples

Sample	Disease State	CFTR Mutation
1	CF	ΔF508+/- (Class II)
2	COPD	-
3	CF	unknown
4	Non-diseased-1	-
5	CF	unknown
6	Bronchopulmonary Dysplasia	-
7	CF	ΔF508+/1717-G>A (Class I & II)
8	Non-diseased-2	-
9	CF	3120 G> A +/- (Class V)
10	IPF	-
11	CF	unknown
12	IPF	-
13	CF	ΔF508+/G542X (Class I & II)
14	ILD, RA	-
15	CF	ΔF508+/+ (Class II)
16	Non-diseased-3	-
17	CF	ΔF508+/+ (Class II)
18	Non-diseased-4	-

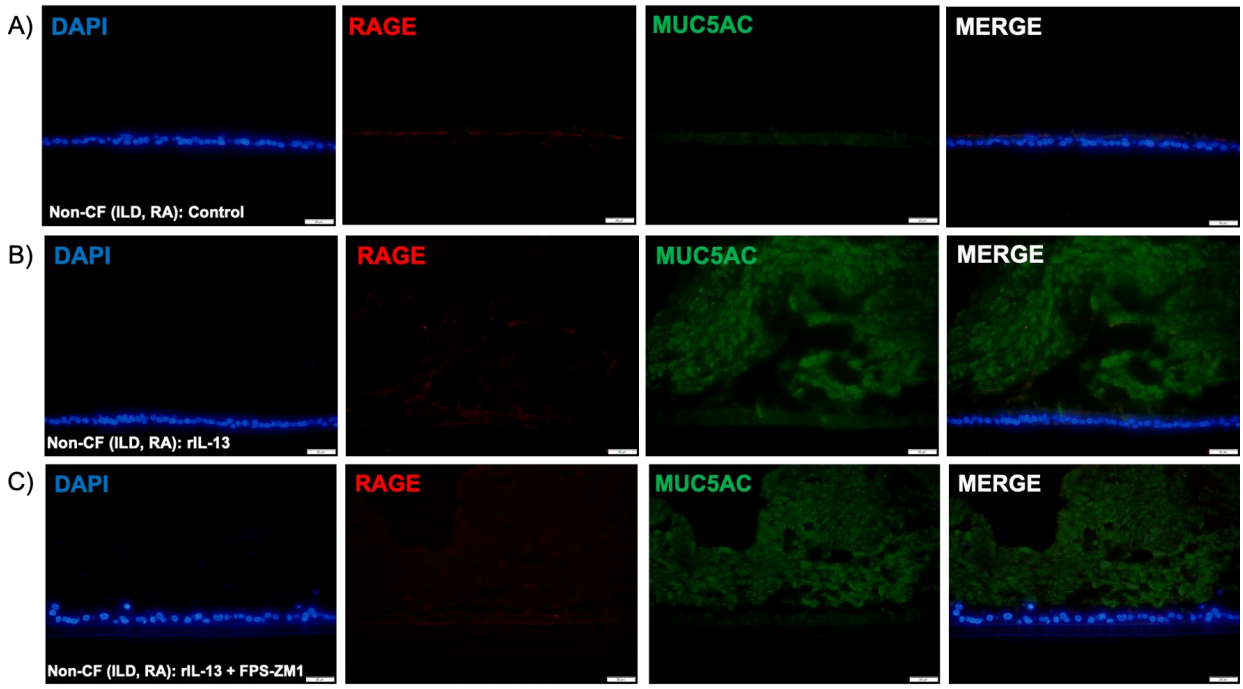

Figure 26: Immunofluorescent images of Non-CF HBECs

Pre-merge immunofluorescent images of Non-CF HBECs cross-sections during control conditions (A), rIL-13 stimulation (B) and RAGE inhibition with FPS-ZM1 (C). Primary antibodies used to target RAGE and MUC5AC were diluted at 1:100 ratio. Secondary antibodies, goat anti-rabbit IgG at (546 nm-red, RAGE) and goat anti-mouse IgG1 (488 nm-green, MUC5AC), were dissolved in PBS at a 1:500 ratio. Nuclei were stained using DAPI. Prior disease states of the Non-CF HBECs were interstitial lung disease (ILD) and rheumatoid arthritis (RA). Images were taken at 200X magnification. Scale bars = 20 µm.

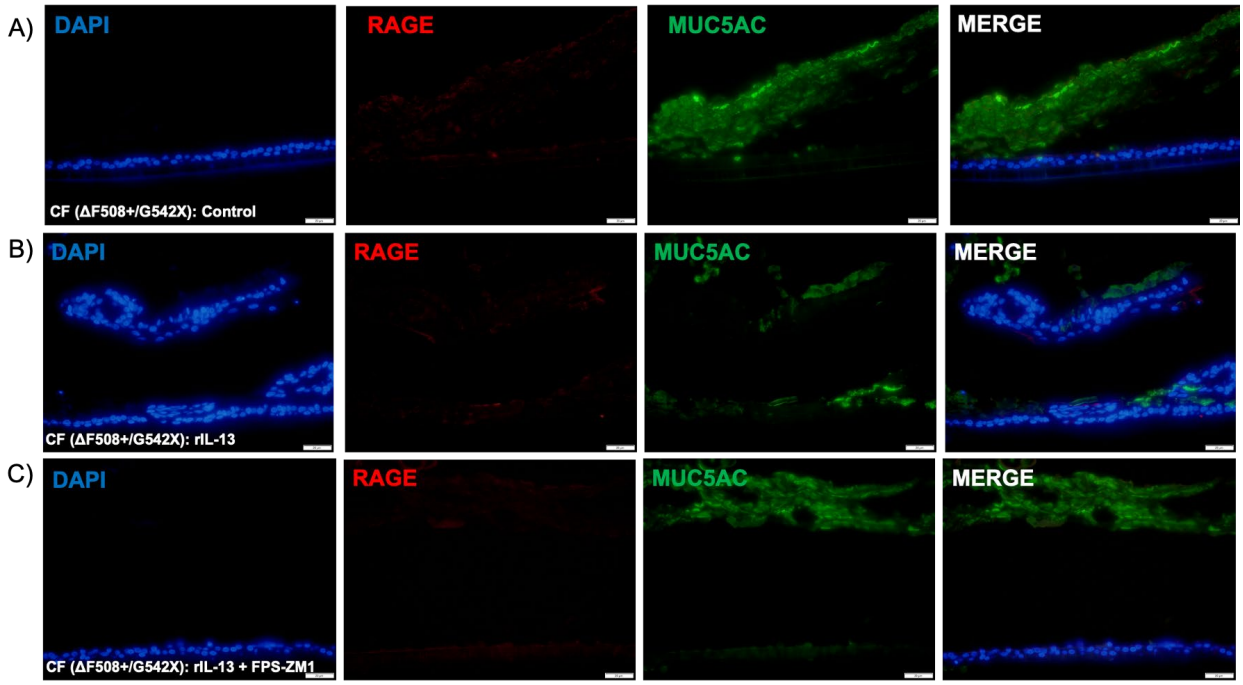

Figure 27: Immunofluorescent images of CF HBECs

Pre-merge immunofluorescent images of CF HBECs cross-sections during control conditions (A) rIL-13 stimulation (B) and RAGE inhibition with FPS-ZM1 (C). Primary antibodies used to target RAGE and MUC5AC were diluted at 1:100 ratio. Secondary antibodies, goat anti-rabbit IgG at (546 nm-red, RAGE) and goat anti-mouse IgG1 (488 nm-green, MUC5AC), were dissolved in PBS at a 1:500 ratio. Nuclei were stained using DAPI. CFTR mutations for the CF HBECs were of class I (G542X) and II (ΔF508+). Images were taken at 200X magnification. Scale bars = 20 μm.

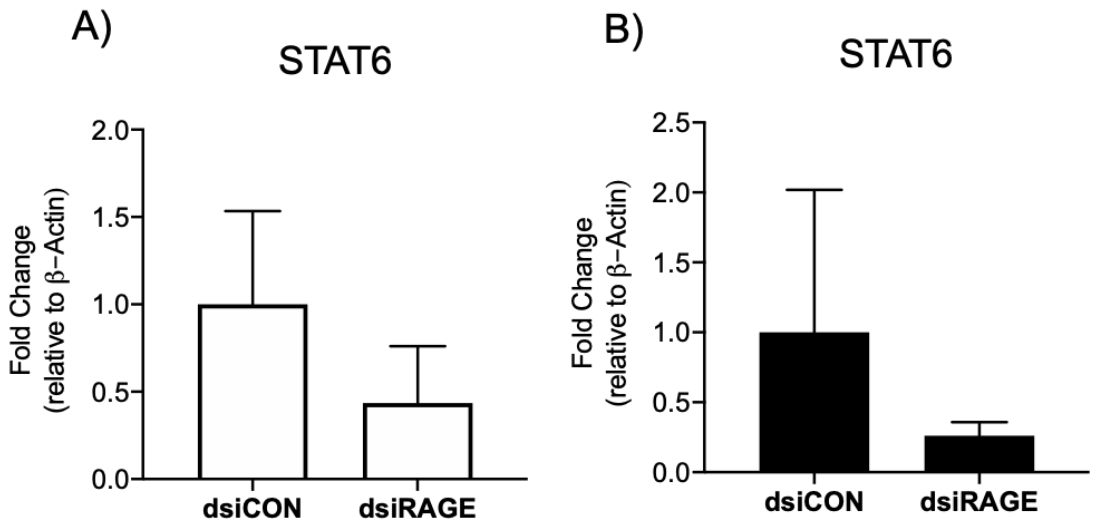

Figure 28: Total STAT6 is not significantly depleted at 24 hours

Fold change expression of STAT6 for Non-CF (white, A) and CF HBECs (black, B) were calculated using Image Studio densitometry software and means represent three replicates for each culture condition. Statistical significance was determined using an Unpaired Student's T-test, $p<0.05$ was considered significant, N=2.

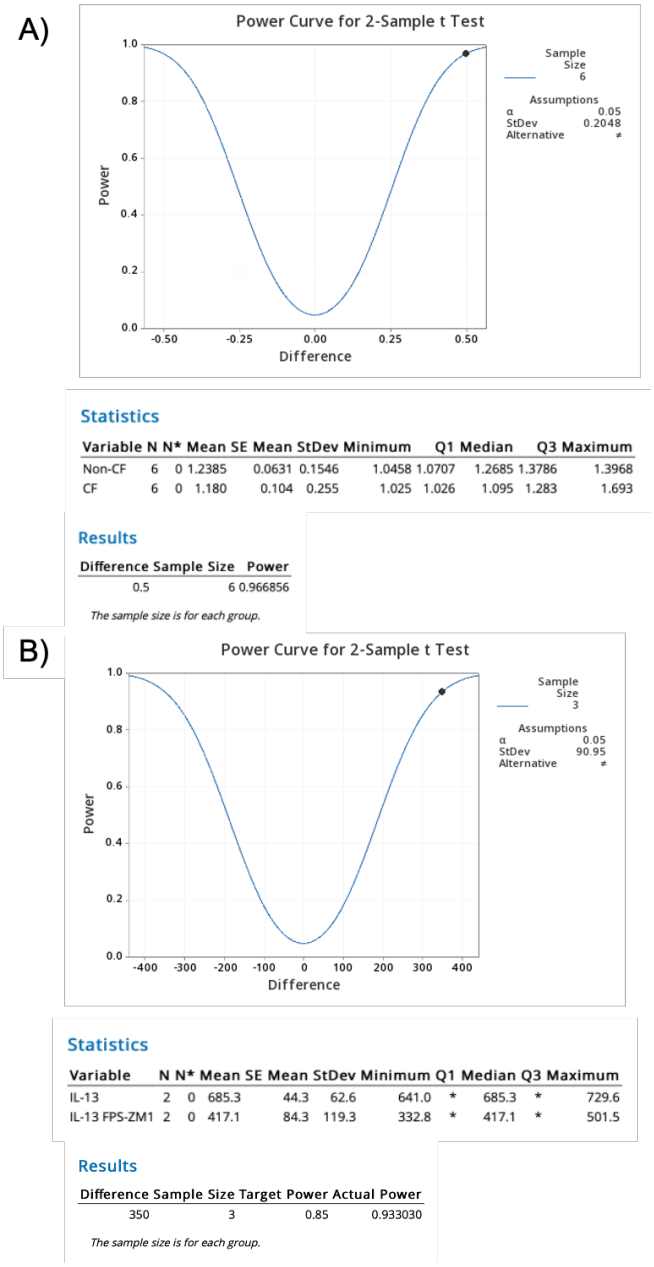

Figure 29: Power analyses on *RAGE* expression and RAGE inhibition experiments

Power analyses were conducted in Minitab (Trialware, State College, PA) to determine if there was adequate statistical power for the *RAGE* expression analysis (Fig. 2, 29 A), and to determine the sample size required for future RAGE inhibition experiments looking at phosphorylation of STAT6 (Fig. 9, 29 B). Statistical power was determined in 29 A (1-β=0.967), whereas in 29 B sample size per treatment group or n was solved for based on a power set to 0.85 (n=3).

A)

Brown-Forsythe test-*MUC5AC*	Non-CF, 48 hours
F (DFn, DFd)	0.7463 (2, 6)
P value	0.5135
P value summary	ns
Are SDs significantly different (P < 0.05)?	No

B)

Brown-Forsythe test-*MUC5AC*	CF, 48 hours
F (DFn, DFd)	0.7195 (2, 6)
P value	0.5247
P value summary	ns
Are SDs significantly different (P < 0.05)?	No

C)

Brown-Forsythe test-*MUC5AC*	Non-CF, 96 hours
F (DFn, DFd)	5.796 (2, 9)
P value	0.0241
P value summary	*
Are SDs significantly different (P < 0.05)?	Yes

D)

Brown-Forsythe test-*MUC5AC*	CF, 96 hours
F (DFn, DFd)	3.169 (2, 9)
P value	0.0908
P value summary	ns
Are SDs significantly different (P < 0.05)?	No

Figure 30: Brown-Forsythe test for *MUC5AC* expression at 48 and 96 hours

The Brown-Forsythe test was conducted for *MUC5AC* expression from Fig. 3 A and D to test for equal variance. The Brown-Forsythe was conducted using GraphPad PRISM 8 software where a $P<0.05$ is considered significant. If $P<0.05$, then the variance is statistically different for a gene's expression. If P is >0.05 variance is not statistically different. Since ANOVA is robust to changes in variance if the sample size is equal, a 3-WAY ANOVA was used to analyze the three effects on gene expression followed by Bonferroni's multiple comparisons test that does not require equal variance: CF, IL13 and the RAGE inhibitor.

A)

Brown-Forsythe test-*CLCA1*	Non-CF, 48 hours
F (DFn, DFd)	1.089 (2, 6)
P value	0.3950
P value summary	ns
Are SDs significantly different (P < 0.05)?	No

B)

Brown-Forsythe test-*CLCA1*	CF, 48 hours
F (DFn, DFd)	3.859 (2, 6)
P value	0.0837
P value summary	ns
Are SDs significantly different (P < 0.05)?	No

C)

Brown-Forsythe test-*SPDEF*	Non-CF, 48 hours
F (DFn, DFd)	1.287 (2, 6)
P value	0.3427
P value summary	ns
Are SDs significantly different (P < 0.05)?	No

D)

Brown-Forsythe test-*SPDEF*	CF, 48 hours
F (DFn, DFd)	2.847 (2, 6)
P value	0.1351
P value summary	ns
Are SDs significantly different (P < 0.05)?	No

E)

Brown-Forsythe test-*FOXA3*	Non-CF, 48 hours
F (DFn, DFd)	1.285 (2, 6)
P value	0.3431
P value summary	ns
Are SDs significantly different (P < 0.05)?	No

F)

Brown-Forsythe test-*FOXA3*	CF, 48 hours
F (DFn, DFd)	0.07084 (2, 6)
P value	0.9324
P value summary	ns
Are SDs significantly different (P < 0.05)?	No

Figure 31: Brown-Forsythe test for *CLCA1*, *SPDEF* and *FOXA3* expression at 48 hours

The Brown-Forsythe test was conducted for *CLCA1, SPDEF* and *FOXA3* expression from Fig. 6 A to test for equal variance. The Brown-Forsythe was conducted using GraphPad PRISM 8 software where a $P<0.05$ is considered significant. If $P<0.05$, then the variance is statistically different for a gene's expression. If P is >0.05 variance is not statistically different. Since ANOVA is robust to changes in variance if the sample size is equal, a 3-WAY ANOVA was used to analyze the three effects on gene expression followed by Bonferroni's multiple comparisons test that does not require equal variance: CF, IL13 and the RAGE inhibitor.

A)

Brown-Forsythe test-*CLCA1*	Non-CF, 96 hours
F (DFn, DFd)	1.700 (2, 9)
P value	0.2364
P value summary	ns
Are SDs significantly different (P < 0.05)?	No

B)

Brown-Forsythe test-*CLCA1*	CF, 96 hours
F (DFn, DFd)	12.05 (2, 9)
P value	0.0028
P value summary	**
Are SDs significantly different (P < 0.05)?	Yes

C)

Brown-Forsythe test-*SPDEF*	Non-CF, 96 hours
F (DFn, DFd)	5.661 (2, 9)
P value	0.0256
P value summary	*
Are SDs significantly different (P < 0.05)?	Yes

D)

Brown-Forsythe test-*SPDEF*	CF, 96 hours
F (DFn, DFd)	1.742 (2, 9)
P value	0.2294
P value summary	ns
Are SDs significantly different (P < 0.05)?	No

E)

Brown-Forsythe test-*FOXA3*	Non-CF, 96 hours
F (DFn, DFd)	10.30 (2, 9)
P value	0.0047
P value summary	**
Are SDs significantly different (P < 0.05)?	Yes

F)

Brown-Forsythe test-*FOXA3*	CF, 96 hours
F (DFn, DFd)	6.305 (2, 9)
P value	0.0194
P value summary	*
Are SDs significantly different (P < 0.05)?	Yes

Figure 32: Brown-Forsythe test for *CLCA1*, *SPDEF* and *FOXA3* expression at 96 hours

The Brown-Forsythe test was conducted for *CLCA1, SPDEF* and *FOXA3* expression from Fig. 6 C to test for equal variance. The Brown-Forsythe was conducted using GraphPad PRISM 8 software where a $P<0.05$ is considered significant. If $P<0.05$, then the variance is statistically different for a gene's expression. If P is >0.05 variance is not statistically different. Since ANOVA is robust to changes in variance if the sample size is equal, a 3-WAY ANOVA was used to analyze the three effects on gene expression followed by Bonferroni's multiple comparisons test that does not require equal variance: CF, IL13 and the RAGE inhibitor.

Bibliography

[1] Xue R, Gu H, Qiu Y, Guo Y, Korteweg C, Huang J, et al. Expression of cystic fibrosis transmembrane conductance regulator in ganglia of human gastrointestinal tract. Sci Rep 2016;6:30926. doi:10.1038/srep30926.

[2] Kreindler JL. Cystic fibrosis: exploiting its genetic basis in the hunt for new therapies. Pharmacol Ther 2010;125:219–29. doi:10.1016/j.pharmthera.2009.10.006.

[3] Locher KP. Mechanistic diversity in ATP-binding cassette (ABC) transporters. Nat Struct Mol Biol 2016;23:487–93. doi:10.1038/nsmb.3216.

[4] Moran O. The gating of the CFTR channel. Cell Mol Life Sci 2017;74:85–92. doi:10.1007/s00018-016-2390-z.

[5] Frizzell RA, Halm DR, Rechkemmer G, Shoemaker RL. Chloride channel regulation in secretory epithelia. Fed Proc 1986;45:2727–31.

[6] Cheng SH, Rich DP, Marshall J, Gregory RJ, Welsh MJ, Smith AE. Phosphorylation of the R domain by cAMP-dependent protein kinase regulates the CFTR chloride channel. Cell 1991;66:1027–36. doi:10.1016/0092-8674(91)90446-6.

[7] Marson FAL, Bertuzzo CS, Ribeiro JD. Classification of CFTR mutation classes. Lancet Respir Med 2016;4:e37–8. doi:10.1016/S2213-2600(16)30188-6.

[8] Bell SC, Mall MA, Gutierrez H, Macek M, Madge S, Davies JC, et al. The future of cystic fibrosis care: a global perspective. Lancet Respir Med 2020;8:65–124. doi:10.1016/S2213-2600(19)30337-6.

[9] Matos AM, Pinto FR, Barros P, Amaral MD, Pepperkok R, Matos P. Inhibition of calpain

1 restores plasma membrane stability to pharmacologically rescued Phe508del-CFTR variant. J Biol Chem 2019;294:13396–410. doi:10.1074/jbc.RA119.008738.

[10] De Boeck K, Amaral MD. Progress in therapies for cystic fibrosis. Lancet Respir Med 2016;4:662–74. doi:10.1016/S2213-2600(16)00023-0.

[11] Li SS, Tumin D, Krone KA, Boyer D, Kirkby SE, Mansour HM, et al. Risks associated with lung transplantation in cystic fibrosis patients. Expert Rev Respir Med 2018;12:893–904. doi:10.1080/17476348.2018.1522254.

[12] Quinton PM. Physiological basis of cystic fibrosis: a historical perspective. Physiol Rev 1999;79:S3–22. doi:10.1152/physrev.1999.79.1.S3.

[13] Saint-Criq V, Gray MA. Role of CFTR in epithelial physiology. Cell Mol Life Sci 2017;74:93–115. doi:10.1007/s00018-016-2391-y.

[14] Gibson-Corley KN, Meyerholz DK, Engelhardt JF. Pancreatic pathophysiology in cystic fibrosis. J Pathol 2016;238:311–20. doi:10.1002/path.4634.

[15] Khan D, Kelsey R, Maheshwari RR, Stone VM, Hasib A, Manderson Koivula FN, et al. Short-term CFTR inhibition reduces islet area in C57BL/6 mice. Sci Rep 2019;9:11244. doi:10.1038/s41598-019-47745-w.

[16] Hart NJ, Aramandla R, Poffenberger G, Fayolle C, Thames AH, Bautista A, et al. Cystic fibrosis-related diabetes is caused by islet loss and inflammation. JCI Insight 2018;3. doi:10.1172/jci.insight.98240.

[17] Barrio R. Management of endocrine disease: Cystic fibrosis-related diabetes: novel pathogenic insights opening new therapeutic avenues. Eur J Endocrinol 2015;172:R131-41. doi:10.1530/EJE-14-0644.

[18] Huang YJ, LiPuma JJ. The microbiome in cystic fibrosis. Clin Chest Med 2016;37:59–67.

doi:10.1016/j.ccm.2015.10.003.

[19] Reznikov LR, Dong Q, Chen J-H, Moninger TO, Park JM, Zhang Y, et al. CFTR-deficient pigs display peripheral nervous system defects at birth. Proc Natl Acad Sci USA 2013;110:3083–8. doi:10.1073/pnas.1222729110.

[20] Marcorelles P, Friocourt G, Uguen A, Ledé F, Férec C, Laquerrière A. Cystic fibrosis transmembrane conductance regulator protein (CFTR) expression in the developing human brain: comparative immunohistochemical study between patients with normal and mutated CFTR. J Histochem Cytochem 2014;62:791–801. doi:10.1369/0022155414546190.

[21] Reznikov LR. Cystic fibrosis and the nervous system. Chest 2017;151:1147–55. doi:10.1016/j.chest.2016.11.009.

[22] El-Salem K, Aburahma S, Rawashdeh M. Peripheral nerve dysfunction in patients with cystic fibrosis. J Clin Neurophysiol 2010;27:216–8. doi:10.1097/01.WNP.0b013e3181e0a9f9.

[23] Moran A, Dunitz J, Nathan B, Saeed A, Holme B, Thomas W. Cystic fibrosis-related diabetes: current trends in prevalence, incidence, and mortality. Diabetes Care 2009;32:1626–31. doi:10.2337/dc09-0586.

[24] Adriaanse MPM, van der Sande LJTM, van den Neucker AM, Menheere PPCA, Dompeling E, Buurman WA, et al. Evidence for a cystic fibrosis enteropathy. PLoS One 2015;10:e0138062. doi:10.1371/journal.pone.0138062.

[25] Frizzell RA, Hanrahan JW. Physiology of epithelial chloride and fluid secretion. Cold Spring Harb Perspect Med 2012;2:a009563. doi:10.1101/cshperspect.a009563.

[26] Guggino WB, Stanton BA. New insights into cystic fibrosis: molecular switches that regulate CFTR. Nat Rev Mol Cell Biol 2006;7:426–36. doi:10.1038/nrm1949.

[27] Lee RJ, Harlow JM, Limberis MP, Wilson JM, Foskett JK. HCO3(-) secretion by murine nasal submucosal gland serous acinar cells during Ca2+-stimulated fluid secretion. J Gen Physiol 2008;132:161–83. doi:10.1085/jgp.200810017.

[28] Cooper JL, Quinton PM, Ballard ST. Mucociliary transport in porcine trachea: differential effects of inhibiting chloride and bicarbonate secretion. Am J Physiol Lung Cell Mol Physiol 2013;304:L184-90. doi:10.1152/ajplung.00143.2012.

[29] Borowitz D. CFTR, bicarbonate, and the pathophysiology of cystic fibrosis. Pediatr Pulmonol 2015;50 Suppl 40:S24–30. doi:10.1002/ppul.23247.

[30] Quinton PM. Cystic fibrosis: impaired bicarbonate secretion and mucoviscidosis. Lancet 2008;372:415–7. doi:10.1016/S0140-6736(08)61162-9.

[31] Ko SBH, Zeng W, Dorwart MR, Luo X, Kim KH, Millen L, et al. Gating of CFTR by the STAS domain of SLC26 transporters. Nat Cell Biol 2004;6:343–50. doi:10.1038/ncb1115.

[32] Bertrand CA, Mitra S, Mishra SK, Wang X, Zhao Y, Pilewski JM, et al. The CFTR trafficking mutation F508del inhibits the constitutive activity of SLC26A9. Am J Physiol Lung Cell Mol Physiol 2017;312:L912–25. doi:10.1152/ajplung.00178.2016.

[33] Boucher RC. Cystic fibrosis: a disease of vulnerability to airway surface dehydration. Trends Mol Med 2007;13:231–40. doi:10.1016/j.molmed.2007.05.001.

[34] Li Z, Kosorok MR, Farrell PM, Laxova A, West SEH, Green CG, et al. Longitudinal development of mucoid Pseudomonas aeruginosa infection and lung disease progression in children with cystic fibrosis. JAMA 2005;293:581–8. doi:10.1001/jama.293.5.581.

[35] Hauser AR, Jain M, Bar-Meir M, McColley SA. Clinical significance of microbial infection and adaptation in cystic fibrosis. Clin Microbiol Rev 2011;24:29–70. doi:10.1128/CMR.00036-10.

[36] Hartl D, Griese M, Kappler M, Zissel G, Reinhardt D, Rebhan C, et al. Pulmonary T(H)2 response in Pseudomonas aeruginosa-infected patients with cystic fibrosis. J Allergy Clin Immunol 2006;117:204–11. doi:10.1016/j.jaci.2005.09.023.

[37] Tiringer K, Treis A, Fucik P, Gona M, Gruber S, Renner S, et al. A Th17- and Th2-skewed cytokine profile in cystic fibrosis lungs represents a potential risk factor for Pseudomonas aeruginosa infection. Am J Respir Crit Care Med 2013;187:621–9. doi:10.1164/rccm.201206-1150OC.

[38] Lucca F, Guarnieri M, Ros M, Muffato G, Rigoli R, Da Dalt L. Antibiotic resistance evolution of Pseudomonas aeruginosa in cystic fibrosis patients (2010-2013). Clin Respir J 2018;12:2189–96. doi:10.1111/crj.12787.

[39] Melvin JA, Montelaro RC, Bomberger JM. Clinical potential of engineered cationic antimicrobial peptides against drug resistant biofilms. Expert Rev Anti Infect Ther 2016;14:989–91. doi:10.1080/14787210.2016.1236687.

[40] Kiedrowski MR, Gaston JR, Kocak BR, Coburn SL, Lee S, Pilewski JM, et al. Staphylococcus aureus Biofilm Growth on Cystic Fibrosis Airway Epithelial Cells Is Enhanced during Respiratory Syncytial Virus Coinfection. MSphere 2018;3. doi:10.1128/mSphere.00341-18.

[41] West NE, Flume PA. Unmet needs in cystic fibrosis: the next steps in improving outcomes. Expert Rev Respir Med 2018;12:585–93. doi:10.1080/17476348.2018.1483723.

[42] Mainz J, Hammer U, Rokahr C, Hubler A, Zintl F, Ballmann M. Cystic fibrosis in 65- and 67-year-old siblings. Clinical feature and nasal potential difference measurement in patients with genotypes F508del and 2789+5G-->A. Respiration 2006;73:698–704. doi:10.1159/000093818.

[43] Castellani C, Assael BM. Cystic fibrosis: a clinical view. Cell Mol Life Sci 2017;74:129–40. doi:10.1007/s00018-016-2393-9.

[44] Schwarzenberg SJ, Hempstead SE, McDonald CM, Powers SW, Wooldridge J, Blair S, et al. Enteral tube feeding for individuals with cystic fibrosis: Cystic Fibrosis Foundation evidence-informed guidelines. J Cyst Fibros 2016;15:724–35. doi:10.1016/j.jcf.2016.08.004.

[45] Morton A, Wolfe S. Enteral tube feeding for cystic fibrosis. Cochrane Database Syst Rev 2015:CD001198. doi:10.1002/14651858.CD001198.pub4.

[46] Souza Dos Santos Simon MI, Forte GC, da Silva Pereira J, da Fonseca Andrade Procianoy E, Drehmer M. Validation of a Nutrition Screening Tool for Pediatric Patients with Cystic Fibrosis. J Acad Nutr Diet 2016;116:813–8. doi:10.1016/j.jand.2016.01.012.

[47] Oates GR, Stepanikova I, Rowe SM, Gamble S, Gutierrez HH, Harris WT. Objective Versus Self-Reported Adherence to Airway Clearance Therapy in Cystic Fibrosis. Respir Care 2019;64:176–81. doi:10.4187/respcare.06436.

[48] Wheatley CM, Baker SE, Daines CM, Phan H, Martinez MG, Morgan WJ, et al. Influence of the Vibralung Acoustical Percussor on pulmonary function and sputum expectoration in individuals with cystic fibrosis. Ther Adv Respir Dis 2018;12:1753466618770997. doi:10.1177/1753466618770997.

[49] Southern KW, Clancy JP, Ranganathan S. Aerosolized agents for airway clearance in cystic fibrosis. Pediatr Pulmonol 2019;54:858–64. doi:10.1002/ppul.24306.

[50] Yang C, Montgomery M. Dornase alfa for cystic fibrosis. Cochrane Database Syst Rev 2018;9:CD001127. doi:10.1002/14651858.CD001127.pub4.

[51] Wheatley CM, Morgan WJ, Cassuto NA, Foxx-Lupo WT, Daines CL, Morgan MA, et al.

Exhaled breath condensate detects baseline reductions in chloride and increases in response to albuterol in cystic fibrosis patients. Clin Med Insights Circ Respir Pulm Med 2013;7:79–90. doi:10.4137/CCRPM.S12882.

[52] Brewington JJ, Backstrom J, Feldman A, Kramer EL, Moncivaiz JD, Ostmann AJ, et al. Chronic β2AR stimulation limits CFTR activation in human airway epithelia. JCI Insight 2018;3. doi:10.1172/jci.insight.93029.

[53] Van Goor F, Hadida S, Grootenhuis PDJ, Burton B, Cao D, Neuberger T, et al. Rescue of CF airway epithelial cell function in vitro by a CFTR potentiator, VX-770. Proc Natl Acad Sci USA 2009;106:18825–30. doi:10.1073/pnas.0904709106.

[54] Bear CE. A Therapy for Most with Cystic Fibrosis. Cell 2020;180:211. doi:10.1016/j.cell.2019.12.032.

[55] Taylor-Cousar JL, Munck A, McKone EF, van der Ent CK, Moeller A, Simard C, et al. Tezacaftor-Ivacaftor in Patients with Cystic Fibrosis Homozygous for Phe508del. N Engl J Med 2017;377:2013–23. doi:10.1056/NEJMoa1709846.

[56] Wainwright CE, Elborn JS, Ramsey BW, Marigowda G, Huang X, Cipolli M, et al. Lumacaftor-Ivacaftor in Patients with Cystic Fibrosis Homozygous for Phe508del CFTR. N Engl J Med 2015;373:220–31. doi:10.1056/NEJMoa1409547.

[57] Rowe SM, Daines C, Ringshausen FC, Kerem E, Wilson J, Tullis E, et al. Tezacaftor-Ivacaftor in Residual-Function Heterozygotes with Cystic Fibrosis. N Engl J Med 2017;377:2024–35. doi:10.1056/NEJMoa1709847.

[58] Middleton PG, Mall MA, Dřevínek P, Lands LC, McKone EF, Polineni D, et al. Elexacaftor-Tezacaftor-Ivacaftor for Cystic Fibrosis with a Single Phe508del Allele. N Engl J Med 2019;381:1809–19. doi:10.1056/NEJMoa1908639.

[59] Jennings MT, Dezube R, Paranjape S, West NE, Hong G, Braun A, et al. An Observational Study of Outcomes and Tolerances in Patients with Cystic Fibrosis Initiated on Lumacaftor/Ivacaftor. Annals of the American Thoracic Society 2017;14:1662–6. doi:10.1513/AnnalsATS.201701-058OC.

[60] Rosenfeld M, Wainwright CE, Higgins M, Wang LT, McKee C, Campbell D, et al. Ivacaftor treatment of cystic fibrosis in children aged 12 to <24 months and with a CFTR gating mutation (ARRIVAL): a phase 3 single-arm study. Lancet Respir Med 2018;6:545–53. doi:10.1016/S2213-2600(18)30202-9.

[61] Rubin BK. Unmet needs in cystic fibrosis. Expert Opin Biol Ther 2018;18:49–52. doi:10.1080/14712598.2018.1484101.

[62] Frost FJ, Nazareth DS, Charman SC, Winstanley C, Walshaw MJ. Ivacaftor Is Associated with Reduced Lung Infection by Key Cystic Fibrosis Pathogens. A Cohort Study Using National Registry Data. Annals of the American Thoracic Society 2019;16:1375–82. doi:10.1513/AnnalsATS.201902-122OC.

[63] Venuta F, Rendina EA, De Giacomo T, Quattrucci S, Vizza D, Ciccone AM, et al. Timing and priorities for cystic fibrosis patients candidates to lung transplantation. Eur J Pediatr Surg 1998;8:274–7. doi:10.1055/s-2008-1071213.

[64] Hadjiliadis D, Steele MP, Chaparro C, Singer LG, Waddell TK, Hutcheon MA, et al. Survival of lung transplant patients with cystic fibrosis harboring panresistant bacteria other than Burkholderia cepacia, compared with patients harboring sensitive bacteria. J Heart Lung Transplant 2007;26:834–8. doi:10.1016/j.healun.2007.05.018.

[65] Morrell MR, Pilewski JM. Lung transplantation for cystic fibrosis. Clin Chest Med 2016;37:127–38. doi:10.1016/j.ccm.2015.11.008.

[66] Alexander BD, Petzold EW, Reller LB, Palmer SM, Davis RD, Woods CW, et al. Survival after lung transplantation of cystic fibrosis patients infected with Burkholderia cepacia complex. Am J Transplant 2008;8:1025–30. doi:10.1111/j.1600-6143.2008.02186.x.

[67] Mitchell RM, Jones AM, Barry PJ. CFTR modulator therapy in patients with cystic fibrosis and an organ transplant. Paediatr Respir Rev 2018;27:6–8. doi:10.1016/j.prrv.2018.04.003.

[68] Yusen RD, Edwards LB, Kucheryavaya AY, Benden C, Dipchand AI, Dobbels F, et al. The registry of the International Society for Heart and Lung Transplantation: thirty-first adult lung and heart-lung transplant report--2014; focus theme: retransplantation. J Heart Lung Transplant 2014;33:1009–24. doi:10.1016/j.healun.2014.08.004.

[69] El-Halfawy OM, Naguib MM, Valvano MA. Novel antibiotic combinations proposed for treatment of Burkholderia cepacia complex infections. Antimicrob Resist Infect Control 2017;6:120. doi:10.1186/s13756-017-0279-8.

[70] Vázquez-Espinosa E, Girón RM, Gómez-Punter RM, García-Castillo E, Valenzuela C, Cisneros C, et al. Long-term safety and efficacy of tobramycin in the management of cystic fibrosis. Ther Clin Risk Manag 2015;11:407–15. doi:10.2147/TCRM.S75208.

[71] Lababidi N, Ofosu Kissi E, Elgaher WAM, Sigal V, Haupenthal J, Schwarz BC, et al. Spray-drying of inhalable, multifunctional formulations for the treatment of biofilms formed in cystic fibrosis. J Control Release 2019. doi:10.1016/j.jconrel.2019.10.038.

[72] Velino C, Carella F, Adamiano A, Sanguinetti M, Vitali A, Catalucci D, et al. Nanomedicine approaches for the pulmonary treatment of cystic fibrosis. Front Bioeng Biotechnol 2019;7:406. doi:10.3389/fbioe.2019.00406.

[73] Pranke I, Golec A, Hinzpeter A, Edelman A, Sermet-Gaudelus I. Emerging therapeutic approaches for cystic fibrosis. from gene editing to personalized medicine. Front Pharmacol

2019;10:121. doi:10.3389/fphar.2019.00121.

[74] Zabner J, Couture LA, Gregory RJ, Graham SM, Smith AE, Welsh MJ. Adenovirus-mediated gene transfer transiently corrects the chloride transport defect in nasal epithelia of patients with cystic fibrosis. Cell 1993;75:207–16. doi:10.1016/0092-8674(93)80063-k.

[75] Joseph PM, O'Sullivan BP, Lapey A, Dorkin H, Oren J, Balfour R, et al. Aerosol and lobar administration of a recombinant adenovirus to individuals with cystic fibrosis. I. Methods, safety, and clinical implications. Hum Gene Ther 2001;12:1369–82. doi:10.1089/104303401750298535.

[76] Moss RB, Rodman D, Spencer LT, Aitken ML, Zeitlin PL, Waltz D, et al. Repeated adeno-associated virus serotype 2 aerosol-mediated cystic fibrosis transmembrane regulator gene transfer to the lungs of patients with cystic fibrosis: a multicenter, double-blind, placebo-controlled trial. Chest 2004;125:509–21.

[77] Moss RB, Milla C, Colombo J, Accurso F, Zeitlin PL, Clancy JP, et al. Repeated aerosolized AAV-CFTR for treatment of cystic fibrosis: a randomized placebo-controlled phase 2B trial. Hum Gene Ther 2007;18:726–32. doi:10.1089/hum.2007.022.

[78] Alton EWFW, Armstrong DK, Ashby D, Bayfield KJ, Bilton D, Bloomfield EV, et al. Repeated nebulisation of non-viral CFTR gene therapy in patients with cystic fibrosis: a randomised, double-blind, placebo-controlled, phase 2b trial. Lancet Respir Med 2015;3:684–91. doi:10.1016/S2213-2600(15)00245-3.

[79] Beumer W, Swildens J, Leal T, Noel S, Anthonijsz H, van der Horst G, et al. Evaluation of eluforsen, a novel RNA oligonucleotide for restoration of CFTR function in in vitro and murine models of p.Phe508del cystic fibrosis. PLoS One 2019;14:e0219182. doi:10.1371/journal.pone.0219182.

[80] Drevinek P, Pressler T, Cipolli M, De Boeck K, Schwarz C, Bouisset F, et al. Antisense oligonucleotide eluforsen is safe and improves respiratory symptoms in F508DEL cystic fibrosis. J Cyst Fibros 2020;19:99–107. doi:10.1016/j.jcf.2019.05.014.

[81] Firth AL, Menon T, Parker GS, Qualls SJ, Lewis BM, Ke E, et al. Functional Gene Correction for Cystic Fibrosis in Lung Epithelial Cells Generated from Patient iPSCs. Cell Rep 2015;12:1385–90. doi:10.1016/j.celrep.2015.07.062.

[82] Schwank G, Koo B-K, Sasselli V, Dekkers JF, Heo I, Demircan T, et al. Functional repair of CFTR by CRISPR/Cas9 in intestinal stem cell organoids of cystic fibrosis patients. Cell Stem Cell 2013;13:653–8. doi:10.1016/j.stem.2013.11.002.

[83] Dekkers JF, Berkers G, Kruisselbrink E, Vonk A, de Jonge HR, Janssens HM, et al. Characterizing responses to CFTR-modulating drugs using rectal organoids derived from subjects with cystic fibrosis. Sci Transl Med 2016;8:344ra84. doi:10.1126/scitranslmed.aad8278.

[84] Yui S, Nakamura T, Sato T, Nemoto Y, Mizutani T, Zheng X, et al. Functional engraftment of colon epithelium expanded in vitro from a single adult $Lgr5^+$ stem cell. Nat Med 2012;18:618–23. doi:10.1038/nm.2695.

[85] Rosen BH, Chanson M, Gawenis LR, Liu J, Sofoluwe A, Zoso A, et al. Animal and model systems for studying cystic fibrosis. J Cyst Fibros 2018;17:S28–34. doi:10.1016/j.jcf.2017.09.001.

[86] Guilbault C, Saeed Z, Downey GP, Radzioch D. Cystic fibrosis mouse models. Am J Respir Cell Mol Biol 2007;36:1–7. doi:10.1165/rcmb.2006-0184TR.

[87] Frizzell RA, Pilewski JM. Finally, mice with CF lung disease. Nat Med 2004;10:452–4. doi:10.1038/nm0504-452.

[88] Caldwell CC, Chen Y, Goetzmann HS, Hao Y, Borchers MT, Hassett DJ, et al. Pseudomonas aeruginosa exotoxin pyocyanin causes cystic fibrosis airway pathogenesis. Am J Pathol 2009;175:2473–88. doi:10.2353/ajpath.2009.090166.

[89] Jeffries JL, Jia J, Choi W, Choe S, Miao J, Xu Y, et al. Pseudomonas aeruginosa pyocyanin modulates mucin glycosylation with sialyl-Lewis(x) to increase binding to airway epithelial cells. Mucosal Immunol 2016;9:1039–50. doi:10.1038/mi.2015.119.

[90] Bielen K, 's Jongers B, Boddaert J, Raju TK, Lammens C, Malhotra-Kumar S, et al. Biofilm-Induced Type 2 Innate Immunity in a Cystic Fibrosis Model of Pseudomonas aeruginosa. Front Cell Infect Microbiol 2017;7:274. doi:10.3389/fcimb.2017.00274.

[91] Awatade NT, Wong SL, Hewson CK, Fawcett LK, Kicic A, Jaffe A, et al. Human primary epithelial cell models: promising tools in the era of cystic fibrosis personalized medicine. Front Pharmacol 2018;9:1429. doi:10.3389/fphar.2018.01429.

[92] Myerburg MM, Latoche JD, McKenna EE, Stabile LP, Siegfried JS, Feghali-Bostwick CA, et al. Hepatocyte growth factor and other fibroblast secretions modulate the phenotype of human bronchial epithelial cells. Am J Physiol Lung Cell Mol Physiol 2007;292:L1352-60. doi:10.1152/ajplung.00328.2006.

[93] Mertens TCJ, Karmouty-Quintana H, Taube C, Hiemstra PS. Use of airway epithelial cell culture to unravel the pathogenesis and study treatment in obstructive airway diseases. Pulm Pharmacol Ther 2017;45:101–13. doi:10.1016/j.pupt.2017.05.008.

[94] Ghaedi M, Niklason LE, Williams J. Development of Lung Epithelium from Induced Pluripotent Stem Cells. Curr Transplant Rep 2015;2:81–9. doi:10.1007/s40472-014-0039-0.

[95] McCauley KB, Hawkins F, Serra M, Thomas DC, Jacob A, Kotton DN. Efficient

Derivation of Functional Human Airway Epithelium from Pluripotent Stem Cells via Temporal Regulation of Wnt Signaling. Cell Stem Cell 2017;20:844–857.e6. doi:10.1016/j.stem.2017.03.001.

[96] Mims JW. Asthma: definitions and pathophysiology. Int Forum Allergy Rhinol 2015;5 Suppl 1:S2-6. doi:10.1002/alr.21609.

[97] Repapi E, Sayers I, Wain LV, Burton PR, Johnson T, Obeidat M, et al. Genome-wide association study identifies five loci associated with lung function. Nat Genet 2010;42:36–44. doi:10.1038/ng.501.

[98] Hancock DB, Eijgelsheim M, Wilk JB, Gharib SA, Loehr LR, Marciante KD, et al. Meta-analyses of genome-wide association studies identify multiple loci associated with pulmonary function. Nat Genet 2010;42:45–52. doi:10.1038/ng.500.

[99] Becker E-C, Wölke G, Heinrich J. Bronchial responsiveness, spirometry and mortality in a cohort of adults. J Asthma 2013;50:427–32. doi:10.3109/02770903.2013.769265.

[100] Wilk JB, Chen T-H, Gottlieb DJ, Walter RE, Nagle MW, Brandler BJ, et al. A genome-wide association study of pulmonary function measures in the Framingham Heart Study. PLoS Genet 2009;5:e1000429. doi:10.1371/journal.pgen.1000429.

[101] Chuang P-T, Kawcak T, McMahon AP. Feedback control of mammalian Hedgehog signaling by the Hedgehog-binding protein, Hip1, modulates Fgf signaling during branching morphogenesis of the lung. Genes Dev 2003;17:342–7. doi:10.1101/gad.1026303.

[102] Wan ES, Li Y, Lao T, Qiu W, Jiang Z, Mancini JD, et al. Metabolomic profiling in a Hedgehog Interacting Protein (Hhip) murine model of chronic obstructive pulmonary disease. Sci Rep 2017;7:2504. doi:10.1038/s41598-017-02701-4.

[103] Mauler M, Bode C, Duerschmied D. Platelet serotonin modulates immune functions. Hamostaseologie 2016;36:11–6. doi:10.5482/HAMO-14-11-0073.

[104] Dupont LJ, Pype JL, Demedts MG, De Leyn P, Deneffe G, Verleden GM. The effects of 5-HT on cholinergic contraction in human airways in vitro. Eur Respir J 1999;14:642–9. doi:10.1034/j.1399-3003.1999.14c26.x.

[105] Kim T-H, An S-H, Cha J-Y, Shin E-K, Lee J-Y, Yoon S-H, et al. Association of 5-hydroxytryptamine (serotonin) receptor 4 (5-HTR4) gene polymorphisms with asthma. Respirology 2011;16:630–8. doi:10.1111/j.1440-1843.2011.01963.x.

[106] Hodge E, Nelson CP, Miller S, Billington CK, Stewart CE, Swan C, et al. HTR4 gene structure and altered expression in the developing lung. Respir Res 2013;14:77. doi:10.1186/1465-9921-14-77.

[107] Chatterjee A, Gupta S. The multifaceted role of glutathione S-transferases in cancer. Cancer Lett 2018;433:33–42. doi:10.1016/j.canlet.2018.06.028.

[108] Mishra V, Banga J, Silveyra P. Oxidative stress and cellular pathways of asthma and inflammation: Therapeutic strategies and pharmacological targets. Pharmacol Ther 2018;181:169–82. doi:10.1016/j.pharmthera.2017.08.011.

[109] Hofmann MA, Drury S, Hudson BI, Gleason MR, Qu W, Lu Y, et al. RAGE and arthritis: the G82S polymorphism amplifies the inflammatory response. Genes Immun 2002;3:123–35. doi:10.1038/sj.gene.6363861.

[110] Xie J, Méndez JD, Méndez-Valenzuela V, Aguilar-Hernández MM. Cellular signalling of the receptor for advanced glycation end products (RAGE). Cell Signal 2013;25:2185–97. doi:10.1016/j.cellsig.2013.06.013.

[111] Oczypok EA, Perkins TN, Oury TD. All the “RAGE” in lung disease: The receptor for

advanced glycation endproducts (RAGE) is a major mediator of pulmonary inflammatory responses. Paediatr Respir Rev 2017;23:40–9. doi:10.1016/j.prrv.2017.03.012.

[112] Perkins TN, Oczypok EA, Dutz RE, Donnell ML, Myerburg MM, Oury TD. The receptor for advanced glycation end products is a critical mediator of type 2 cytokine signaling in the lungs. J Allergy Clin Immunol 2019;144:796–808.e12. doi:10.1016/j.jaci.2019.03.019.

[113] Perkins TN, Oczypok EA, Milutinovic PS, Dutz RE, Oury TD. RAGE-dependent VCAM-1 expression in the lung endothelium mediates IL-33 induced allergic airway inflammation. Allergy 2018. doi:10.1111/all.13500.

[114] Oczypok EA, Milutinovic PS, Alcorn JF, Khare A, Crum LT, Manni ML, et al. Pulmonary receptor for advanced glycation end-products promotes asthma pathogenesis through IL-33 and accumulation of group 2 innate lymphoid cells. J Allergy Clin Immunol 2015;136:747–756.e4. doi:10.1016/j.jaci.2015.03.011.

[115] Torgerson DG, Ampleford EJ, Chiu GY, Gauderman WJ, Gignoux CR, Graves PE, et al. Meta-analysis of genome-wide association studies of asthma in ethnically diverse North American populations. Nat Genet 2011;43:887–92. doi:10.1038/ng.888.

[116] D'Amato G, Holgate ST, Pawankar R, Ledford DK, Cecchi L, Al-Ahmad M, et al. Meteorological conditions, climate change, new emerging factors, and asthma and related allergic disorders. A statement of the World Allergy Organization. World Allergy Organiz J 2015;8:25. doi:10.1186/s40413-015-0073-0.

[117] Brandt EB, Kovacic MB, Lee GB, Gibson AM, Acciani TH, Le Cras TD, et al. Diesel exhaust particle induction of IL-17A contributes to severe asthma. J Allergy Clin Immunol 2013;132:1194–1204.e2. doi:10.1016/j.jaci.2013.06.048.

[118] Weng C-M, Lee M-J, He J-R, Chao M-W, Wang C-H, Kuo H-P. Diesel exhaust particles

up-regulate interleukin-17A expression via ROS/NF-κB in airway epithelium. Biochem Pharmacol 2018;151:1–8. doi:10.1016/j.bcp.2018.02.028.

[119] Brandt EB, Bolcas PE, Ruff BP, Khurana Hershey GK. IL33 contributes to diesel pollution-mediated increase in experimental asthma severity. Allergy 2020. doi:10.1111/all.14181.

[120] Arsalane K, Gosset P, Vanhee D, Voisin C, Hamid Q, Tonnel AB, et al. Ozone stimulates synthesis of inflammatory cytokines by alveolar macrophages in vitro. Am J Respir Cell Mol Biol 1995;13:60–8. doi:10.1165/ajrcmb.13.1.7598938.

[121] Tillie-Leblond I, Pugin J, Marquette CH, Lamblin C, Saulnier F, Brichet A, et al. Balance between proinflammatory cytokines and their inhibitors in bronchial lavage from patients with status asthmaticus. Am J Respir Crit Care Med 1999;159:487–94. doi:10.1164/ajrccm.159.2.9805115.

[122] Rincon M, Irvin CG. Role of IL-6 in asthma and other inflammatory pulmonary diseases. Int J Biol Sci 2012;8:1281–90. doi:10.7150/ijbs.4874.

[123] Sunil VR, Vayas KN, Massa CB, Gow AJ, Laskin JD, Laskin DL. Ozone-induced injury and oxidative stress in bronchiolar epithelium are associated with altered pulmonary mechanics. Toxicol Sci 2013;133:309–19. doi:10.1093/toxsci/kft071.

[124] Nassikas N, Spangler K, Fann N, Nolte CG, Dolwick P, Spero TL, et al. Ozone-related asthma emergency department visits in the US in a warming climate. Environ Res 2020;183:109206. doi:10.1016/j.envres.2020.109206.

[125] Habre R, Zhou H, Eckel SP, Enebish T, Fruin S, Bastain T, et al. Short-term effects of airport-associated ultrafine particle exposure on lung function and inflammation in adults with asthma. Environ Int 2018;118:48–59. doi:10.1016/j.envint.2018.05.031.

[126] Onishi T, Honda A, Tanaka M, Chowdhury PH, Okano H, Okuda T, et al. Ambient fine and coarse particles in Japan affect nasal and bronchial epithelial cells differently and elicit varying immune response. Environ Pollut 2018;242:1693–701. doi:10.1016/j.envpol.2018.07.103.

[127] Timblin CR, Shukla A, Berlanger I, BeruBe KA, Churg A, Mossman BT. Ultrafine airborne particles cause increases in protooncogene expression and proliferation in alveolar epithelial cells. Toxicol Appl Pharmacol 2002;179:98–104. doi:10.1006/taap.2001.9343.

[128] Steinbacher M, Pfleger A, Schwantzer G, Jauk S, Weinhandl E, Eber E. Small airway function before and after cold dry air challenge in pediatric asthma patients during remission. Pediatr Pulmonol 2017;52:873–9. doi:10.1002/ppul.23724.

[129] Dreßler M, Friedrich T, Lasowski N, Herrmann E, Zielen S, Schulze J. Predictors and reproducibility of exercise-induced bronchoconstriction in cold air. BMC Pulm Med 2019;19:94. doi:10.1186/s12890-019-0845-3.

[130] Menzel A, Sparks TH, Estrella N, Koch E, Aasa A, Ahas R, et al. European phenological response to climate change matches the warming pattern. Glob Change Biol 2006;12:1969–76. doi:10.1111/j.1365-2486.2006.01193.x.

[131] Wayne P, Foster S, Connolly J, Bazzaz F, Epstein P. Production of allergenic pollen by ragweed (Ambrosia artemisiifolia L.) is increased in CO2-enriched atmospheres. Ann Allergy Asthma Immunol 2002;88:279–82. doi:10.1016/S1081-1206(10)62009-1.

[132] Ribeiro H, Costa C, Abreu I, Esteves da Silva JCG. Effect of O3 and NO2 atmospheric pollutants on Platanus x acerifolia pollen: Immunochemical and spectroscopic analysis. Sci Total Environ 2017;599–600:291–7. doi:10.1016/j.scitotenv.2017.04.206.

[133] Sun X, Waller A, Yeatts KB, Thie L. Pollen concentration and asthma exacerbations in

Wake County, North Carolina, 2006-2012. Sci Total Environ 2016;544:185–91. doi:10.1016/j.scitotenv.2015.11.100.

[134] Singh RK, Chang H-W, Yan D, Lee KM, Ucmak D, Wong K, et al. Influence of diet on the gut microbiome and implications for human health. J Transl Med 2017;15:73. doi:10.1186/s12967-017-1175-y.

[135] Rosshart SP, Herz J, Vassallo BG, Hunter A, Wall MK, Badger JH, et al. Laboratory mice born to wild mice have natural microbiota and model human immune responses. Science 2019;365. doi:10.1126/science.aaw4361.

[136] Yassour M, Jason E, Hogstrom LJ, Arthur TD, Tripathi S, Siljander H, et al. Strain-Level Analysis of Mother-to-Child Bacterial Transmission during the First Few Months of Life. Cell Host Microbe 2018;24:146–154.e4. doi:10.1016/j.chom.2018.06.007.

[137] Michalovich D, Rodriguez-Perez N, Smolinska S, Pirozynski M, Mayhew D, Uddin S, et al. Obesity and disease severity magnify disturbed microbiome-immune interactions in asthma patients. Nat Commun 2019;10:5711. doi:10.1038/s41467-019-13751-9.

[138] Kanoh S, Tanabe T, Rubin BK. IL-13-induced MUC5AC production and goblet cell differentiation is steroid resistant in human airway cells. Clin Exp Allergy 2011;41:1747–56. doi:10.1111/j.1365-2222.2011.03852.x.

[139] Patrick DM, Sbihi H, Dai DLY, Al Mamun A, Rasali D, Rose C, et al. Decreasing antibiotic use, the gut microbiota, and asthma incidence in children: evidence from population-based and prospective cohort studies. Lancet Respir Med 2020. doi:10.1016/S2213-2600(20)30052-7.

[140] Yaghoubi M, Adibi A, Safari A, FitzGerald JM, Sadatsafavi M. The projected economic and health burden of uncontrolled asthma in the united states. Am J Respir Crit Care Med

2019;200:1102–12. doi:10.1164/rccm.201901-0016OC.

[141] Ealey KN, Moro K, Koyasu S. Are ILC2s Jekyll and Hyde in airway inflammation? Immunol Rev 2017;278:207–18. doi:10.1111/imr.12547.

[142] Artis D, Spits H. The biology of innate lymphoid cells. Nature 2015;517:293–301. doi:10.1038/nature14189.

[143] Yang Z, Tang T, Wei X, Yang S, Tian Z. Type 1 innate lymphoid cells contribute to the pathogenesis of chronic hepatitis B. Innate Immun 2015;21:665–73. doi:10.1177/1753425915586074.

[144] Tait Wojno ED, Artis D. Emerging concepts and future challenges in innate lymphoid cell biology. J Exp Med 2016;213:2229–48. doi:10.1084/jem.20160525.

[145] Mantovani A, Dinarello CA, Molgora M, Garlanda C. Interleukin-1 and Related Cytokines in the Regulation of Inflammation and Immunity. Immunity 2019;50:778–95. doi:10.1016/j.immuni.2019.03.012.

[146] Romera-Hernández M, Aparicio-Domingo P, Papazian N, Karrich JJ, Cornelissen F, Hoogenboezem RM, et al. Yap1-Driven Intestinal Repair Is Controlled by Group 3 Innate Lymphoid Cells. Cell Rep 2020;30:37–45.e3. doi:10.1016/j.celrep.2019.11.115.

[147] Mantis NJ, Rol N, Corthésy B. Secretory IgA's complex roles in immunity and mucosal homeostasis in the gut. Mucosal Immunol 2011;4:603–11. doi:10.1038/mi.2011.41.

[148] Samitas K, Zervas E, Gaga M. T2-low asthma: current approach to diagnosis and therapy. Curr Opin Pulm Med 2017;23:48–55. doi:10.1097/MCP.0000000000000342.

[149] Fahy JV. Type 2 inflammation in asthma--present in most, absent in many. Nat Rev Immunol 2015;15:57–65. doi:10.1038/nri3786.

[150] Byers DE, Alexander-Brett J, Patel AC, Agapov E, Dang-Vu G, Jin X, et al. Long-term

IL-33-producing epithelial progenitor cells in chronic obstructive lung disease. J Clin Invest 2013;123:3967–82. doi:10.1172/JCI65570.

[151] Le Goffic R, Arshad MI, Rauch M, L'Helgoualc'h A, Delmas B, Piquet-Pellorce C, et al. Infection with influenza virus induces IL-33 in murine lungs. Am J Respir Cell Mol Biol 2011;45:1125–32. doi:10.1165/rcmb.2010-0516OC.

[152] Chen F, Liu Z, Wu W, Rozo C, Bowdridge S, Millman A, et al. An essential role for TH2-type responses in limiting acute tissue damage during experimental helminth infection. Nat Med 2012;18:260–6. doi:10.1038/nm.2628.

[153] Gause WC, Urban JF, Stadecker MJ. The immune response to parasitic helminths: insights from murine models. Trends Immunol 2003;24:269–77. doi:10.1016/S1471-4906(03)00101-7.

[154] Schuijs MJ, Hammad H, Lambrecht BN. Professional and "Amateur" Antigen-Presenting Cells In Type 2 Immunity. Trends Immunol 2019;40:22–34. doi:10.1016/j.it.2018.11.001.

[155] Palm NW, Rosenstein RK, Medzhitov R. Allergic host defences. Nature 2012;484:465–72. doi:10.1038/nature11047.

[156] Kotsias F, Cebrian I, Alloatti A. Antigen processing and presentation. Int Rev Cell Mol Biol 2019;348:69–121. doi:10.1016/bs.ircmb.2019.07.005.

[157] Lloyd CM, Harker JA. Location, location, location: localized memory cells take residence in the allergic lung. Immunity 2016;44:13–5. doi:10.1016/j.immuni.2015.12.012.

[158] Berger A. Th1 and Th2 responses: what are they? BMJ 2000;321:424.

[159] Tau G, Rothman P. Biologic functions of the IFN-gamma receptors. Allergy 1999;54:1233–51. doi:10.1034/j.1398-9995.1999.00099.x.

[160] Gould HJ, Sutton BJ, Beavil AJ, Beavil RL, McCloskey N, Coker HA, et al. The biology

of IGE and the basis of allergic disease. Annu Rev Immunol 2003;21:579–628. doi:10.1146/annurev.immunol.21.120601.141103.

[161] Perfect JR, Dismukes WE, Dromer F, Goldman DL, Graybill JR, Hamill RJ, et al. Clinical practice guidelines for the management of cryptococcal disease: 2010 update by the infectious diseases society of america. Clin Infect Dis 2010;50:291–322. doi:10.1086/649858.

[162] Yamanishi Y, Miyake K, Iki M, Tsutsui H, Karasuyama H. Recent advances in understanding basophil-mediated Th2 immune responses. Immunol Rev 2017;278:237–45. doi:10.1111/imr.12548.

[163] Galli SJ, Tsai M. IgE and mast cells in allergic disease. Nat Med 2012;18:693–704. doi:10.1038/nm.2755.

[164] Sawaguchi M, Tanaka S, Nakatani Y, Harada Y, Mukai K, Matsunaga Y, et al. Role of mast cells and basophils in IgE responses and in allergic airway hyperresponsiveness. J Immunol 2012;188:1809–18. doi:10.4049/jimmunol.1101746.

[165] Klein Wolterink RGJ, Kleinjan A, van Nimwegen M, Bergen I, de Bruijn M, Levani Y, et al. Pulmonary innate lymphoid cells are major producers of IL-5 and IL-13 in murine models of allergic asthma. Eur J Immunol 2012;42:1106–16. doi:10.1002/eji.201142018.

[166] Lv J, Yu Q, Lv J, Di C, Lin X, Su W, et al. Airway epithelial TSLP production of TLR2 drives type 2 immunity in allergic airway inflammation. Eur J Immunol 2018;48:1838–50. doi:10.1002/eji.201847663.

[167] Barlow JL, Peel S, Fox J, Panova V, Hardman CS, Camelo A, et al. IL-33 is more potent than IL-25 in provoking IL-13-producing nuocytes (type 2 innate lymphoid cells) and airway contraction. J Allergy Clin Immunol 2013;132:933–41.

doi:10.1016/j.jaci.2013.05.012.

[168] Zhang DH, Cohn L, Ray P, Bottomly K, Ray A. Transcription factor GATA-3 is differentially expressed in murine Th1 and Th2 cells and controls Th2-specific expression of the interleukin-5 gene. J Biol Chem 1997;272:21597–603. doi:10.1074/jbc.272.34.21597.

[169] Fulkerson PC, Rothenberg ME. Targeting eosinophils in allergy, inflammation and beyond. Nat Rev Drug Discov 2013;12:117–29. doi:10.1038/nrd3838.

[170] Woodruff PG, Modrek B, Choy DF, Jia G, Abbas AR, Ellwanger A, et al. T-helper type 2-driven inflammation defines major subphenotypes of asthma. Am J Respir Crit Care Med 2009;180:388–95. doi:10.1164/rccm.200903-0392OC.

[171] Corren J. Asthma phenotypes and endotypes: an evolving paradigm for classification. Discov Med 2013;15:243–9.

[172] Park SC, Kim H, Bak Y, Shim D, Kwon KW, Kim CH, et al. An Alternative Dendritic Cell-Induced Murine Model of Asthma Exhibiting a Robust Th2/Th17-Skewed Response. Allergy Asthma Immunol Res 2020;12:537–55. doi:10.4168/aair.2020.12.3.537.

[173] Sun L, Ren X, Wang I-C, Pradhan A, Zhang Y, Flood HM, et al. The FOXM1 inhibitor RCM-1 suppresses goblet cell metaplasia and prevents IL-13 and STAT6 signaling in allergen-exposed mice. Sci Signal 2017;10. doi:10.1126/scisignal.aai8583.

[174] Ramakrishnan RK, Al Heialy S, Hamid Q. Role of IL-17 in asthma pathogenesis and its implications for the clinic. Expert Rev Respir Med 2019;13:1057–68. doi:10.1080/17476348.2019.1666002.

[175] Reichard A, Wanner N, Stuehr E, Alemagno M, Weiss K, Queisser K, et al. Quantification of airway fibrosis in asthma by flow cytometry. Cytometry A 2018;93:952–8.

doi:10.1002/cyto.a.23373.

[176] Damera G, Panettieri RA. Irreversible airway obstruction in asthma: what we lose, we lose early. Allergy Asthma Proc 2014;35:111–8. doi:10.2500/aap.2013.34.3724.

[177] Dunican EM, Fahy JV. The role of type 2 inflammation in the pathogenesis of asthma exacerbations. Annals of the American Thoracic Society 2015;12 Suppl 2:S144-9. doi:10.1513/AnnalsATS.201506-377AW.

[178] Xu M, Xu J, Yang X. Asthma and risk of cardiovascular disease or all-cause mortality: a meta-analysis. Ann Saudi Med 2017;37:99–105. doi:10.5144/0256-4947.2017.99.

[179] Yuan Y, Ran N, Xiong L, Wang G, Guan X, Wang Z, et al. Obesity-Related Asthma: Immune Regulation and Potential Targeted Therapies. J Immunol Res 2018;2018:1943497. doi:10.1155/2018/1943497.

[180] Kuenzig ME, Bishay K, Leigh R, Kaplan GG, Benchimol EI, Crowdscreen SR Review Team. Co-occurrence of Asthma and the Inflammatory Bowel Diseases: A Systematic Review and Meta-analysis. Clin Transl Gastroenterol 2018;9:188. doi:10.1038/s41424-018-0054-z.

[181] Fergeson JE, Patel SS, Lockey RF. Acute asthma, prognosis, and treatment. J Allergy Clin Immunol 2017;139:438–47. doi:10.1016/j.jaci.2016.06.054.

[182] Delmotte P, Sanderson MJ. Effects of albuterol isomers on the contraction and Ca2+ signaling of small airways in mouse lung slices. Am J Respir Cell Mol Biol 2008;38:524–31. doi:10.1165/rcmb.2007-0214OC.

[183] Horvath G, Wanner A. Inhaled corticosteroids: effects on the airway vasculature in bronchial asthma. Eur Respir J 2006;27:172–87. doi:10.1183/09031936.06.00048605.

[184] Alangari AA. Corticosteroids in the treatment of acute asthma. Ann Thorac Med

2014;9:187–92. doi:10.4103/1817-1737.140120.

[185] Price D, Castro M, Bourdin A, Fucile S, Altman P. Short-course systemic corticosteroids in asthma: striking the balance between efficacy and safety. Eur Respir Rev 2020;29. doi:10.1183/16000617.0151-2019.

[186] Iramain R, Castro-Rodriguez JA, Jara A, Cardozo L, Bogado N, Morinigo R, et al. Salbutamol and ipratropium by inhaler is superior to nebulizer in children with severe acute asthma exacerbation: Randomized clinical trial. Pediatr Pulmonol 2019;54:372–7. doi:10.1002/ppul.24244.

[187] Fajt ML, Wenzel SE. Asthma phenotypes and the use of biologic medications in asthma and allergic disease: the next steps toward personalized care. J Allergy Clin Immunol 2015;135:299–310; quiz 311. doi:10.1016/j.jaci.2014.12.1871.

[188] McCracken JL, Tripple JW, Calhoun WJ. Biologic therapy in the management of asthma. Curr Opin Allergy Clin Immunol 2016;16:375–82. doi:10.1097/ACI.0000000000000284.

[189] Moran A, Pavord ID. Anti-IL-4/IL-13 for the treatment of asthma: the story so far. Expert Opin Biol Ther 2020;20:283–94. doi:10.1080/14712598.2020.1714027.

[190] Busse WW, Holgate S, Kerwin E, Chon Y, Feng J, Lin J, et al. Randomized, double-blind, placebo-controlled study of brodalumab, a human anti-IL-17 receptor monoclonal antibody, in moderate to severe asthma. Am J Respir Crit Care Med 2013;188:1294–302. doi:10.1164/rccm.201212-2318OC.

[191] David MMC, Gomes EL de FD, Mello MC, Costa D. Noninvasive ventilation and respiratory physical therapy reduce exercise-induced bronchospasm and pulmonary inflammation in children with asthma: randomized clinical trial. Ther Adv Respir Dis 2018;12:1753466618777723. doi:10.1177/1753466618777723.

[192] Eijkemans M, Mommers M, Draaisma JMT, Thijs C, Prins MH. Physical activity and asthma: a systematic review and meta-analysis. PLoS One 2012;7:e50775. doi:10.1371/journal.pone.0050775.

[193] Zhang W, Wang Q, Liu L, Yang W, Liu H. Effects of physical therapy on lung function in children with asthma: a systematic review and meta-analysis. Pediatr Res 2020. doi:10.1038/s41390-020-0874-x.

[194] Trompette A, Gollwitzer ES, Yadava K, Sichelstiel AK, Sprenger N, Ngom-Bru C, et al. Gut microbiota metabolism of dietary fiber influences allergic airway disease and hematopoiesis. Nat Med 2014;20:159–66. doi:10.1038/nm.3444.

[195] Vuolo F, Abreu SC, Michels M, Xisto DG, Blanco NG, Hallak JE, et al. Cannabidiol reduces airway inflammation and fibrosis in experimental allergic asthma. Eur J Pharmacol 2019;843:251–9. doi:10.1016/j.ejphar.2018.11.029.

[196] Shin YS, Takeda K, Gelfand EW. Understanding asthma using animal models. Allergy Asthma Immunol Res 2009;1:10–8. doi:10.4168/aair.2009.1.1.10.

[197] Hall S, Agrawal DK. Key mediators in the immunopathogenesis of allergic asthma. Int Immunopharmacol 2014;23:316–29. doi:10.1016/j.intimp.2014.05.034.

[198] Nials AT, Uddin S. Mouse models of allergic asthma: acute and chronic allergen challenge. Dis Model Mech 2008;1:213–20. doi:10.1242/dmm.000323.

[199] Kumar RK, Foster PS. Modeling allergic asthma in mice: pitfalls and opportunities. Am J Respir Cell Mol Biol 2002;27:267–72. doi:10.1165/rcmb.F248.

[200] Koya T, Matsuda H, Matsubara S, Miyahara N, Dakhama A, Takeda K, et al. Differential effects of dendritic cell transfer on airway hyperresponsiveness and inflammation. Am J Respir Cell Mol Biol 2009;41:271–80. doi:10.1165/rcmb.2008-0256OC.

[201] Ramu S, Menzel M, Bjermer L, Andersson C, Akbarshahi H, Uller L. Allergens produce serine proteases-dependent distinct release of metabolite DAMPs in human bronchial epithelial cells. Clin Exp Allergy 2018;48:156–66. doi:10.1111/cea.13071.

[202] Kouzaki H, Iijima K, Kobayashi T, O'Grady SM, Kita H. The danger signal, extracellular ATP, is a sensor for an airborne allergen and triggers IL-33 release and innate Th2-type responses. J Immunol 2011;186:4375–87. doi:10.4049/jimmunol.1003020.

[203] Wark PAB, Johnston SL, Bucchieri F, Powell R, Puddicombe S, Laza-Stanca V, et al. Asthmatic bronchial epithelial cells have a deficient innate immune response to infection with rhinovirus. J Exp Med 2005;201:937–47. doi:10.1084/jem.20041901.

[204] Devalia JL, Bayram H, Abdelaziz MM, Sapsford RJ, Davies RJ. Differences between cytokine release from bronchial epithelial cells of asthmatic patients and non-asthmatic subjects: effect of exposure to diesel exhaust particles. Int Arch Allergy Immunol 1999;118:437–9. doi:10.1159/000024157.

[205] Nichols JE, Niles JA, Vega SP, Argueta LB, Eastaway A, Cortiella J. Modeling the lung: Design and development of tissue engineered macro- and micro-physiologic lung models for research use. Exp Biol Med 2014;239:1135–69. doi:10.1177/1535370214536679.

[206] Wang C, Hei F, Ju Z, Yu J, Yang S, Chen M. Differentiation of Urine-Derived Human Induced Pluripotent Stem Cells to Alveolar Type II Epithelial Cells. Cell Reprogram 2016;18:30–6. doi:10.1089/cell.2015.0015.

[207] Banerjee ER, Laflamme MA, Papayannopoulou T, Kahn M, Murry CE, Henderson WR. Human embryonic stem cells differentiated to lung lineage-specific cells ameliorate pulmonary fibrosis in a xenograft transplant mouse model. PLoS One 2012;7:e33165. doi:10.1371/journal.pone.0033165.

[208] Jacob A, Morley M, Hawkins F, McCauley KB, Jean JC, Heins H, et al. Differentiation of Human Pluripotent Stem Cells into Functional Lung Alveolar Epithelial Cells. Cell Stem Cell 2017;21:472–488.e10. doi:10.1016/j.stem.2017.08.014.

[209] Ghaedi M, Le AV, Hatachi G, Beloiartsev A, Rocco K, Sivarapatna A, et al. Bioengineered lungs generated from human iPSCs-derived epithelial cells on native extracellular matrix. J Tissue Eng Regen Med 2018;12:e1623–35. doi:10.1002/term.2589.

[210] Neeper M, Schmidt AM, Brett J, Yan SD, Wang F, Pan YC, et al. Cloning and expression of a cell surface receptor for advanced glycosylation end products of proteins. J Biol Chem 1992;267:14998–5004.

[211] Brett J, Schmidt AM, Yan SD, Zou YS, Weidman E, Pinsky D, et al. Survey of the distribution of a newly characterized receptor for advanced glycation end products in tissues. Am J Pathol 1993;143:1699–712.

[212] Malherbe P, Richards JG, Gaillard H, Thompson A, Diener C, Schuler A, et al. cDNA cloning of a novel secreted isoform of the human receptor for advanced glycation end products and characterization of cells co-expressing cell-surface scavenger receptors and Swedish mutant amyloid precursor protein. Brain Res Mol Brain Res 1999;71:159–70. doi:10.1016/S0169-328X(99)00174-6.

[213] Yonekura H, Yamamoto Y, Sakurai S, Petrova RG, Abedin MJ, Li H, et al. Novel splice variants of the receptor for advanced glycation end-products expressed in human vascular endothelial cells and pericytes, and their putative roles in diabetes-induced vascular injury. Biochem J 2003;370:1097–109. doi:10.1042/BJ20021371.

[214] Hudson BI, Carter AM, Harja E, Kalea AZ, Arriero M, Yang H, et al. Identification, classification, and expression of RAGE gene splice variants. FASEB J 2008;22:1572–80.

doi:10.1096/fj.07-9909com.

[215] Kalea AZ, Reiniger N, Yang H, Arriero M, Schmidt AM, Hudson BI. Alternative splicing of the murine receptor for advanced glycation end-products (RAGE) gene. FASEB J 2009;23:1766–74. doi:10.1096/fj.08-117739.

[216] Park IH, Yeon SI, Youn JH, Choi JE, Sasaki N, Choi I-H, et al. Expression of a novel secreted splice variant of the receptor for advanced glycation end products (RAGE) in human brain astrocytes and peripheral blood mononuclear cells. Mol Immunol 2004;40:1203–11. doi:10.1016/j.molimm.2003.11.027.

[217] López-Díez R, Rastrojo A, Villate O, Aguado B. Complex tissue-specific patterns and distribution of multiple RAGE splice variants in different mammals. Genome Biol Evol 2013;5:2420–35. doi:10.1093/gbe/evt188.

[218] Yatime L, Betzer C, Jensen RK, Mortensen S, Jensen PH, Andersen GR. The structure of the RAGE:S100A6 complex reveals a unique mode of homodimerization for S100 proteins. Structure 2016;24:2043–52. doi:10.1016/j.str.2016.09.011.

[219] Ishihara K, Tsutsumi K, Kawane S, Nakajima M, Kasaoka T. The receptor for advanced glycation end-products (RAGE) directly binds to ERK by a D-domain-like docking site. FEBS Lett 2003;550:107–13. doi:10.1016/S0014-5793(03)00846-9.

[220] Englert JM, Hanford LE, Kaminski N, Tobolewski JM, Tan RJ, Fattman CL, et al. A role for the receptor for advanced glycation end products in idiopathic pulmonary fibrosis. Am J Pathol 2008;172:583–91. doi:10.2353/ajpath.2008.070569.

[221] Blondonnet R, Audard J, Belville C, Clairefond G, Lutz J, Bouvier D, et al. RAGE inhibition reduces acute lung injury in mice. Sci Rep 2017;7:7208. doi:10.1038/s41598-017-07638-2.

[222] Zhang L, Bukulin M, Kojro E, Roth A, Metz VV, Fahrenholz F, et al. Receptor for advanced glycation end products is subjected to protein ectodomain shedding by metalloproteinases. J Biol Chem 2008;283:35507–16. doi:10.1074/jbc.M806948200.

[223] Buckley ST, Ehrhardt C. The receptor for advanced glycation end products (RAGE) and the lung. J Biomed Biotechnol 2010;2010:917108. doi:10.1155/2010/917108.

[224] Jules J, Maiguel D, Hudson BI. Alternative splicing of the RAGE cytoplasmic domain regulates cell signaling and function. PLoS One 2013;8:e78267. doi:10.1371/journal.pone.0078267.

[225] Bargagli E, Penza F, Bianchi N, Olivieri C, Bennett D, Prasse A, et al. Controversial role of RAGE in the pathogenesis of idiopathic pulmonary fibrosis. Respir Physiol Neurobiol 2009;165:119–20; author reply 121. doi:10.1016/j.resp.2008.10.017.

[226] Ding H, Ji X, Chen R, Ma T, Tang Z, Fen Y, et al. Antifibrotic properties of receptor for advanced glycation end products in idiopathic pulmonary fibrosis. Pulm Pharmacol Ther 2015;35:34–41. doi:10.1016/j.pupt.2015.10.010.

[227] Makam M, Diaz D, Laval J, Gernez Y, Conrad CK, Dunn CE, et al. Activation of critical, host-induced, metabolic and stress pathways marks neutrophil entry into cystic fibrosis lungs. Proc Natl Acad Sci USA 2009;106:5779–83. doi:10.1073/pnas.0813410106.

[228] Mulrennan S, Baltic S, Aggarwal S, Wood J, Miranda A, Frost F, et al. The role of receptor for advanced glycation end products in airway inflammation in CF and CF related diabetes. Sci Rep 2015;5:8931. doi:10.1038/srep08931.

[229] Wu L, Ma L, Nicholson LFB, Black PN. Advanced glycation end products and its receptor (RAGE) are increased in patients with COPD. Respir Med 2011;105:329–36. doi:10.1016/j.rmed.2010.11.001.

[230] Gopal P, Reynaert NL, Scheijen JLJM, Schalkwijk CG, Franssen FME, Wouters EFM, et al. Association of plasma sRAGE, but not esRAGE with lung function impairment in COPD. Respir Res 2014;15:24. doi:10.1186/1465-9921-15-24.

[231] Sambamurthy N, Leme AS, Oury TD, Shapiro SD. The receptor for advanced glycation end products (RAGE) contributes to the progression of emphysema in mice. PLoS One 2015;10:e0118979. doi:10.1371/journal.pone.0118979.

[232] Lee H, Lee J, Hong S-H, Rahman I, Yang S-R. Inhibition of RAGE Attenuates Cigarette Smoke-Induced Lung Epithelial Cell Damage via RAGE-Mediated Nrf2/DAMP Signaling. Front Pharmacol 2018;9:684. doi:10.3389/fphar.2018.00684.

[233] Milutinovic PS, Alcorn JF, Englert JM, Crum LT, Oury TD. The receptor for advanced glycation end products is a central mediator of asthma pathogenesis. Am J Pathol 2012;181:1215–25. doi:10.1016/j.ajpath.2012.06.031.

[234] Yao L, Zhao H, Tang H, Liang J, Liu L, Dong H, et al. The receptor for advanced glycation end products is required for β-catenin stabilization in a chemical-induced asthma model. Br J Pharmacol 2016;173:2600–13. doi:10.1111/bph.13539.

[235] Yonchuk JG, Silverman EK, Bowler RP, Agustí A, Lomas DA, Miller BE, et al. Circulating soluble receptor for advanced glycation end products (sRAGE) as a biomarker of emphysema and the RAGE axis in the lung. Am J Respir Crit Care Med 2015;192:785–92. doi:10.1164/rccm.201501-0137PP.

[236] Manichaikul A, Sun L, Borczuk AC, Onengut-Gumuscu S, Farber EA, Mathai SK, et al. Plasma soluble receptor for advanced glycation end products in idiopathic pulmonary fibrosis. Annals of the American Thoracic Society 2017;14:628–35. doi:10.1513/AnnalsATS.201606-485OC.

[237] Yao D, Brownlee M. Hyperglycemia-induced reactive oxygen species increase expression of the receptor for advanced glycation end products (RAGE) and RAGE ligands. Diabetes 2010;59:249–55. doi:10.2337/db09-0801.

[238] Sirois CM, Jin T, Miller AL, Bertheloot D, Nakamura H, Horvath GL, et al. RAGE is a nucleic acid receptor that promotes inflammatory responses to DNA. J Exp Med 2013;210:2447–63. doi:10.1084/jem.20120201.

[239] Singh R, Barden A, Mori T, Beilin L. Advanced glycation end-products: a review. Diabetologia 2001;44:129–46. doi:10.1007/s001250051591.

[240] Nowotny K, Schröter D, Schreiner M, Grune T. Dietary advanced glycation end products and their relevance for human health. Ageing Res Rev 2018;47:55–66. doi:10.1016/j.arr.2018.06.005.

[241] Feldman N, Rotter-Maskowitz A, Okun E. DAMPs as mediators of sterile inflammation in aging-related pathologies. Ageing Res Rev 2015;24:29–39. doi:10.1016/j.arr.2015.01.003.

[242] Hori O, Brett J, Slattery T, Cao R, Zhang J, Chen JX, et al. The receptor for advanced glycation end products (RAGE) is a cellular binding site for amphoterin. Mediation of neurite outgrowth and co-expression of rage and amphoterin in the developing nervous system. J Biol Chem 1995;270:25752–61.

[243] Hofmann MA, Drury S, Fu C, Qu W, Taguchi A, Lu Y, et al. RAGE Mediates a Novel Proinflammatory Axis. Cell 1999;97:889–901. doi:10.1016/S0092-8674(00)80801-6.

[244] Wang H, Bloom O, Zhang M, Vishnubhakat JM, Ombrellino M, Che J, et al. HMG-1 as a late mediator of endotoxin lethality in mice. Science 1999;285:248–51. doi:10.1126/science.285.5425.248.

[245] Rovere-Querini P, Capobianco A, Scaffidi P, Valentinis B, Catalanotti F, Giazzon M, et al. HMGB1 is an endogenous immune adjuvant released by necrotic cells. EMBO Rep 2004;5:825–30. doi:10.1038/sj.embor.7400205.

[246] Sakaguchi M, Kinoshita R, Putranto EW, Ruma IMW, Sumardika IW, Youyi C, et al. Signal diversity of receptor for advanced glycation end products. Acta Med Okayama 2017;71:459–65. doi:10.18926/AMO/55582.

[247] Huttunen HJ, Kuja-Panula J, Sorci G, Agneletti AL, Donato R, Rauvala H. Coregulation of neurite outgrowth and cell survival by amphoterin and S100 proteins through receptor for advanced glycation end products (RAGE) activation. J Biol Chem 2000;275:40096–105. doi:10.1074/jbc.M006993200.

[248] Heizmann CW, Fritz G, Schäfer BW. S100 proteins: structure, functions and pathology. Front Biosci 2002;7:d1356-68.

[249] Foell D, Wittkowski H, Vogl T, Roth J. S100 proteins expressed in phagocytes: a novel group of damage-associated molecular pattern molecules. J Leukoc Biol 2007;81:28–37. doi:10.1189/jlb.0306170.

[250] Kang JH, Hwang SM, Chung IY. S100A8, S100A9 and S100A12 activate airway epithelial cells to produce MUC5AC via extracellular signal-regulated kinase and nuclear factor-κB pathways. Immunology 2015;144:79–90. doi:10.1111/imm.12352.

[251] Yan SD, Chen X, Fu J, Chen M, Zhu H, Roher A, et al. RAGE and amyloid-beta peptide neurotoxicity in Alzheimer's disease. Nature 1996;382:685–91. doi:10.1038/382685a0.

[252] Du Yan S, Zhu H, Fu J, Yan SF, Roher A, Tourtellotte WW, et al. Amyloid-beta peptide-receptor for advanced glycation endproduct interaction elicits neuronal expression of macrophage-colony stimulating factor: a proinflammatory pathway in Alzheimer disease.

Proc Natl Acad Sci USA 1997;94:5296–301.

[253] Serrano-Pozo A, Gómez-Isla T, Growdon JH, Frosch MP, Hyman BT. A phenotypic change but not proliferation underlies glial responses in Alzheimer disease. Am J Pathol 2013;182:2332–44. doi:10.1016/j.ajpath.2013.02.031.

[254] Deane R, Du Yan S, Submamaryan RK, LaRue B, Jovanovic S, Hogg E, et al. RAGE mediates amyloid-beta peptide transport across the blood-brain barrier and accumulation in brain. Nat Med 2003;9:907–13. doi:10.1038/nm890.

[255] Demling N, Ehrhardt C, Kasper M, Laue M, Knels L, Rieber EP. Promotion of cell adherence and spreading: a novel function of RAGE, the highly selective differentiation marker of human alveolar epithelial type I cells. Cell Tissue Res 2006;323:475–88. doi:10.1007/s00441-005-0069-0.

[256] Milutinovic PS, Englert JM, Crum LT, Mason NS, Ramsgaard L, Enghild JJ, et al. Clearance kinetics and matrix binding partners of the receptor for advanced glycation end products. PLoS One 2014;9:e88259. doi:10.1371/journal.pone.0088259.

[257] Chavakis T, Bierhaus A, Al-Fakhri N, Schneider D, Witte S, Linn T, et al. The pattern recognition receptor (RAGE) is a counterreceptor for leukocyte integrins: a novel pathway for inflammatory cell recruitment. J Exp Med 2003;198:1507–15. doi:10.1084/jem.20030800.

[258] Murakami Y, Fujino T, Kurachi R, Hasegawa T, Usui T, Hayase F, et al. Identification of pyridinoline, a collagen crosslink, as a novel intrinsic ligand for the receptor for advanced glycation end-products (RAGE). Biosci Biotechnol Biochem 2018;82:1–7. doi:10.1080/09168451.2018.1475213.

[259] Yan SD, Schmidt AM, Anderson GM, Zhang J, Brett J, Zou YS, et al. Enhanced cellular

oxidant stress by the interaction of advanced glycation end products with their receptors/binding proteins. J Biol Chem 1994;269:9889–97.

[260] Lander HM, Tauras JM, Ogiste JS, Hori O, Moss RA, Schmidt AM. Activation of the receptor for advanced glycation end products triggers a p21(ras)-dependent mitogen-activated protein kinase pathway regulated by oxidant stress. J Biol Chem 1997;272:17810–4.

[261] Zhong Y, Cheng C, Luo Y, Tian C, Yang H, Liu B, et al. C-reactive protein stimulates RAGE expression in human coronary artery endothelial cells in vitro via ROS generation and ERK/NF-κB activation. Acta Pharmacol Sin 2015;36:440–7. doi:10.1038/aps.2014.163.

[262] Li J, Schmidt AM. Characterization and functional analysis of the promoter of RAGE, the receptor for advanced glycation end products. J Biol Chem 1997;272:16498–506. doi:10.1074/jbc.272.26.16498.

[263] Hudson BI, Kalea AZ, Del Mar Arriero M, Harja E, Boulanger E, D'Agati V, et al. Interaction of the RAGE cytoplasmic domain with diaphanous-1 is required for ligand-stimulated cellular migration through activation of Rac1 and Cdc42. J Biol Chem 2008;283:34457–68. doi:10.1074/jbc.M801465200.

[264] Sorci G, Riuzzi F, Arcuri C, Giambanco I, Donato R. Amphoterin stimulates myogenesis and counteracts the antimyogenic factors basic fibroblast growth factor and S100B via RAGE binding. Mol Cell Biol 2004;24:4880–94. doi:10.1128/MCB.24.11.4880-4894.2004.

[265] Harja E, Bu D, Hudson BI, Chang JS, Shen X, Hallam K, et al. Vascular and inflammatory stresses mediate atherosclerosis via RAGE and its ligands in apoE-/- mice. J Clin Invest

2008;118:183–94. doi:10.1172/JCI32703.

[266] Basta G, Lazzerini G, Massaro M, Simoncini T, Tanganelli P, Fu C, et al. Advanced glycation end products activate endothelium through signal-transduction receptor RAGE: a mechanism for amplification of inflammatory responses. Circulation 2002;105:816–22. doi:10.1161/hc0702.104183.

[267] Skrha J, Kalousová M, Svarcová J, Muravská A, Kvasnička J, Landová L, et al. Relationship of soluble RAGE and RAGE ligands HMGB1 and EN-RAGE to endothelial dysfunction in type 1 and type 2 diabetes mellitus. Exp Clin Endocrinol Diabetes 2012;120:277–81. doi:10.1055/s-0031-1283161.

[268] Taguchi A, Blood DC, del Toro G, Canet A, Lee DC, Qu W, et al. Blockade of RAGE-amphoterin signalling suppresses tumour growth and metastases. Nature 2000;405:354–60. doi:10.1038/35012626.

[269] Guh JY, Huang JS, Chen HC, Hung WC, Lai YH, Chuang LY. Advanced glycation end product-induced proliferation in NRK-49F cells is dependent on the JAK2/STAT5 pathway and cyclin D1. Am J Kidney Dis 2001;38:1096–104. doi:10.1053/ajkd.2001.28616.

[270] Huang JS, Guh JY, Hung WC, Yang ML, Lai YH, Chen HC, et al. Role of the Janus kinase (JAK)/signal transducters and activators of transcription (STAT) cascade in advanced glycation end-product-induced cellular mitogenesis in NRK-49F cells. Biochem J 1999;342 (Pt 1):231–8.

[271] Aleshin A, Ananthakrishnan R, Li Q, Rosario R, Lu Y, Qu W, et al. RAGE modulates myocardial injury consequent to LAD infarction via impact on JNK and STAT signaling in a murine model. Am J Physiol Heart Circ Physiol 2008;294:H1823-32. doi:10.1152/ajpheart.01210.2007.

[272] Meloche J, Paulin R, Courboulin A, Lambert C, Barrier M, Bonnet P, et al. RAGE-dependent activation of the oncoprotein Pim1 plays a critical role in systemic vascular remodeling processes. Arterioscler Thromb Vasc Biol 2011;31:2114–24. doi:10.1161/ATVBAHA.111.230573.

[273] Brizzi MF, Dentelli P, Rosso A, Calvi C, Gambino R, Cassader M, et al. RAGE- and TGF-beta receptor-mediated signals converge on STAT5 and p21waf to control cell-cycle progression of mesangial cells: a possible role in the development and progression of diabetic nephropathy. FASEB J 2004;18:1249–51. doi:10.1096/fj.03-1053fje.

[274] Li JH, Huang XR, Zhu H-J, Oldfield M, Cooper M, Truong LD, et al. Advanced glycation end products activate Smad signaling via TGF-beta-dependent and independent mechanisms: implications for diabetic renal and vascular disease. FASEB J 2004;18:176–8. doi:10.1096/fj.02-1117fje.

[275] Fukami K, Ueda S, Yamagishi S, Kato S, Inagaki Y, Takeuchi M, et al. AGEs activate mesangial TGF-beta-Smad signaling via an angiotensin II type I receptor interaction. Kidney Int 2004;66:2137–47. doi:10.1111/j.1523-1755.2004.66004.x.

[276] Lappas M, Permezel M, Georgiou HM, Rice GE. Nuclear factor kappa B regulation of proinflammatory cytokines in human gestational tissues in vitro. Biol Reprod 2002;67:668–73. doi:10.1095/biolreprod67.2.668.

[277] Sharma I, Tupe RS, Wallner AK, Kanwar YS. Contribution of myo-inositol oxygenase in AGE:RAGE-mediated renal tubulointerstitial injury in the context of diabetic nephropathy. Am J Physiol Renal Physiol 2018;314:F107–21. doi:10.1152/ajprenal.00434.2017.

[278] Ohtsu A, Shibutani Y, Seno K, Iwata H, Kuwayama T, Shirasuna K. Advanced glycation end products and lipopolysaccharides stimulate interleukin-6 secretion via the

RAGE/TLR4-NF-κB-ROS pathways and resveratrol attenuates these inflammatory responses in mouse macrophages. Exp Ther Med 2017;14:4363–70. doi:10.3892/etm.2017.5045.

[279] Schmidt AM, Yan SD, Yan SF, Stern DM. The multiligand receptor RAGE as a progression factor amplifying immune and inflammatory responses. J Clin Invest 2001;108:949–55. doi:10.1172/JCI14002.

[280] Cheng P, Dai W, Wang F, Lu J, Shen M, Chen K, et al. Ethyl pyruvate inhibits proliferation and induces apoptosis of hepatocellular carcinoma via regulation of the HMGB1-RAGE and AKT pathways. Biochem Biophys Res Commun 2014;443:1162–8. doi:10.1016/j.bbrc.2013.12.064.

[281] Li DX, Deng TZ, Lv J, Ke J. Advanced glycation end products (AGEs) and their receptor (RAGE) induce apoptosis of periodontal ligament fibroblasts. Braz J Med Biol Res 2014;47:1036–43.

[282] Ibrahim ZA, Armour CL, Phipps S, Sukkar MB. RAGE and TLRs: relatives, friends or neighbours? Mol Immunol 2013;56:739–44. doi:10.1016/j.molimm.2013.07.008.

[283] Breuer O, Caudri D, Stick S, Turkovic L. Predicting disease progression in cystic fibrosis. Expert Rev Respir Med 2018;12:905–17. doi:10.1080/17476348.2018.1519400.

[284] Keating C, Poor AD, Liu X, Chiuzan C, Backenroth D, Zhang Y, et al. Reduced survival in adult cystic fibrosis despite attenuated lung function decline. J Cyst Fibros 2017;16:78–84. doi:10.1016/j.jcf.2016.07.012.

[285] Ma JT, Tang C, Kang L, Voynow JA, Rubin BK. Cystic fibrosis sputum rheology correlates with both acute and longitudinal changes in lung function. Chest 2018;154:370–7. doi:10.1016/j.chest.2018.03.005.

[286] Donaldson SH, Corcoran TE, Laube BL, Bennett WD. Mucociliary clearance as an outcome measure for cystic fibrosis clinical research. Proc Am Thorac Soc 2007;4:399–405. doi:10.1513/pats.200703-042BR.

[287] Abdullah LH, Coakley R, Webster MJ, Zhu Y, Tarran R, Radicioni G, et al. Mucin Production and Hydration Responses to Mucopurulent Materials in Normal versus Cystic Fibrosis Airway Epithelia. Am J Respir Crit Care Med 2018;197:481–91. doi:10.1164/rccm.201706-1139OC.

[288] Henderson AG, Ehre C, Button B, Abdullah LH, Cai L-H, Leigh MW, et al. Cystic fibrosis airway secretions exhibit mucin hyperconcentration and increased osmotic pressure. J Clin Invest 2014;124:3047–60. doi:10.1172/JCI73469.

[289] Kreda SM, Davis CW, Rose MC. CFTR, mucins, and mucus obstruction in cystic fibrosis. Cold Spring Harb Perspect Med 2012;2:a009589. doi:10.1101/cshperspect.a009589.

[290] Mall MA. Unplugging mucus in cystic fibrosis and chronic obstructive pulmonary disease. Annals of the American Thoracic Society 2016;13 Suppl 2:S177-85. doi:10.1513/AnnalsATS.201509-641KV.

[291] Zhu Z, Homer RJ, Wang Z, Chen Q, Geba GP, Wang J, et al. Pulmonary expression of interleukin-13 causes inflammation, mucus hypersecretion, subepithelial fibrosis, physiologic abnormalities, and eotaxin production. J Clin Invest 1999;103:779–88. doi:10.1172/JCI5909.

[292] Erle DJ, Sheppard D. The cell biology of asthma. J Cell Biol 2014;205:621–31. doi:10.1083/jcb.201401050.

[293] Beucher J, Boëlle P-Y, Busson P-F, Muselet-Charlier C, Clement A, Corvol H, et al. AGER -429T/C is associated with an increased lung disease severity in cystic fibrosis.

PLoS One 2012;7:e41913. doi:10.1371/journal.pone.0041913.

[294] Hao Y, Kuang Z, Walling BE, Bhatia S, Sivaguru M, Chen Y, et al. Pseudomonas aeruginosa pyocyanin causes airway goblet cell hyperplasia and metaplasia and mucus hypersecretion by inactivating the transcriptional factor FoxA2. Cell Microbiol 2012;14:401–15. doi:10.1111/j.1462-5822.2011.01727.x.

[295] Castellani S, Di Gioia S, di Toma L, Conese M. Human cellular models for the investigation of lung inflammation and mucus production in cystic fibrosis. Anal Cell Pathol (Amst) 2018;2018:3839803. doi:10.1155/2018/3839803.

[296] Deane R, Singh I, Sagare AP, Bell RD, Ross NT, LaRue B, et al. A multimodal RAGE-specific inhibitor reduces amyloid β-mediated brain disorder in a mouse model of Alzheimer disease. J Clin Invest 2012;122:1377–92. doi:10.1172/JCI58642.

[297] Ramachandran S, Krishnamurthy S, Jacobi AM, Wohlford-Lenane C, Behlke MA, Davidson BL, et al. Efficient delivery of RNA interference oligonucleotides to polarized airway epithelia in vitro. Am J Physiol Lung Cell Mol Physiol 2013;305:L23-32. doi:10.1152/ajplung.00426.2012.

[298] Booth BW, Adler KB, Bonner JC, Tournier F, Martin LD. Interleukin-13 induces proliferation of human airway epithelial cells in vitro via a mechanism mediated by transforming growth factor-alpha. Am J Respir Cell Mol Biol 2001;25:739–43. doi:10.1165/ajrcmb.25.6.4659.

[299] Taniguchi K, Yamamoto S, Aoki S, Toda S, Izuhara K, Hamasaki Y. Epigen is induced during the interleukin-13-stimulated cell proliferation in murine primary airway epithelial cells. Exp Lung Res 2011;37:461–70. doi:10.3109/01902148.2011.596894.

[300] Park K-S, Korfhagen TR, Bruno MD, Kitzmiller JA, Wan H, Wert SE, et al. SPDEF

regulates goblet cell hyperplasia in the airway epithelium. J Clin Invest 2007;117:978–88. doi:10.1172/JCI29176.

[301] Chen G, Korfhagen TR, Xu Y, Kitzmiller J, Wert SE, Maeda Y, et al. SPDEF is required for mouse pulmonary goblet cell differentiation and regulates a network of genes associated with mucus production. J Clin Invest 2009;119:2914–24. doi:10.1172/JCI39731.

[302] Lambrecht BN, Hammad H. The airway epithelium in asthma. Nat Med 2012;18:684–92. doi:10.1038/nm.2737.

[303] Matsukura S, Stellato C, Georas SN, Casolaro V, Plitt JR, Miura K, et al. Interleukin-13 upregulates eotaxin expression in airway epithelial cells by a STAT6-dependent mechanism. Am J Respir Cell Mol Biol 2001;24:755–61. doi:10.1165/ajrcmb.24.6.4351.

[304] Wen T, Rothenberg ME. The regulatory function of eosinophils. Microbiol Spectr 2016;4. doi:10.1128/microbiolspec.MCHD-0020-2015.

[305] Tashkin DP, Wechsler ME. Role of eosinophils in airway inflammation of chronic obstructive pulmonary disease. Int J Chron Obstruct Pulmon Dis 2018;13:335–49. doi:10.2147/COPD.S152291.

[306] Davoine F, Lacy P. Eosinophil cytokines, chemokines, and growth factors: emerging roles in immunity. Front Immunol 2014;5:570. doi:10.3389/fimmu.2014.00570.

[307] Marguet C, Jouen-Boedes F, Dean TP, Warner JO. Bronchoalveolar cell profiles in children with asthma, infantile wheeze, chronic cough, or cystic fibrosis. Am J Respir Crit Care Med 1999;159:1533–40. doi:10.1164/ajrccm.159.5.9805028.

[308] Snead NM, Wu X, Li A, Cui Q, Sakurai K, Burnett JC, et al. Molecular basis for improved gene silencing by Dicer substrate interfering RNA compared with other siRNA variants. Nucleic Acids Res 2013;41:6209–21. doi:10.1093/nar/gkt200.

[309] Chirico V, Lacquaniti A, Leonardi S, Grasso L, Rotolo N, Romano C, et al. Acute pulmonary exacerbation and lung function decline in patients with cystic fibrosis: high-mobility group box 1 (HMGB1) between inflammation and infection. Clin Microbiol Infect 2015;21:368.e1-9. doi:10.1016/j.cmi.2014.11.004.

[310] Barry J, Loh Z, Collison A, Mazzone S, Lalwani A, Zhang V, et al. Absence of Toll-IL-1 receptor 8/single immunoglobulin IL-1 receptor-related molecule reduces house dust mite-induced allergic airway inflammation in mice. Am J Respir Cell Mol Biol 2013;49:481–90. doi:10.1165/rcmb.2012-0425OC.

[311] Kuperman DA, Huang X, Nguyenvu L, Hölscher C, Brombacher F, Erle DJ. IL-4 receptor signaling in Clara cells is required for allergen-induced mucus production. J Immunol 2005;175:3746–52. doi:10.4049/jimmunol.175.6.3746.

[312] Arora S, Ahmad S, Irshad R, Goyal Y, Rafat S, Siddiqui N, et al. TLRs in pulmonary diseases. Life Sci 2019;233:116671. doi:10.1016/j.lfs.2019.116671.

[313] Lennox AT, Coburn SL, Leech JA, Heidrich EM, Kleyman TR, Wenzel SE, et al. ATP12A promotes mucus dysfunction during Type 2 airway inflammation. Sci Rep 2018;8:2109. doi:10.1038/s41598-018-20444-8.

[314] Antonelli A, Di Maggio S, Rejman J, Sanvito F, Rossi A, Catucci A, et al. The shedding-derived soluble receptor for advanced glycation endproducts sustains inflammation during acute Pseudomonas aeruginosa lung infection. Biochim Biophys Acta Gen Subj 2017;1861:354–64. doi:10.1016/j.bbagen.2016.11.040.

[315] Lau GW, Ran H, Kong F, Hassett DJ, Mavrodi D. *Pseudomonas aeruginosa* pyocyanin is critical for lung infection in mice. Infect Immun 2004;72:4275–8. doi:10.1128/IAI.72.7.4275-4278.2004.

[316] Sandri A, Ortombina A, Boschi F, Cremonini E, Boaretti M, Sorio C, et al. Inhibition of Pseudomonas aeruginosa secreted virulence factors reduces lung inflammation in CF mice. Virulence 2018;9:1008–18. doi:10.1080/21505594.2018.1489198.

[317] Schmitz J, Owyang A, Oldham E, Song Y, Murphy E, McClanahan TK, et al. IL-33, an interleukin-1-like cytokine that signals via the IL-1 receptor-related protein ST2 and induces T helper type 2-associated cytokines. Immunity 2005;23:479–90. doi:10.1016/j.immuni.2005.09.015.

[318] Dinarello CA. Overview of the IL-1 family in innate inflammation and acquired immunity. Immunol Rev 2018;281:8–27. doi:10.1111/imr.12621.

[319] Liu X, Hammel M, He Y, Tainer JA, Jeng U-S, Zhang L, et al. Structural insights into the interaction of IL-33 with its receptors. Proc Natl Acad Sci USA 2013;110:14918–23. doi:10.1073/pnas.1308651110.

[320] Carriere V, Roussel L, Ortega N, Lacorre D-A, Americh L, Aguilar L, et al. IL-33, the IL-1-like cytokine ligand for ST2 receptor, is a chromatin-associated nuclear factor in vivo. Proc Natl Acad Sci USA 2007;104:282–7. doi:10.1073/pnas.0606854104.

[321] Lüthi AU, Cullen SP, McNeela EA, Duriez PJ, Afonina IS, Sheridan C, et al. Suppression of interleukin-33 bioactivity through proteolysis by apoptotic caspases. Immunity 2009;31:84–98. doi:10.1016/j.immuni.2009.05.007.

[322] Saglani S, Lui S, Ullmann N, Campbell GA, Sherburn RT, Mathie SA, et al. IL-33 promotes airway remodeling in pediatric patients with severe steroid-resistant asthma. J Allergy Clin Immunol 2013;132:676–685.e13. doi:10.1016/j.jaci.2013.04.012.

[323] Bessa J, Meyer CA, de Vera Mudry MC, Schlicht S, Smith SH, Iglesias A, et al. Altered subcellular localization of IL-33 leads to non-resolving lethal inflammation. J Autoimmun

2014;55:33–41. doi:10.1016/j.jaut.2014.02.012.

[324] Perkins C, Wills-Karp M, Finkelman FD. IL-4 induces IL-13-independent allergic airway inflammation. J Allergy Clin Immunol 2006;118:410–9. doi:10.1016/j.jaci.2006.06.004.

[325] Moro K, Yamada T, Tanabe M, Takeuchi T, Ikawa T, Kawamoto H, et al. Innate production of T(H)2 cytokines by adipose tissue-associated c-Kit(+)Sca-1(+) lymphoid cells. Nature 2010;463:540–4. doi:10.1038/nature08636.

[326] Moffatt MF, Gut IG, Demenais F, Strachan DP, Bouzigon E, Heath S, et al. A large-scale, consortium-based genomewide association study of asthma. N Engl J Med 2010;363:1211–21. doi:10.1056/NEJMoa0906312.

[327] Cayrol C, Duval A, Schmitt P, Roga S, Camus M, Stella A, et al. Environmental allergens induce allergic inflammation through proteolytic maturation of IL-33. Nat Immunol 2018;19:375–85. doi:10.1038/s41590-018-0067-5.

[328] Cayrol C, Girard J-P. IL-33: an alarmin cytokine with crucial roles in innate immunity, inflammation and allergy. Curr Opin Immunol 2014;31:31–7. doi:10.1016/j.coi.2014.09.004.

[329] Ohno T, Morita H, Arae K, Matsumoto K, Nakae S. Interleukin-33 in allergy. Allergy 2012;67:1203–14. doi:10.1111/all.12004.

[330] Leclerc E, Fritz G, Vetter SW, Heizmann CW. Binding of S100 proteins to RAGE: an update. Biochim Biophys Acta 2009;1793:993–1007. doi:10.1016/j.bbamcr.2008.11.016.

[331] Ullah MA, Loh Z, Gan WJ, Zhang V, Yang H, Li JH, et al. Receptor for advanced glycation end products and its ligand high-mobility group box-1 mediate allergic airway sensitization and airway inflammation. J Allergy Clin Immunol 2014;134:440–50. doi:10.1016/j.jaci.2013.12.1035.

[332] Eschenbacher WL. Defining Airflow Obstruction. Chronic Obstr Pulm Dis (Miami) 2016;3:515–8. doi:10.15326/jcopdf.3.2.2015.0166.

[333] Neill DR, Wong SH, Bellosi A, Flynn RJ, Daly M, Langford TKA, et al. Nuocytes represent a new innate effector leukocyte that mediates type-2 immunity. Nature 2010;464:1367–70. doi:10.1038/nature08900.

[334] Price AE, Liang H-E, Sullivan BM, Reinhardt RL, Eisley CJ, Erle DJ, et al. Systemically dispersed innate IL-13-expressing cells in type 2 immunity. Proc Natl Acad Sci USA 2010;107:11489–94. doi:10.1073/pnas.1003988107.

[335] Ishizaka T, Saito H, Hatake K, Dvorak AM, Leiferman KM, Arai N, et al. Preferential differentiation of inflammatory cells by recombinant human interleukins. Int Arch Allergy Immunol 1989;88:46–9. doi:10.1159/000234746.

[336] Chand N, Harrison JE, Rooney S, Pillar J, Jakubicki R, Nolan K, et al. Anti-IL-5 monoclonal antibody inhibits allergic late phase bronchial eosinophilia in guinea pigs: a therapeutic approach. Eur J Pharmacol 1992;211:121–3.

[337] Kuperman DA, Huang X, Koth LL, Chang GH, Dolganov GM, Zhu Z, et al. Direct effects of interleukin-13 on epithelial cells cause airway hyperreactivity and mucus overproduction in asthma. Nat Med 2002;8:885–9. doi:10.1038/nm734.

[338] Shirasawa M, Fujiwara N, Hirabayashi S, Ohno H, Iida J, Makita K, et al. Receptor for advanced glycation end-products is a marker of type I lung alveolar cells. Genes Cells 2004;9:165–74. doi:10.1111/j.1356-9597.2004.00712.x.

[339] Fehrenbach H. Alveolar epithelial type II cell: defender of the alveolus revisited. Respir Res 2001;2:33–46. doi:10.1186/rr36.

[340] Oczypok EA, Perkins TN, Oury TD. Alveolar Epithelial Cell-Derived Mediators: Potential

Direct Regulators of Large Airway and Vascular Responses. Am J Respir Cell Mol Biol 2017;56:694–9. doi:10.1165/rcmb.2016-0151PS.

[341] Liu T, Barrett NA, Kanaoka Y, Yoshimoto E, Garofalo D, Cirka H, et al. Type 2 Cysteinyl Leukotriene Receptors Drive IL-33-Dependent Type 2 Immunopathology and Aspirin Sensitivity. J Immunol 2018;200:915–27. doi:10.4049/jimmunol.1700603.

[342] Hawkins F, Kramer P, Jacob A, Driver I, Thomas DC, McCauley KB, et al. Prospective isolation of NKX2-1-expressing human lung progenitors derived from pluripotent stem cells. J Clin Invest 2017;127:2277–94. doi:10.1172/JCI89950.

[343] Kurmann AA, Serra M, Hawkins F, Rankin SA, Mori M, Astapova I, et al. Regeneration of thyroid function by transplantation of differentiated pluripotent stem cells. Cell Stem Cell 2015;17:527–42. doi:10.1016/j.stem.2015.09.004.

[344] Barth K, Bläsche R, Kasper M. T1alpha/podoplanin shows raft-associated distribution in mouse lung alveolar epithelial E10 cells. Cell Physiol Biochem 2010;25:103–12. doi:10.1159/000272065.

[345] Williams MC, Cao Y, Hinds A, Rishi AK, Wetterwald A. T1 alpha protein is developmentally regulated and expressed by alveolar type I cells, choroid plexus, and ciliary epithelia of adult rats. Am J Respir Cell Mol Biol 1996;14:577–85. doi:10.1165/ajrcmb.14.6.8652186.

[346] Nakano H, Nakano K, Cook DN. Isolation and Purification of Epithelial and Endothelial Cells from Mouse Lung. Methods Mol Biol 2018;1799:59–69. doi:10.1007/978-1-4939-7896-0_6.

[347] Hasegawa K, Sato A, Tanimura K, Uemasu K, Hamakawa Y, Fuseya Y, et al. Fraction of MHCII and EpCAM expression characterizes distal lung epithelial cells for alveolar type 2

cell isolation. Respir Res 2017;18:150. doi:10.1186/s12931-017-0635-5.

[348] Xia J, Zhao J, Shang J, Li M, Zeng Z, Zhao J, et al. Increased IL-33 expression in chronic obstructive pulmonary disease. Am J Physiol Lung Cell Mol Physiol 2015;308:L619-27. doi:10.1152/ajplung.00305.2014.

[349] Castranova V, Rabovsky J, Tucker JH, Miles PR. The alveolar type II epithelial cell: a multifunctional pneumocyte. Toxicol Appl Pharmacol 1988;93:472–83.

[350] Draper JS, Pigott C, Thomson JA, Andrews PW. Surface antigens of human embryonic stem cells: changes upon differentiation in culture. J Anat 2002;200:249–58. doi:10.1046/j.1469-7580.2002.00030.x.

[351] Wosen JE, Mukhopadhyay D, Macaubas C, Mellins ED. Epithelial MHC class II expression and its role in antigen presentation in the gastrointestinal and respiratory tracts. Front Immunol 2018;9:2144. doi:10.3389/fimmu.2018.02144.

[352] Gereke M, Jung S, Buer J, Bruder D. Alveolar type II epithelial cells present antigen to CD4(+) T cells and induce Foxp3(+) regulatory T cells. Am J Respir Crit Care Med 2009;179:344–55. doi:10.1164/rccm.200804-592OC.

[353] ANTIGEN PRESENTATION. Immunology Guidebook, Elsevier; 2004, p. 267–76. doi:10.1016/B978-012198382-6/50031-5.

[354] Fanta CH. Clinical aspects of mucus and mucous plugging in asthma. J Asthma 1985;22:295–301.

[355] Mao B, Yang J-W, Lu H-W, Xu J-F. Asthma and bronchiectasis exacerbation. Eur Respir J 2016;47:1680–6. doi:10.1183/13993003.01862-2015.

[356] Roussel L, Farias R, Rousseau S. IL-33 is expressed in epithelia from patients with cystic fibrosis and potentiates neutrophil recruitment. J Allergy Clin Immunol 2013;131:913–6.

doi:10.1016/j.jaci.2012.10.019.

[357] Farias R, Rousseau S. The TAK1→IKKβ→TPL2→MKK1/MKK2 Signaling Cascade Regulates IL-33 Expression in Cystic Fibrosis Airway Epithelial Cells Following Infection by Pseudomonas aeruginosa. Front Cell Dev Biol 2015;3:87. doi:10.3389/fcell.2015.00087.

[358] Lyczak JB, Cannon CL, Pier GB. Lung infections associated with cystic fibrosis. Clin Microbiol Rev 2002;15:194–222. doi:10.1128/cmr.15.2.194-222.2002.

[359] Jefferis BJMH, Papacosta O, Owen CG, Wannamethee SG, Humphries SE, Woodward M, et al. Interleukin 18 and coronary heart disease: prospective study and systematic review. Atherosclerosis 2011;217:227–33. doi:10.1016/j.atherosclerosis.2011.03.015.

[360] Hanford LE, Enghild JJ, Valnickova Z, Petersen SV, Schaefer LM, Schaefer TM, et al. Purification and characterization of mouse soluble receptor for advanced glycation end products (sRAGE). J Biol Chem 2004;279:50019–24. doi:10.1074/jbc.M409782200.

[361] Zhang F, Wen Y, Guo X. CRISPR/Cas9 for genome editing: progress, implications and challenges. Hum Mol Genet 2014;23:R40-6. doi:10.1093/hmg/ddu125.

[362] Jeong SJ, Lim BJ, Park S, Choi D, Kim HW, Ku NS, et al. The effect of sRAGE-Fc fusion protein attenuates inflammation and decreases mortality in a murine cecal ligation and puncture model. Inflamm Res 2012;61:1211–8. doi:10.1007/s00011-012-0518-7.

[363] Pichery M, Mirey E, Mercier P, Lefrancais E, Dujardin A, Ortega N, et al. Endogenous IL-33 is highly expressed in mouse epithelial barrier tissues, lymphoid organs, brain, embryos, and inflamed tissues: in situ analysis using a novel Il-33-LacZ gene trap reporter strain. J Immunol 2012;188:3488–95. doi:10.4049/jimmunol.1101977.

[364] Katsuoka F, Kawakami Y, Arai T, Imuta H, Fujiwara M, Kanma H, et al. Type II alveolar

epithelial cells in lung express receptor for advanced glycation end products (RAGE) gene. Biochem Biophys Res Commun 1997;238:512–6. doi:10.1006/bbrc.1997.7263.